

The Hops Tethering Complex and the Dynamin Homolog Vps1 Coordinate Distinct Stages in Intracellular Membrane Fusion

The Hops Tethering Complex and the Dynamin Homolog Vps1 Coordinate Distinct Stages in Intracellular Membrane Fusion

A Dissertation (Thesis) Submitted to the Faculty of the Graduate School

Baylor College of Medicine

In Partial Fulfillment of the

Requirements for the Degree of Doctor of Philosophy by

Aditya Kulkarni

APPROVED BY THE DISSERTATION (THESIS) COMMITTEE

Christopher Peters, Ph.D. (Chairman)

Adam Kuspa, Ph.D.

Kimberley Tolias, Ph.D.

Zheng Zhou, Ph.D.

Anna Sokac, Ph.D.

Approved By the Department of

Biochemistry and Molecular Biology

John Wilson, Ph.D.

Director of Graduate Studies

Theodore Wensel, Ph.D.

Chairman of Department

Approved By the Dean of Graduate Sciences

Deborah L. Johnson, Ph.D.

Published By

MedCrave Group

October 17, 2016

Contents

Acknowledgments	1
Abstract	2
Chapter I	3
Background	4
Chapter II	21
A HOPS Tethering Complex Dimer Catalyzes Trans-SNARE Complex Formation In Yeast	22
Vacuolar Fusion	22
Introduction	25
Materials and Methods	26
Results	35
Discussion	39
Chapter III	39
The dynamin homolog Vps1 promotes the transition from hemifusion to content mixing in yeast vacuolar fusion	40
Introduction	40
Materials and Methods	42
Results	55
Discussion	58
Chapter IV	59
Summary, Significance, Outlook and Future Goals	59
Summary	62
References	

Acknowledgements

I would like to thank my advisor Dr. Christopher Peters for his exceptional guidance, motivation, advice and support throughout my PhD. His mentorship in regards to elucidation of both theoretical and practical biochemistry; identification and conceptualization of a biological problem; planning and execution of experiments; outlining and drafting of a manuscript; and effective communication of research output has been extremely vital for me to excel as graduate student. I also want to thank all my former and current lab members, especially Dr. Kannan Alpadi, for offering constructive inputs and sharing their skills and perspectives. I wish to acknowledge my committee members, Dr. Zheng Zhou, Dr. Kim Tolias, Dr. Anna Sokac and Dr. Adam Kuspa, for being extremely approachable, for their eagerness to provide helpful feedback and resources, and for helping me set and maintain a direction to my projects. I would like to thank our program director, Dr. John Wilson, for his initiatives in overall student development, and for making the Biochemistry department a cohesive family.

I want to thank all my batchmates from the entering class of 2009, especially Michael Chen, for helping me through the course work, the qualifying examination, oral and poster presentations and for being really great friends. A very special mention goes to Ms. Ruth Reeves for being a constant pillar of encouragement, for taking care of all my deadlines and paperwork, and for planning wonderful events. It was a great learning experience and a pleasure to share my knowledge and skills with all rotation students and undergrads we had in the lab, including Vlatko Stojanoski, Swetha Mandalaju and Dominic Nguyen.

I am greatly indebted to my parents Smita Kulkarni and Vivek Kulkarni for standing by me unconditionally throughout my PhD. I am extremely grateful to my wife Vishakha Bhedasgaonkar for being my rock through the process. Their presence has been invaluable.

Abstract

Part 1

Cells in almost all eukaryotes ranging from yeast to humans contain membrane-enclosed compartments called organelles. To survive and proliferate, cells must communicate signals within themselves and with their environment and this is achieved through membrane trafficking. It involves generation of a vesicle carrying specific soluble or membrane-anchored cargo from a precursor membrane, transport of the vesicle to its destination and ultimately fusion of the vesicle with the target membrane. Soluble N-ethylmaleimide sensitive factor Attachment protein Receptors (SNAREs) have been identified as key components of membrane fusion in the endomembrane system. SNARE proteins typically consist of a single transmembrane domain at the carboxy terminal and a coiled-coil SNARE domain and are designated as Qa, Qb, Qc and R depending upon the presence of a Glutamine or Arginine residue at a conserved position in the SNARE domain. A critical intermediate in the membrane fusion pathway is the trans-SNARE complex generated by the assembly of SNAREs residing in opposing membrane compartments destined to fuse. Mechanistic details of trans-SNARE complex formation and topology in a physiological system remain largely unresolved. This study on native yeast vacuoles revealed that SNAREs alone are insufficient to form trans-SNARE complexes and that additional factors, potentially tethering complexes and Rab GTPases, are required for the process. HOmotypic fusion and vacuole Protein Sorting (HOPS) is a tethering complex that is known to function in endosome to vacuole/lysosome transport and is well conserved across multiple species. Ypt7 is the Rab7 homolog in yeast that coordinates endolysosomal trafficking. I found that the HOPS complex exists as a dimer on the surface of yeast vacuoles. I report a new finding that a HOPS tethering complex dimer catalyzes Ypt7-dependent formation of a topologically preferred QbQcR-Qa trans-SNARE complex in yeast vacuole fusion.

Part 2

Dynamin family members are the classically recognized core components driving membrane fission reactions in the endomembrane system. The yeast dynamin homolog Vps1 (Vacuolar protein sorting 1) is a dynamin-related protein involved in vesicle trafficking along the secretory and endocytic pathways converging at the vacuolar compartment. Vps1 is known to self-assemble into higher order oligomers as rings and form collar-like constrictions of membranes. These results in membrane deformation leading to the hemifused state from the opposite direction compared to that in fusion. SNARE-mediated fusion and dynamin-driven fission are fundamental membrane remodeling processes underlying ubiquitous cellular events such as exocytosis, endocytosis, intracellular trafficking and mitosis. Depending on environmental, nutritional and cell cycle conditions, organelles and vesicles exist in an equilibrium of fragmentation into smaller units and fusion into larger structures. Simultaneous fusion and fission events are futile and hence need to be strictly controlled. Regulation of this fusion-fission equilibrium which is critical for maintenance of cellular homeostasis, is an obvious but poorly explored problem. Moreover, the convergence of the antagonistic reactions of membrane fusion and fission at the hemifusion/hemifission intermediate has generated a captivating enigma of whether SNAREs and dynamin have unusual counter-functions in fission and fusion respectively. Here I have demonstrated the influence of Vps1 on the content mixing and lipid mixing properties of yeast vacuoles, and on the incorporation of SNAREs into fusogenic complexes. I identified specific Vps1 mutations that impair vacuolar content mixing and trans-SNARE complex formation, but allow comparable lipid mixing relative to wild type. I discovered that the vacuole fusion defects caused by these Vps1 mutations can be attributed to the loss of oligomerization capacity of Vps1. I propose a novel concept that Vps1, through its oligomerization and SNARE domain binding, promotes the hemifusion-content mixing transition in yeast vacuole fusion by increasing the number of trans-SNAREs.

Chapter 1

Background

Chapter I

Background

The endomembrane system in eukaryotic cells

A cell is considered as the fundamental structural and functional unit of life. Cells are categorized into two basic types: prokaryotic (pro = before, karyon = nucleus) and eukaryotic (eu = true, karyon = nucleus). These cell types are as alike as they are different. Both are enclosed by a cell membrane. Both have DNA as their genetic material. Both are made from the same basic chemicals: proteins, lipids, carbohydrates, nucleic acids and vitamins. To survive and proliferate, each cell must communicate external or internal stimuli and downstream signals within itself and with its environment. Accordingly, both prokaryotic and eukaryotic cells regulate the flow of the nutrients and metabolic products that enter and leave them. That's what prokaryotic and eukaryotic cells have in common. But there are significant differences between them too. The two main differences lie in their age and structure. Prokaryotes such as bacteria were the first life forms on earth, originating around 3.5 billion years ago. This occurred 2 billion years prior to the evolution of eukaryotes [1]. Unlike a bacterium that consists of a plasma membrane enveloping a cell body typically with free-floating DNA and no internal structures, a eukaryotic cell has its DNA packaged inside a double-membrane nucleus and is elaborately subdivided into functionally distinct, membrane-bound compartments called organelles. These membranous systems form functionally specialized zones within the cell to catalyze particular biochemical reactions. Intracellular organelles have distinct biochemical and morphological characteristics defined by their unique protein and lipid compositions. Each organelle membrane must have a mechanism to incorporate specific proteins and lipids that make the organelle structurally and functionally distinct. Finely regulated transport systems are therefore required to accurately deliver cargo to its correct intracellular location. The pool of different membrane-bound organelles and vesicles suspended in the cytosol constitute the endomembrane system in a eukaryotic cell [2]. Figure 1, adapted from [2] illustrates the general framework of major organelles common to most eukaryotic cells. As displayed in this figure, the plasma membrane, the nucleus, cytosol, endoplasmic reticulum (ER), Golgi apparatus, mitochondrion, lysosome, endosome and peroxisome are distinct compartments separated from the rest of the cell by at least one selectively permeable membrane.

The plasma membrane is a phospholipids' bilayer and forms the bounding membrane that separates the cell from its environment and regulates the transport of molecules and signals into and out of the cell. The plasma membrane of a cell thereby maintains the pH and preserves the osmotic pressure of the cytosol. The nucleus wrapped in a double membrane envelope contains the cell's genome and is the principal site of DNA and RNA synthesis. The surrounding cytoplasm consists of the cytosol and organelles suspended in it. The cytosol or intracellular aqueous fluid is composed

of a complex mixture of substances and has multiple levels of organization. These include macromolecules such as enzymes and protein complexes associating to carry out metabolic processes, and concentration gradients of ions. The ER has ribosomes bound to its cytosolic surface where both soluble and integral membrane proteins are synthesized. The ER also produces most of the lipid for the cell and acts as a Ca^{++} reservoir. Many of these proteins and lipids are further transported to other organelles or secreted to the cell exterior by being sorted into small membrane-bound compartments called vesicles. The Golgi apparatus consists of stacks of disc-like compartments called cisternae. Each Golgi stack has two distinct faces: a cis face (or entry face) and a trans face (or exit face) in relation to the ER. The Golgi receives proteins and lipids from the ER and dispatches them to various destinations such as lysosome, endosome, plasma membrane via vesicles or other intermediate compartments. Nascent proteins or lipids arriving from the ER are usually covalently modified as they traverse the Golgi. Mitochondria generate most of the ATP that cells need as their energy currency to drive biochemical reactions.

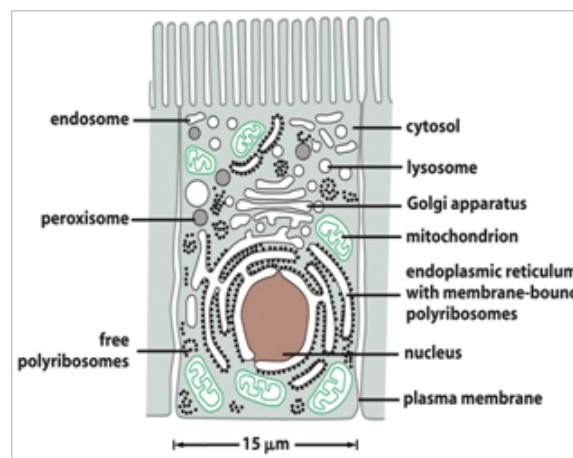


Figure 1: Schematic of the endomembrane system in a eukaryotic cell.

Lysosomes (lysis from lyein = to separate; soma = body) can be described as the stomach of the cell. They contain digestive acid hydrolase enzymes that break down toxic or waste material from various sources. Lysosomes digest macromolecules from phagocytosis (ingestion of other dying cells or invading microbes), endocytosis (internalization of receptors and other proteins that are either degraded and released into the cytosol or recycled to the cell surface), and autophagy (wherein old, excess or unnecessary organelles or proteins, or microbes that have invaded the cytoplasm are delivered to the lysosome). Depending upon the cell type, the size of a lysosome may vary from 0.1-1.2 μm . The membrane around a lysosome allows the digestive enzymes to work at the acidic pH that they require. At pH 4.8, the interior or lumen of the lysosome is acidic compared to the slightly alkaline cytosol at pH 7.2. The lysosome maintains this pH differential by pumping protons

Chapter 1

(H⁺ ions) from the cytosol across its membrane via proton pumps. The lysosomal membrane protects the cytosol, and therefore the rest of the cell, from the degradative enzymes within the lysosome. The cell is additionally protected from any lysosomal acid hydrolases that drain into the cytosol, as these enzymes are pH-sensitive and do not function well or at all in the alkaline environment of the cytosol. This ensures that cytosolic molecules and organelles are not lysed in case there is leakage of the hydrolytic enzymes from the lysosome.

Different types of endosomes exist to provide an environment for cellular cargo to be sorted to or from the Golgi, plasma membrane and lysosome. Endosomes comprise three different compartments: early endosomes, late endosomes, and recycling endosomes. They are distinguished by the time it takes for material internalized from the plasma membrane to reach them. They also have different morphologies. Early endosomes consist of a dynamic tubular-vesicular network. Molecules are sorted into smaller vesicles that bud from the perimeter membrane into the endosome lumen, forming luminal vesicles. This leads to the multivesicular appearance of late endosomes and hence they are also known as multivesicular bodies (MVBs). Some material recycles to the plasma membrane directly from early endosomes, but most traffics via recycling endosomes. Finally, peroxisomes are compartments that contain enzymes catalyzing various oxidation reactions. In general, each organelle performs the same set of primary functions in all cell types. To serve specialized functions in cells, these organelles may vary in abundance and may have additional properties that vary according to cell type. To understand the relationships between the various organelles, it is helpful to consider how they might have evolved. The precursors of the first eukaryotic cells are thought to be bacteria-like organisms in which the plasma membrane itself performs all membrane-dependent functions including synthesis and transport of biomolecules. Typical present-day eukaryotic cells are 1000-10000 times

greater in volume and 10-30 times larger in linear dimension than a typical bacterium. An increase in the overall volume of a cell would require the plasma membrane to fold profusely in order to maintain a constant surface area to volume ratio so as to be able to sustain the many vital membrane functions. These folds may have led to the emergence of specialized internal membranes to maintain communication with the environment. The invagination and pinching off of intracellular membrane structures from the plasma membrane is likely to have created the ER, Golgi, lysosomes and endosomes. According to this evolutionary scheme, the interior of these organelles must be topologically equivalent to the exterior of the cell and we can think of all these organelles as members of the same family [2]. Their interiors are known to communicate extensively with one another and with the cell exterior via transport intermediates or vesicles, which bud out from one organelle and fuse with another.

Secretory and endocytic membrane trafficking pathways

To remain healthy, every cell must adapt and respond rapidly to its environment. The cell must therefore adjust the composition of its plasma membrane in a dynamic manner. The framework of the endomembrane system described before facilitates the incorporation or depletion of cell-surface proteins. Through the process of exocytosis, the secretory pathway delivers newly synthesized proteins, lipids and carbohydrates to the plasma membrane or extracellular space. By the converse process of endocytosis, the endocytic pathway captures nutrients together with the macromolecules to which they bind and is also able to remove plasma membrane components. The internalized material is then delivered to endosomes from where it can either be transported to the lysosome for degradation or released into the cytosol or recycled to the same or different region of the plasma membrane. Figure 2, obtained from [2], depicts a road map of the membrane trafficking pathways in a typical eukaryotic cell.

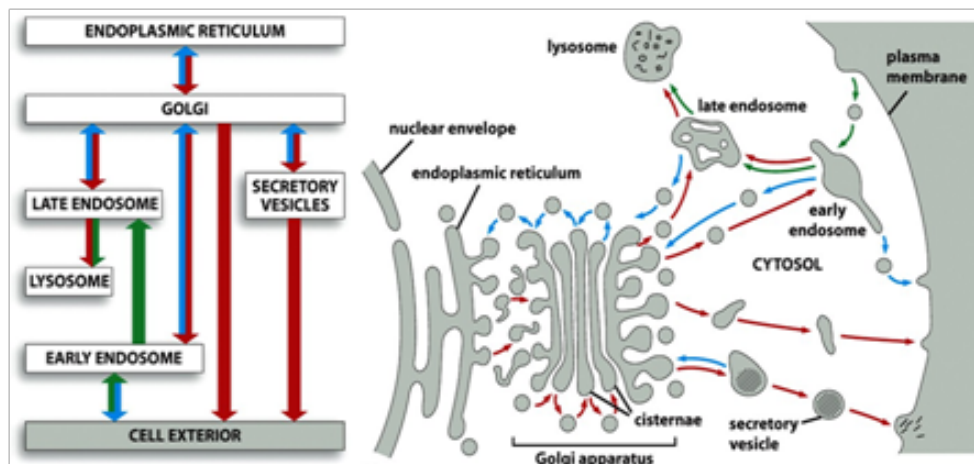


Figure 2: A road map of the secretory and endocytic pathways.

Left panel shows the directionality of communication between different organelles. Red arrows indicate secretory pathway, green arrows indicate endocytic pathway and blue arrows denote retrieval pathways. Right panel depicts the different organelles in the trafficking pathways communicating via vesicular transport.

In the secretory pathway, molecules are transported from the ER to (i) the plasma membrane via the Golgi and secretory vesicles and (ii) the lysosome via the Golgi and endosomes. In the endocytic pathway, molecules are incorporated in vesicles derived from the plasma membrane and delivered to early endosomes and then to lysosomes via late endosomes. Retrieval pathways also operate wherein cargo is retrieved from endosomes and returned to either the plasma membrane for reuse or the Golgi and further to the ER [2]. Communication between the various compartments generally occurs through vesicles.

Steps in vesicular transport

Molecules can move between compartments by three

fundamentally different mechanisms: gated transport, transmembrane transport and vesicular transport. In vesicular transport, membrane-enclosed transport intermediates - which may be small spherical vesicles or larger, irregularly shaped organelle fragments - ferry molecules from one organelle to another. Typically, vesicles carry material as cargo from the lumen and membrane of one compartment (donor) from where they bud and pinch off. They discharge their cargo into a second compartment by fusing with the membrane enclosing that compartment (target). Vesicular transport mediates a continuous exchange of components between biochemically distinct membrane-bound compartments that collectively comprise the secretory and endocytic pathways. As represented in **figure 3** adapted from [3], the broad steps in vesicular transport involve vesicle budding, movement, tethering and fusion. These steps are strictly regulated to ensure that a vesicles generated from a donor compartment is delivered to its appropriate target compartment.

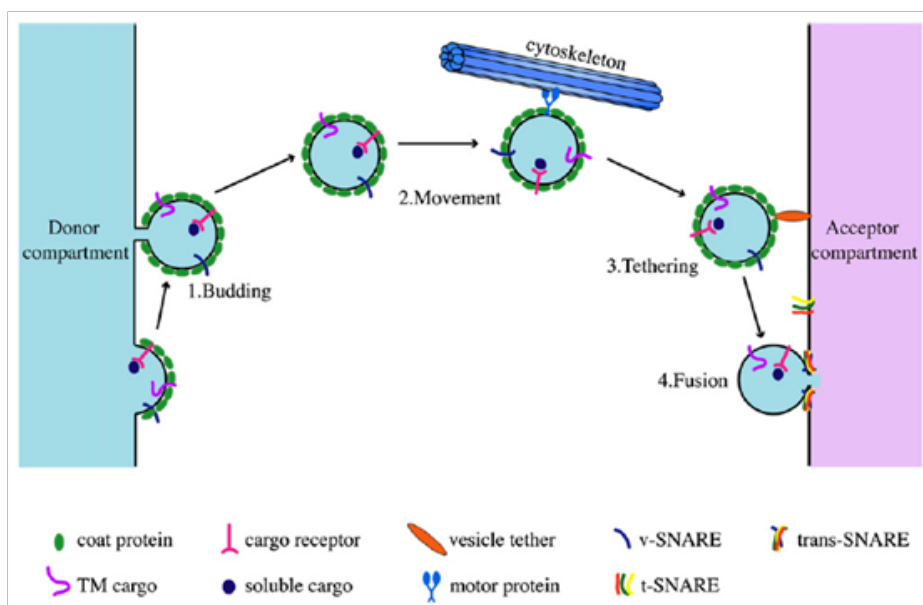


Figure 3: Steps in vesicle transport.

During budding, coat proteins are recruited from the cytosol to the site of an emerging bud. Coat proteins participate in cargo selection by recognizing and concentrating specific membrane proteins in a specialized patch on the donor membrane from which the vesicle membrane arises. Coat proteins assemble into a curved, basket-like lattice that deforms flat membranes and thereby shapes the vesicle. Clathrin, COPI and COPII are three well characterized coat proteins that distinguish transport vesicles operating in different pathways. For instance, clathrin-coated vesicles mediate transport from the plasma membrane and the trans-Golgi network. There is, however, much more diversity and complexity in coated vesicles and their functions than

suggested here. After budding, vesicles are transported to their destination by simple diffusion or with the aid of a cytoskeletal track. The initial interaction (bridging or linking) between a vesicle and its target membrane is referred to as tethering. This precedes the pairing of certain integral membrane proteins, termed as SNAREs, on apposed membranes destined to fuse. Tethers facilitate membrane recognition early in the fusion cascade and along with Rab proteins (small GTPases of the Ras superfamily), play a critical role in determining the specificity of vesicle targeting. Subsequently, the vesicle-associated SNARE (v-SNARE) and the target membrane associated-SNARE (t-SNARE) assemble into a four-helix bundle as a cognate set of

SNAREs. Thereafter, the membranes enclosing the two compartments fuse and their luminal contents mix leading to the delivery of cargo to the target compartment [3].

Fusion in the endomembrane system involves at least three conserved protein families whose members collaborate in compartment-specific combinations: Soluble *N*-ethylmaleimide-sensitive factor Attachment protein REceptors (SNAREs), tethering factors and Rab GTPases. Each pathway has its own set of cognate factors specifying the membrane fission and fusion events in that pathway. The distribution of these factors is important in the determination of fusion specificity. For example, an ER-derived vesicle has never been reported to fuse directly with the plasma membrane, since those compartments do not contain the cognate sets of interacting proteins. The impression until recently has been that SNAREs are the principal determinants of fusion specificity. However this concept has now been challenged. Ubiquitous distribution of SNAREs, promiscuous pairing of snares, a single SNARE participating in multiple transport pathways and hence in multiple membrane fusion events has suggested that the specificity of membrane fusion is unlikely to be solely due to the intrinsic specificity of SNARE pairing [4-6]. Analysis of a mixture of purified snares shows that both cognate and non-cognate SNARE complexes can form with no particular preference [7]. Therefore, other factors would be necessary for ensuring the fidelity of the fusion process. Most promising among these are tethers and Rabs that are capable of providing additional layers of regulation prior to or accompanying SNARE-mediated fusion.

In summary, inter-compartmental traffic involves budding out of a vesicle induced by coat proteins and carrying specifically sorted cargo from a donor compartment, transport of the vesicle to its destination guided by Rab GTPases, cytoskeletal elements, specific recognition of the correct fusion partner by tethering complexes as well as Rabs, and ultimately SNARE-mediated fusion with the target compartment. Complete specificity of membrane fusion is likely determined by a series of inter-related steps and components and not by a single factor. It is important to note that despite enormous diversity in the size and shape of organelles, the basic reactions of membrane fusion and fission are carried out by multiprotein complexes that consist of protein families that have been conserved throughout eukaryotic evolution.

Conserved protein families governing membrane fusion SNAREs

A convergence of independent research tracks in the 1980s and 1990s led to the identification of SNAREs. Beginning from the identification of SNAREs as components of the synapse [8-11], as targets of neurotoxins [12], as homologs of yeast *sec/vam* genes [4,13], as receptors of NSF adaptor proteins in brain detergent extracts [14], to the functional data from electrophysiological studies on mutants in *Drosophila melanogaster*, *Caenorhabditis elegans* and

Mus musculus [15-20], SNAREs are now regarded as the perpetrators of membrane fusion in vesicular trafficking.

Although cell-cell fusion and the fusion events of mitochondria and peroxisomes involve unrelated proteins, SNAREs are the central players that mediate membrane fusion in all of the trafficking steps of the secretory and endocytic pathways. According to the currently accepted mechanistic model, SNARE proteins that are localized in opposing membranes drive membrane fusion by harnessing the energy that is released during the thermodynamically favorable process of formation of a four-helix SNARE bundle [21]. The zippering of appropriate SNARE partners from opposing membranes into this bundle leads to a tight connection of the membranes and initiates the merger of their lipid bilayers. A central tenet of the zippering hypothesis of SNARE function is that for fusion to proceed, SNAREs must assemble in a trans configuration, with at least one SNARE that has a transmembrane domain being contributed by each of the fusing membranes. During trans-SNARE complex formation, nucleation begins at the N termini of the SNARE domains and then proceeds in a zipper-like fashion towards the C-terminal membrane anchors [22,23]. As a result, a mechanical pulling force is exerted on the membranes, which draws them in closer proximity and helps overcome the energy barrier for fusion. The recycling of SNAREs for subsequent cycles of fusion is achieved through the dissociation of the alpha helical SNARE bundle into separated SNAREs, which is mediated by the AAA+ protein NSF (*N*-ethylmaleimide-sensitive factor) [24]. As is the case for every other intermediate in the SNARE cycle, trans-SNARE complexes are subject to regulation by other proteins. More specifically, in chapter II, I will describe how a tethering complex and a Rab GTPase govern trans-SNARE complex establishment in yeast vacuolar fusion. Further in chapter III, I will elucidate how a dynamin-related protein unexpectedly influences trans-SNARE complex formation.

SNARE proteins form a superfamily of proteins with 25 members in *Saccharomyces cerevisiae*, 36 members in humans and 54 members in *Arabidopsis thaliana*. Generally speaking, each member in each organism is localized at a distinct subcellular compartment, as shown schematically in figure 4 adapted from [21]. SNAREs have a simple domain structure, and the most important feature of SNAREs is the SNARE domain - an evolutionarily conserved stretch of 60-70 amino acids that are arranged in heptad repeats. At their C-terminal ends, most SNAREs have a single transmembrane domain that is connected to the SNARE domain by a short linker [21]. Many SNAREs have independently folded domains that are positioned N-terminal to the SNARE domain and that vary between the subgroups of SNAREs. Although this prototypic structure applies to most SNAREs, there are important exceptions. A subset of SNAREs lacks the N-terminal domain. Another subset lacks transmembrane domain, but most of these SNAREs contain sites for hydrophobic post-translational modifications that mediate membrane attachment.

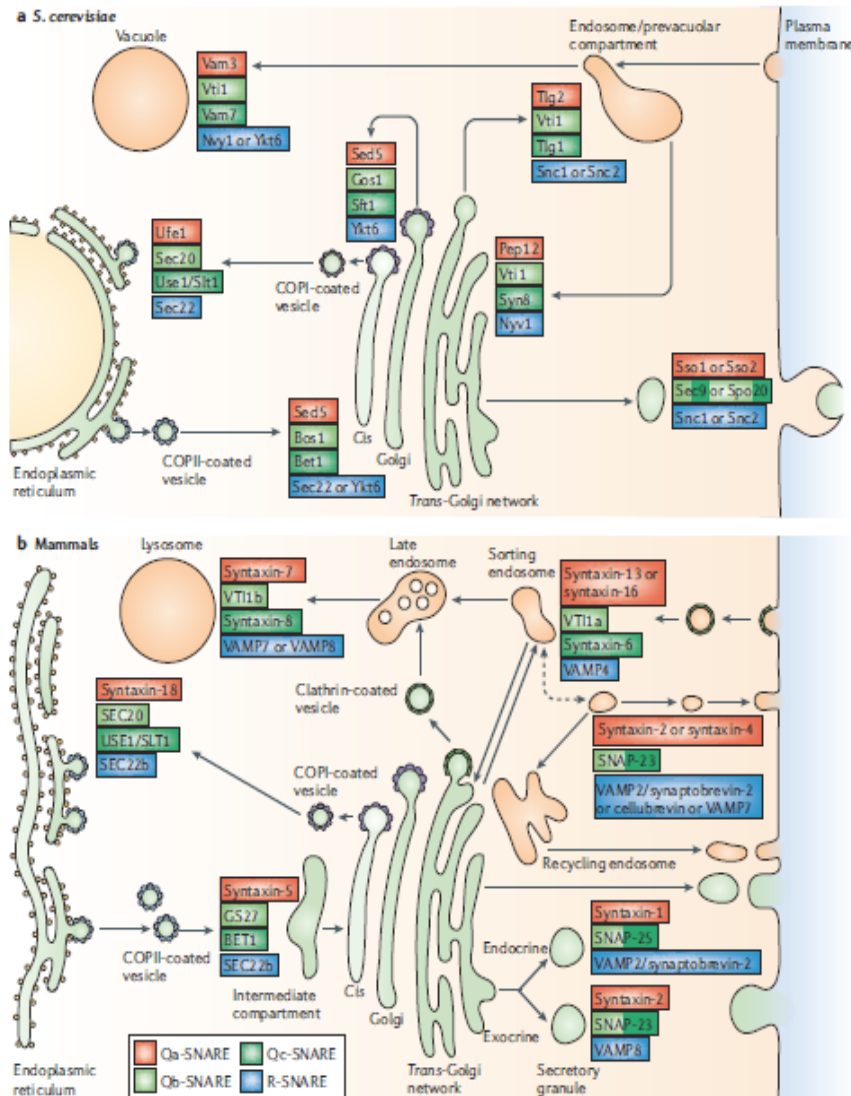


Figure 4: Assignment of SNAREs to intracellular membrane-trafficking pathways.

SNARE localization at each compartment within the eukaryotic endomembrane system has been characterized in yeast (top panel) as well as mammalian cells (bottom panel).

Originally, it was thought that there was a strict division between SNAREs on the ‘donor’ compartment and the ‘acceptor’ compartment, which led to their functional classification as v-SNAREs (vesicle membrane SNAREs) or t-SNAREs (target-membrane SNAREs). This could explain the fusion occurring between dissimilar membrane compartments present in a heterotypic orientation, for example between late endosomes and lysosomes, or between ER-derived COPII vesicles and the cis-Golgi compartment. However, this terminology is not useful in describing homotypic fusion events where both fusion partners are identical, and for certain SNAREs that function

in several transport steps with varying partners. For example, vacuole-vacuole fusion in budding yeast is of homotypic architecture. Similarly, fusion of early endosomes and ER membranes is homotypic. Also, the *S. cerevisiae* SNARE Sec22 functions in both anterograde and retrograde traffic between the ER and the Golgi apparatus. In its anterograde transport, Sec22 is colocalized with the SNAREs Bos1 and Bet1 on COPII vesicles, but only Bet1 was classified as a v-SNARE, whereas Bos1 and Sec22 were classified as t-SNAREs [25]. In its retrograde transport, Sec22 was described as the only functional SNARE on COPI vesicles [26].

A more rigorous and invariant classification is derived from understanding the components of SNARE complexes. Complex formation is mediated by the SNARE domains, and is associated with conformational and energy changes.

When SNARE proteins are monomeric, their SNARE domains are unstructured. However, when appropriate sets of SNAREs combine, their SNARE domains spontaneously associate to form alpha helical core complexes of extraordinary stability [26]. The crystal structures of different SNARE core complexes have revealed a remarkable degree of conservation. Core complexes are composed of elongated coiled coils of four intertwined, parallel alpha helices, with each helix being contributed by a different SNARE domain. The centre of the bundle contains 16 stacked layers of interacting amino acid side chains. Each layer has 4 residues, 1 from each SNARE domain. These layers are largely hydrophobic, except for the central or zero layer that contains three highly conserved glutamine (Q) residues and one highly conserved arginine (R) residue. Accordingly, the contributing SNARE domains are classified into Qa, Qb, Qc and R-SNAREs [28]. Functional SNARE complexes that drive membrane fusion are hetero-oligomeric, parallel four-helix bundles. Each such bundle must contain one of each of the Qa, Qb, Qc and R-SNAREs forming a classical QabcR SNARE complex.

Tethering complexes: The concept of tethering emerged from observations indicating that SNARE proteins alone cannot entirely account for the specificity and efficiency of vesicle fusion. The original idea of tethering involved linking molecules that extended over distances of more than about half the diameter of a vesicle from a given membrane surface (>25 nm) to specifically bridge vesicles to their target membrane [29]. However, since the discovery of factors that can extend only 5 nm from the surface and still act as tethers [30], tethering is now considered a regulatory event after coat protein-mediated vesicle scission and before SNARE-mediated docking and membrane fusion which is required for proper vesicle recruitment to the respective target membrane. Tethering complexes are a heterogeneous family of proteins involved in regulating multiple steps in the emergence, journey and consumption of any membrane-bound vesicle. Their best studied role which gives them their name is to facilitate the bridging and recognition of membranes early in the fusion cascade, i.e. prior to or accompanying trans-SNARE complex formation. Tethers form two broad classes: elongated coiled-coil tethers and multisubunit tethering complexes.

Coiled-coil tethers are generally known to form stable homodimers and associate with the membrane either directly or via anchor proteins including activated or GTP-bound Rabs or other coiled-coil proteins. For example, among the best characterized coiled-coil tethers is yeast Uso1 and its mammalian homolog, the golgin p115 operating within the Golgi apparatus [31]. The architecture of p115 comprises a C-terminal acidic region, the central coiled-coil core and a large globular N-terminal domain. The central region mediates homodimerization and also binds to the active GTP-bound form of Rab1. Rab1 is thus the membrane receptor for p115, and this interaction is thought to tether COP II vesicles to each other, thus promoting homotypic vesicle fusion [32]. The C-terminal region of p115 binds to

GM130 and giantin, two further Golgi-localized coiled-coil tethers. This interaction in turn enhances Rab1 binding and establishes a link to the cis-Golgi network [33]. Interestingly, p115 also interacts with the v-SNARE Gos28 and the t-SNARE Syntaxin-5, which recruits p115 to COP II vesicles [34]. This interaction scheme represents an intersection between Rab, tethering and fusion machineries.

Eight different multisubunit tethers have been characterized in yeast operating in different trafficking steps, and many of their mammalian homologs have also been identified. Biochemical and structural analyses have revealed that these multisubunit tethering complexes are quite diverse in their functions, molecular interactions and structure [35]. The eight complexes can be divided into two groups: those that have a common domain at the N-terminus of at least some, if not all, of their subunits, and those that do not. The family of complexes related to each other by virtue of their shared domain, or the 'quatrefoil' complexes, consists of: (i) the exocyst, located at the plasma membrane at sites of active secretion (termed the Sec6/8 complex in mammalian studies), (ii) the conserved oligomeric Golgi [COG] complex required for retrograde transport through the Golgi and interacting with SNAREs and COPI vesicles (previously known as the Sec34/35 complex, and in mammals also as the Golgi transport complex [GTC]) and (iii) the Golgi-associated retrograde protein [GARP] complex (which is also known in yeast as the Vps52/53/54 or VFT complex) involved in recycling of proteins from the endosome to trans-Golgi. The other group consists of complexes that seem to bear no relation to each other or to the quatrefoil complexes and comprises: (i) two isoforms of TRAPP (Transport Protein Particle, TRAPPI operating at cis-Golgi to recruit ER-derived vesicles and TRAPPII functioning at trans-Golgi receiving endosomal traffic), (ii) two related Class C Vps complexes (including the homotypic fusion and vacuole protein sorting [HOPS] complex required for proper sorting of proteins to the vacuole, and the class C core vacuole/endosome tethering [CORVET] complex located at endosomes) and (iii) the Dsl1 (Dependence on SLY1) complex implicated in Golgi to ER transport. The modular structure of multisubunit tethers can combine multiple functions within the same complex and hence achieve coupling of processes more efficiently. Due to their structural disposition and affinities for coat proteins, adaptors, small GTPases, lipids and SNAREs, multisubunit tethers are poised to link the recognition of membranes (via coats/ GTPases/ lipids) with subsequent fusion (via SNAREs).

Rab GTPases: The Rab family of proteins is a subdivision of the Ras superfamily of monomeric G proteins. Approximately 70 different Rabs have now been identified in humans. Complete sequencing of the yeast genome has revealed the existence of 11 Rab proteins, referred to as Ypt products (Yeast protein two), with some redundancy in their function [36]. Like Ras proteins, Rabs have an average length of 200–230 amino acids and a similar spacing within the first 150–160 residues of the conserved sequence regions G1

- G5 that are collectively involved in Guanine nucleoside phosphate binding and hydrolysis. Structurally, Rabs belong to the P-loop containing nucleoside triphosphate hydrolase family [37].

Rab proteins are peripheral membrane proteins, anchored to a membrane via a lipid moiety covalently linked to an amino acid. Specifically, Rabs insert into membrane leaflets via prenyl groups harbored on two cysteines at their C-terminus [38]. Rab escort proteins (REPs) deliver the newly synthesized and prenylated Rab to its destination membrane by binding the hydrophobic, insoluble prenyl groups and carrying the Rab through the cytoplasm. The lipid prenyl groups can then insert into the membrane, anchoring Rab at the cytoplasmic face of a vesicle, organelle or the plasma membrane.

Like other GTPases, Rabs switch between two conformations, an inactive, cytosolic form bound to GDP (guanosine diphosphate), and an active, membrane-anchored form bound to GTP (guanosine triphosphate). A Guanine nucleotide exchange factor (GEF) catalyzes the conversion from GDP-bound to GTP-bound form, thereby activating the Rab. The inherent GTP hydrolysis of Rabs can be enhanced by a GTPase-activating protein (GAP) leading to Rab inactivation [39]. REPs carry only the GDP-bound form of Rab, and Rab effectors, proteins with which the Rab physically interacts and through which it functions, only bind the GTP-bound form of Rab. Rab effectors are very heterogeneous, and each Rab isoform has a multitude of effectors through which it perpetuates multiple functions.

After membrane fusion, Rab is recycled back to its membrane of origin. A GDP dissociation inhibitor (GDI) binds the prenyl groups of the inactive, GDP-bound form of Rab, inhibits the exchange of GDP for GTP (which would reactivate the Rab) and delivers Rab to its original membrane. Partitioning of the prenylated tail moiety between the hydrophobic pocket in GDI and the membrane bilayer allows Rabs to rapidly and reversibly sample membrane surfaces. Nucleotide exchange occurs when the GDP-bound inactive Rab encounters a cognate GEF. This GTP-bound active Rab species does not interact with GDI and can therefore accumulate on the membrane surface, where it may further recruit effector proteins with specific biological functions. This cycle is reset when a GTP-bound Rab encounters a GAP (GTPase-activating protein) and the bound GTP is hydrolyzed to generate GDP and inorganic phosphate [40]. The concomitant action of GAPs and GEFs, determined by the actions of their associated Rab, labels the boundaries of each membrane compartment. Emerging evidence indicates that Rab activation and inactivation are under complex feedback control. Such a mechanism can promote the rapid membrane accumulation and removal of Rabs to create spatiotemporally restricted membrane domains with a unique composition, and can explain how Rabs define the identity of vesicle and organelle membranes.

Rabs form another family of conserved proteins that regulate virtually all steps of membrane traffic from the

formation of the transport vesicle at the donor membrane to its fusion at the target membrane. Some of the many regulatory functions performed by Rabs include interacting with diverse effector proteins that may select cargo before vesicle scission, aid in vesicle uncoating after budding or tether membranes prior to fusion. Rabs are also implicated in promoting vesicle movement and verifying the correct site of fusion. Rabs organize distinct protein scaffolds within a single organelle and act in a combinatorial manner with their effectors to regulate all stages of membrane traffic. Figure 5 adapted from [41] presents an overview of multisubunit tethering complexes with their corresponding Rabs operating in the various trafficking pathways.

MTCs are indicated in orange (secretory pathway) and brown (endolysosomal circuit). Associated Rabs are indicated in yellow (using the yeast nomenclature). (ER, endoplasmic reticulum; EE, early endosome; MVB/LE, multivesicular body/late endosome; CPY, carboxypeptidase Y, a cargo of the biosynthetic pathway to the vacuole; AP-3, adaptor protein complex 3.)

Conserved protein families controlling membrane fission

Dynamin superfamily: Like SNAREs are universal fusion molecules mediating lipid bilayer fusion, dynamins are universal lipid bilayer stretching/tubulating/scission molecules that have been adapted to function at many different compartments in various cell types. Dynamins are large GTPases that encompass a protein family of classical dynamins, dynamin-like proteins, Mx proteins, mitofusins and atlascins. Historically, they have been known to function in membrane-remodeling processes associated with endocytic membrane fission, budding of transport vesicles from a donor membrane and fragmentation of organelles. Information about dynamin from genomic sequences and phenotypic studies on many organisms as well as crystal structures has been helpful in proposing a common mechanism of dynamin-driven membrane tubulation.

As depicted in figure 6 modified from [42], classical dynamin is a cytosolic protein typically comprising an N-terminal GTPase domain, a middle or stalk region, a pleckstrin homology (PH) domain, a GTPase Effector/Assembly Domain (GED) so called because of its involvement in dynamin self-assembly thereby interacting with the GTPase domain, and a C-terminal proline-rich domain (PRD). The GTPase domain sits on top of a helical bundle, called the bundle signaling element (BSE) or neck, which is formed by three helices contributed by the N and C-terminal regions of the GTPase domain and by the C-terminal region of the GED. This region of the GED lies in close physical proximity with and is functionally linked to the GTPase domain. The BSE is followed by a stalk composed of helices from the middle domain and N-terminal region of the GED. The PH domain forms the vertex or foot of the stalk and is involved in membrane binding. The PH domain binds acidic phospholipids at the cytosolic leaflets of membranes and PI(4,5)P₂ in particular via a positively charged surface. The

Chapter 1

PRD, expected to be projecting away from the membrane, emerges at the boundary between the BSE and GTPase domain and is likely to interact with other proteins. The PRD contains an array of PxxP motifs that interact with

many SH3 (Src homology 3) domain containing proteins to localize dynamin at endocytic sites and coordinate dynamin's function with other factors.

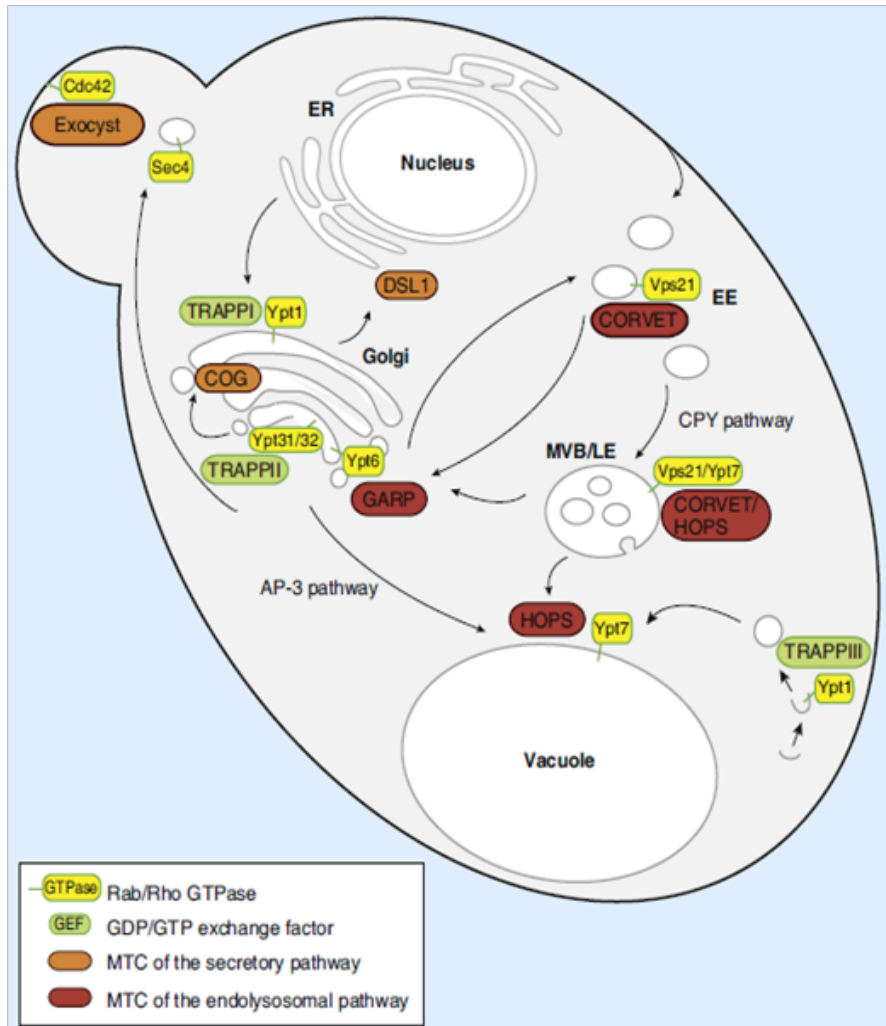


Figure 5: Multisubunit tethering complexes (MTCs) with their corresponding Rab GTPases.

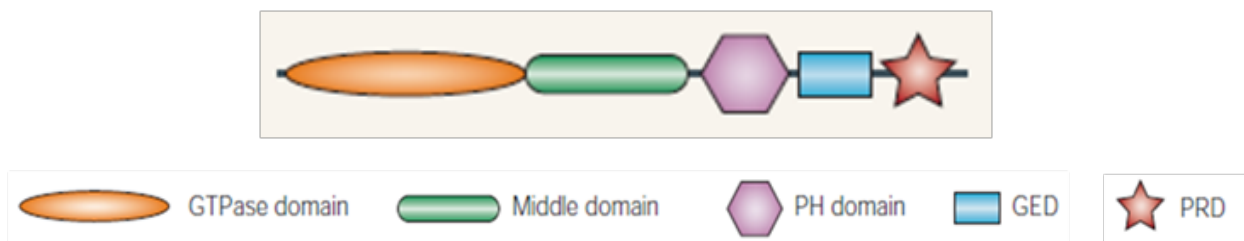


Figure 6: Domain organization of classical dynamin.

Self-oligomerization and GTP hydrolysis are important properties of dynamins that execute its well documented membrane fission function. An oligomer normally refers to a complex of more than one monomer, but as the basic building block of native dynamin is a dimer or a tetramer,

oligomerization here can be considered as the ordered assembly of these building blocks into rings or helices. Regarding the mechanism by which dynamin catalyzes membrane fission, it has been proposed that assembly of dynamin into spirals or helical oligomers around the

neck of emerging vesicles promotes the demonomization of GTPase domains of adjacent helical rungs, leading to GTP hydrolysis. This triggers a conformational change in the dynamin polymer, allowing the constriction of the dynamin ring. This further drives the constriction of the underlying membrane, increasing membrane curvature. This reduces the energy barrier to fission, subsequently triggering fission at the boundary between the dynamin ring and the bare membrane. It is believed that once a critical mass of oligomers is reached, the resulting cooperative GTP hydrolysis leads to helix disassembly and ultimately to dynamin depolymerization. Thereafter membrane fission is discontinued. This model [43] describes dynamin as a mechanochemical enzyme wherein GTP hydrolysis is necessary for vesicle scission and the GED contributes to the catalytic activity indirectly through oligomerization.

Purified dynamin spontaneously polymerizes into rings and helices when incubated in low ionic strength solutions or in the presence of synthetic membranes [44]. It can also tubulate membrane bilayers under appropriate conditions by forming a continuous coat around them [45-47]. The tetrameric form of dynamin, which can be abundant in solution, may represent an intermediate in its higher order assembly [48]. This oligomerization capacity of dynamin has been widely exploited in assembly tests for other members of the dynamin family.

The crystal structures of a range of dynamin family members, with or without bound nucleotide, and in different

oligomeric states, have recently been solved. These have been critical in understanding how dynamins harness self-assembly and GTP-dependent conformational changes along with other protein interaction modes to remodel membranes. The crystal structure of the endocytic DRP, mammalian dynamin1 [49], lacking the proline-rich domain, in its nucleotide-free state depicts the dynamin1 monomer as an extended structure with the GTPase domain and bundle signaling element positioned on top of a long helical stalk composed of the GED, with the pleckstrin homology domain flexibly attached on its opposing end. Dynamin1 dimer and higher order dimer multimers were predicted to form via at least three different interfaces located in the stalk, as shown in figure 7A [49]. The sequence space covering these oligomerization interfaces has been remarkably conserved from yeast to humans across various dynamin family members. The dynamin1 crystal lattice contains linear filaments assembled via three stalk interfaces resulting in layers of interacting stalks separated by GTPase and PH domains. Interface 2, detailed in figure 7B [49], is the largest, has two-fold symmetry and is relatively rigid. Each dynamin1 protomer in a tetramer participating at interface 2 contributes seven direct hydrogen bonds and eight hydrophobic residues. Interfaces 1 and 3 are also stalk-localized and mediate higher order assembly of dynamin1 dimers. Interface 1 is at the tips of interacting stalks, proximal to the GTPase domain and BSE. Interface 3 is at the distal end of the stalk.

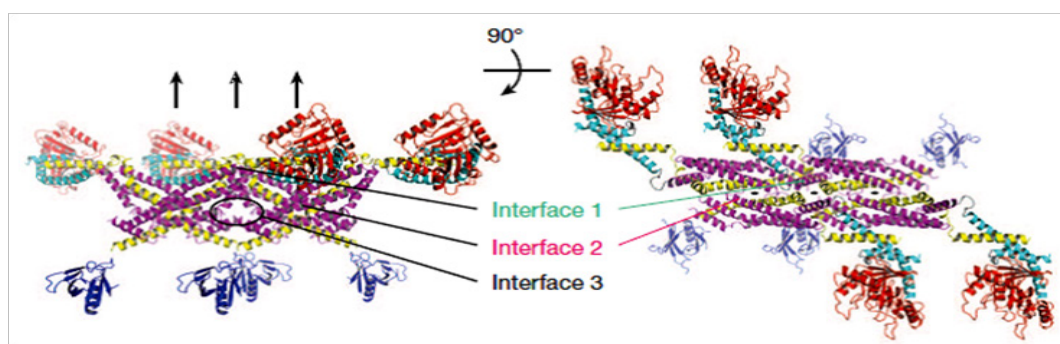


Figure 7A: Image of four dynamin1 monomers showing interfaces 1, 2 and 3 in the crystal lattice.

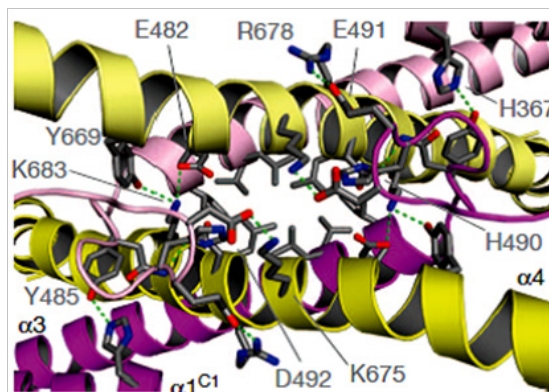


Figure 7B: Details of interface 2: Protomers are shown in different colors. Green dotted lines denote hydrogen bonds. Residues K683 and Y669, among others, are well conserved from yeast to mammals.

Coat proteins and adaptors: Although dynamin alone can constrict and cut lipid tubules, the constriction of the dynamin ring *in vivo* is likely to be assisted or regulated by other factors to achieve fission. Dynamin may contribute to membrane fission in a variety of subcellular contexts, but its action is best understood in the context of clathrin-mediated vesicle scission. Clathrin is a coat protein that performs critical roles in shaping rounded vesicles budding out from patches in the plasma membrane, trans-Golgi network, and endosomal compartments and targeted to multiple membrane trafficking pathways. It forms a triskelion shape composed of three heavy chains and three light chains. When the clathrin triskelia interact they form a polyhedral lattice that surrounds the emerging vesicle like a basket. After a vesicle buds into the cytoplasm, the coat disassembles, allowing the clathrin to recycle while the vesicle gets transported to its destination. Adaptor molecules are responsible for the recruitment and self-assembly of clathrin at sites of vesicle formation. For instance, during formation of endocytic buds at the plasma membrane, a subset of scaffold proteins (such as FCHO1, Eps15 and intersectin) [50] and clathrin adaptors (for example the AP-2 complex, AP180/CALM and epsin) are first recruited to the PI(4,5)P₂-rich plasma membrane, coincident with the binding of some of these proteins to endocytic sorting motifs of integral membrane proteins [51]. Such components cluster cargo and induce membrane curvature. The coat subsequently grows through the assembly of the clathrin lattice, which, through positive feedback, recruits additional cargo adaptors and endocytic factors. Dynamin eventually accumulates around the growing clathrin-coated pit. Deep invagination of the bud and formation of a narrow neck involves the recruitment of BAR (Bin-Amphiphysin-Rvs) domain-containing proteins, several of which bind dynamin [52,53]. Dynamin is then rapidly and efficiently able to accomplish membrane fission.

Yeast vacuoles as a model system to study membrane fusion-fission dynamics

Every intracellular transport pathway culminates with membrane fusion. This fusion process relies on the collaborative action of SNAREs, tethers and Rabs. Powerful *in vitro* fusion systems using isolated organelles were pivotal in obtaining mechanistic insights into the process of membrane fusion having apparently complex interdependencies among components involved in successive stages - from the initiation of fusion to luminal content mixing. Among these, yeast vacuoles serve as an elegant model system, particularly useful as they are biochemically and genetically highly accessible and tunable. Yeast vacuoles are easy to purify in satisfactory amounts. There are established rapid quantitative assays to measure fusion of vacuoles, fluorescent tools to trace them, and available agents to induce or inhibit their fusion or fission *in vitro* and *in vivo*.

The yeast vacuole, which resembles the lysosome of higher eukaryotes, is positioned at a crucial point of the eukaryotic endomembrane system, i.e., at the intersection of the two

major trafficking pathways in the cell - the endocytic and the secretory pathways - which deliver cargo to the vacuole/lysosome. Several screens in yeast have been designed to identify mutants defective in endocytosis (End), vacuolar protein sorting (Vps), vacuolar protease activity (Pep), vacuole inheritance (Vac), and vacuole morphology (Vam) [54]. Not surprisingly, since multiple pathways feed into the vacuole, in many yeast mutants identified, vacuolar proteins were found to be missorted or incompletely processed, and/or vacuolar morphology strongly perturbed. Subsequent characterization of these genes unraveled the underlying machinery of a number of trafficking pathways that are critical for vacuole biogenesis and vacuole fusion. Additional biochemical investigation of protein transport in numerous experimental systems has identified several proteins proposed to be involved in the fusion of transport vesicles with their target membranes. These proteins have been found to be highly homologous among the various systems, suggesting that the fusion of transport vesicles utilizes a conserved mechanism.

Trafficking pathways to/from the vacuole, outlined in figure 8 adapted from [55], have been named according to the most prominent cargo they shuttle. The vacuolar enzyme carboxypeptidase Y (CPY) travels from the trans-Golgi-Network (TGN) to the late endosome, from where it is subsequently delivered to the vacuole [56]. At the TGN, it is recognized by the receptor protein Vps10, concentrated and packed into vesicles that pinch off from the TGN in an AP-1 (Adaptor Protein-1)/ clathrin-dependent manner. After fusion with the late endosomal compartment, CPY dissociates from its receptor and is then transported to the vacuole upon endosomal maturation. Vps10 is subsequently recycled back to the TGN with the help of the retromer complex. Various other hydrolases have additionally been shown to interact with Vps10 and therefore follow the same route to the vacuole. Consequently, this generic pathway has been termed the CPY pathway. However, a small subgroup of vacuolar resident proteins, namely the *pho8* gene product alkaline phosphatase (ALP), the SNAREs Vam3 and Nvy1 and the vacuolar casein kinase Yck3, travel to the vacuole in a more direct Golgi-to-vacuole trafficking event omitting the endosome [57-60]. This pathway is termed the ALP or AP-3-pathway after the adaptor complex which is involved in the generation of vesicles at the TGN in a clathrin-independent fashion. The SNARE Vti1 plays a role in *cis*-Golgi membrane traffic which is essential for yeast viability, and a nonessential role in the fusion of Golgi-derived vesicles with the prevacuolar/late endosomal compartment via the CPY pathway [61]. The SNARE Vam7 has been shown to regulate a late step in protein trafficking to the vacuole, also likely via the CPY pathway [54]. Additional pathways are linked to the vacuole. The cytoplasm to vacuole targeting (Cvt) pathway and the macroautophagy pathway use a similar set of components to transport proteins to the vacuole [62]. Whereas the Cvt pathway is a biosynthetic route to direct aminopeptidase I (Ape1) to the vacuole lumen, macroautophagy is a catabolic pathway, which plays a crucial role in cell survival upon

starvation. In both cases, a double membrane of unknown origin engulfs oligomeric Ape1 (Cvt pathway) or organelles

and cytosolic material (macroautophagy) and targets them directly to the yeast vacuole.

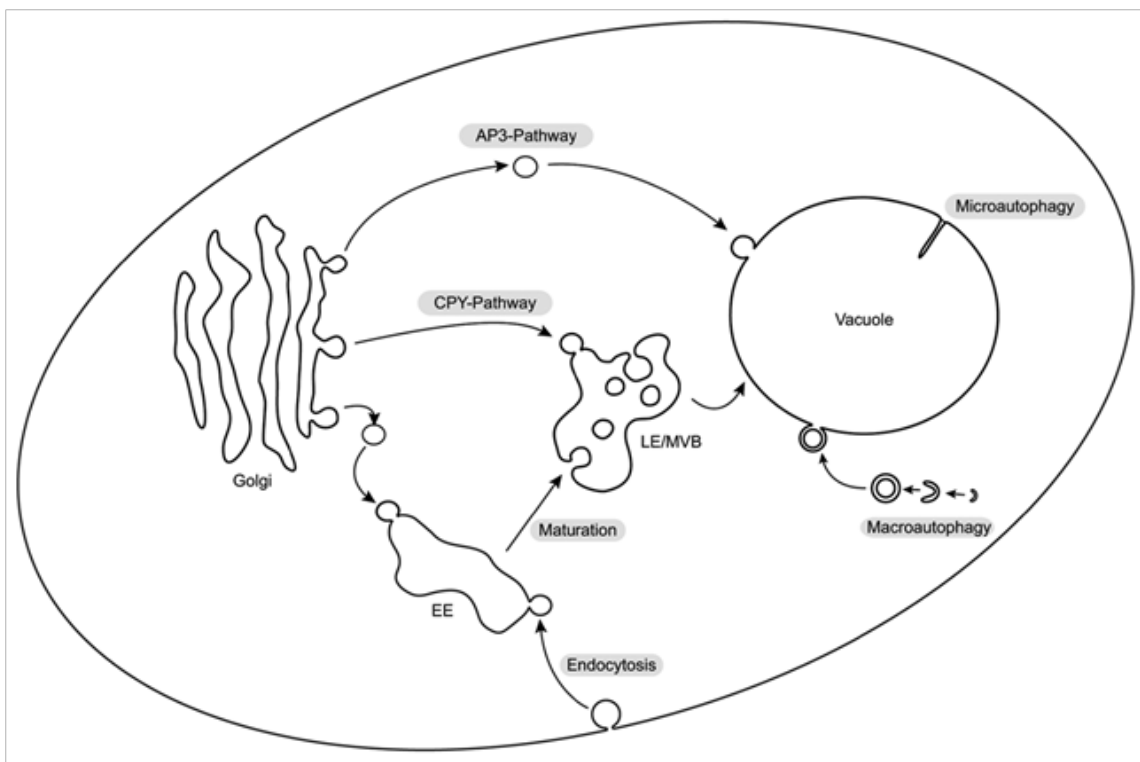


Figure 8: Trafficking pathways leading to the yeast vacuole. (EE, early endosome; LE, late endosome; MVB, multivesicular body.)

The *in vitro* vacuole fusion assay, devised as a rapid colorimetric tool to measure content mixing, exploits the fact that vacuolar hydrolases are synthesized as catalytically inactive proenzymes in the endoplasmic reticulum and are activated only on arriving at the vacuole, through proteolytic cleavage by vacuolar luminal proteases [63,64]. The principle of this assay is explained in figure 9. The unprocessed precursor form of the vacuolar membrane protein alkaline phosphatase (pho8 gene product, pro-ALP) is C-terminally cleaved by proteinase A (pep4 gene product), a vacuolar protease to yield mature, active ALP. One of the yeast strains employed in this assay (called DKY) expresses the vacuolar proteases but lacks alkaline phosphatase (Δ pho8). The other strain (called BJ) lacks the vacuolar protease (Δ pep4) and thus has the pro-ALP form. Hence neither strain is able to express mature ALP by itself. Maturation of pro-ALP can occur only by luminal content mixing upon fusion of the two vacuole populations. Level of ALP activity is a measure of pro-ALP maturation and hence reflects the extent of fusion. Acquisition of ALP activity is quantified spectrophotometrically by using the substrate para-nitrophenyl phosphate (PNPP) after detergent lysis of fused vacuoles. PNPP turns yellow on being converted into PNP in the presence of mature active ALP. Absorbance is recorded at 400 nm.

The intracellular compartments of eukaryotic cells are largely defined by the composition of the resident proteins contained therein. Thus, efficient biosynthetic trafficking of these resident proteins must be maintained to ensure the integrity and functionality of individual organelles. The acidified vacuole of the budding yeast *Saccharomyces cerevisiae* is one such organelle. Analogous to the lysosome of mammalian cells, the vacuole is a dynamic organelle that functions in a variety of cellular processes including macromolecular degradation, metabolite storage, and cytosolic ion and pH homeostasis [65]. Thus, vacuolar function requires an influx of resident proteins such as hydrolytic proteases, lipases, and transporters. These proteins traffic via vesicle-mediated transport reactions that require appropriate cargo selection and vesicle budding from donor membranes, followed by the docking and fusion of the transport intermediates with the correct target organelle. Homotypic (self) fusion of yeast vacuoles, which is essential for the low copy number of this organelle, uses elements similar to those occurring in heterotypic vesicular trafficking reactions between different organelles throughout the endomembrane system. Studies on homotypic vacuole fusion have helped in chalking out a model of membrane fusion in which SNAREs can form stable complexes in *cis* (when on the same membrane) as well as in *trans* (when

Chapter 1

anchored to opposing membranes). Chaperones (NSF/yeast Sec 18, and α -SNAP/yeast Sec17) disassemble cis-SNARE complexes to prepare for the docking of organelles. The specificity of organelle docking is considered to reside

in a cascade of trans-interactions involving Rab GTPases, tethering factors and trans-SNARE pairing. Fusion itself, i.e. the mixing of both the membrane leaflets and the organelle contents, is further triggered by various factors.

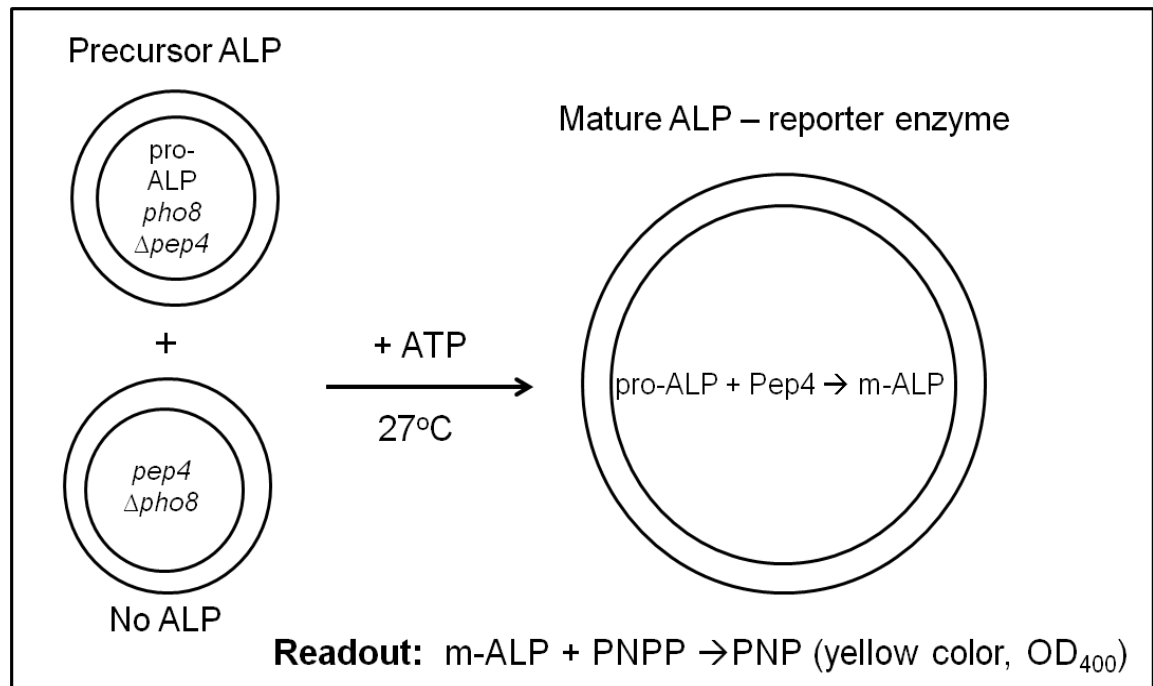


Figure 9: Principle of the *in vitro* vacuole fusion or content mixing assay.

As broadly outlined in figure 10 adapted from [55], a typical vacuole fusion reaction can be subdivided into multiple

stages involving priming, tethering, docking and hemifusion leading to luminal content mixing [21,55,66].

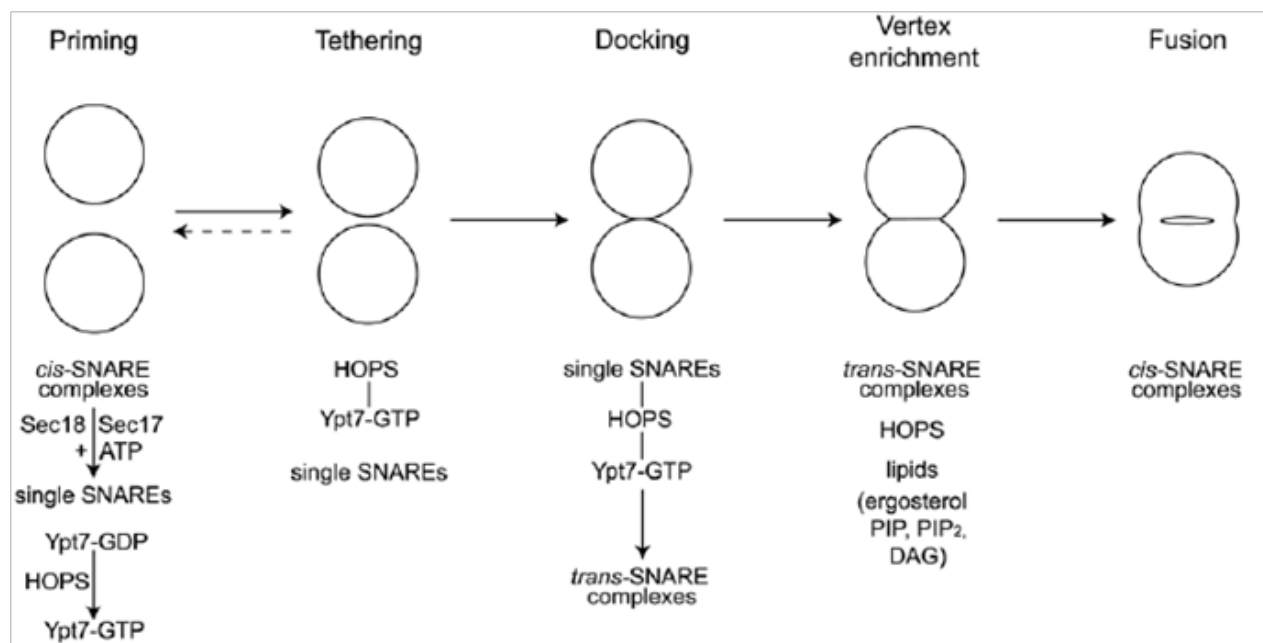


Figure 10: Stages of *in vitro* vacuole fusion.

Priming: The cis-SNARE complex is disassembled and reorganized into SNARE subcomplexes via ATP hydrolysis by the ATPase N-ethylmaleimide-Sensitive Factor (NSF/yeast Sec18) and its adaptor α-Soluble N-ethylmaleimide-sensitive factor Attachment Protein (α-SNAP/yeast Sec17) [24]. After the dissociation of the tetrameric cis-SNARE complex, new, complementary sets of SNAREs compatible and “primed” (or ready/available) for trans-interactions, are formed on the opposing membranes. Priming can be monitored biochemically by the stable persistence of specific SNAREs on the vacuolar membrane upon treatment with ATP, or by the sensitivity of the fusion reaction to antibodies against Sec18 or Sec17. The main reactions involving Ypt7, HOPS and SNAREs are indicated below the cartoon.

Tethering: It is the initial reversible (sensitive to dilution) interaction between membranes through protein complexes that act as linkers. Tethering may occur prior to or alongside trans-SNARE pairing. The tethering complex operating during yeast vacuolar fusion is termed HOMotypic fusion and vacuole Protein Sorting or HOPS. The unique Rab GTPase that marks the vacuolar compartment is Ypt7. Tethering during homotypic yeast vacuole fusion is thought to be mediated by Ypt7 and its effector, the HOPS complex, however this mechanism remains to be detailed.

Docking: It is the subsequent tighter, productive association of tethered vacuoles rendered irreversible through the establishment of trans-SNARE complexes. A trans-SNARE complex is composed of a parallel four-helix bundle with each α-helix being contributed by one SNARE. Formation of a stable coiled-coil trans-SNARE bundle releases sufficient energy to cause localized destabilization of the lipid bilayer and drive the formation of a fusion pore. Docking can be defined morphologically by the observation of ATP-dependent vacuole clusters or biochemically as the acquisition of resistance to (i) dilution of the fusion reaction and (ii) disassembly of the SNARE complex by Sec18/Sec17.

Hemifusion: This stage is also referred to as lipid mixing in which only the outer leaflets of opposed lipid bilayers merge but the inner leaflets remain separated. This hemifusion stage is followed by opening and enlargement of the fusion pore allowing content mixing leading to completion of fusion. This is a relatively little explored phase in the fusion cascade since only few quantitative assays to measure lipid mixing between physiological membranes are available.

Fusion: Fusion per se may be the least understood step of this *in vitro* reaction. Steps between docking and the completion of fusion have been proposed to require multiple components including the vacuolar V-ATPase (proton pump), calcium signaling through Calmodulin and Protein phosphatase I.

On the contrary, during cell division the vacuole of budding yeast fragments partially, producing vesicular and tubular structures, which are transported into the emerging bud. In order to control the overall shape of the vacuolar organelle, inherited vacuole-derived vesicles fuse later in

the bud, maintaining a low copy number for this organelle. Vacuole fragmentation and fusion are also connected to osmoregulation, and to the synthesis and turnover of phosphoinositides. Several molecules that seem to support the various stages of vacuolar fusion and fission are still being defined. It will be interesting to investigate whether there is any known component that is able to serve as a master regulator achieving fusion-fission control. Drawing from recent endocytosis studies in yeast [67] and exocytosis studies in insulin secreting beta-cells and neurons [68] [69], as well as studies on fusion-fission equilibrium [70], the yeast dynamin homolog Vps1, principally implicated in vacuole fission, appears to be one such unexpected candidate that might be playing a role in vacuolar fusion.

Components of yeast vacuolar membrane fusion and their known interactions

Table 1 framed from [66] and [71] below enlists the different factors implicated in yeast vacuolar fusion. The t-SNAREs of one membrane can bind to v-SNAREs on a fusion partner. This has been proposed to provide at least part of the targeting specificity during trafficking, as well as the binding affinity during membrane docking, and even to contribute to organelle identity. The t-SNARE Vam3, the soluble SNARE Vam7 and the v-SNAREs Nyv1 and Vti1 are each present in the vacuolar cis-SNARE complex and are each needed for normal rates of fusion, normal rates of protein delivery to the vacuole and for normal vacuole size. After priming, they are transposed to a trans-SNARE complex, of identical composition but different topological arrangement. Trans-SNARE pairing can be assayed by priming a mixture of vacuoles harboring differentially tagged SNAREs, for example, Vam3-HA (with untagged Nyv1) and Nyv1-VSV (with untagged Vam3) and measuring SNARE pairs by immunoprecipitation. Trans-SNARE pairing, which renders docking irreversible, depends on the prior action of Ypt7 and HOPS. It is not clear whether these proteins participate directly with the SNAREs on each vacuole to promote pairing in trans or act merely by supporting tethering.

The homotypic fusion and vacuole protein sorting (HOPS) complex is a six-subunit complex that acts during the docking stage of yeast vacuole fusion. The HOPS complex is also termed the Class C vacuolar protein sorting (Vps) complex because it is composed of Vps proteins, which are encoded by genes required for proper protein sorting to the yeast vacuole. HOPS complex subunits are also involved in transport between endocytic compartments, as well as transport to the vacuole. The HOPS complex contains six subunits: Vps11, Vps16, Vps18, Vps33, Vps39 and Vps41. Vps 39 and Vps41 are accessory vacuole-specific subunits while the rest are core subunits. A pull-down of any one vacuolar HOPS subunit will pull down the entire complex [72]. HOPS has multiple membrane binding modes and has no known transmembrane domain. It has known affinities for the GTP-bound form of the Rab7 homolog Ypt7, phosphoinositides and the SNAREs Vam7 and Vam3 [73-77]. It is therefore engaged in highly dynamic protein-protein

Chapter 1

interactions during fusion. Individual subunits of HOPS exhibit domain architecture designed to mediate protein-protein interactions, and in particular signify oligomerization potential. Structural features of the HOPS subunits are summarized in figure 11 modified from [78]. Each HOPS subunit has a predicted N-terminal β -propeller followed by a C-terminal α -solenoid. Around 200 residues of sequence

homology to the clathrin heavy chain was detected in the C-terminal regions of Vps11, Vps18, Vps39, and Vps41. Vps11 and Vps18 have C-terminal RING (really interesting new gene) domains and Vps39 has a partial RING domain, although this region lacks residues that would coordinate a second Zn⁺⁺ ion.

Table 1: A glance at factors involved in yeast vacuolar fusion.

Factor	Protein Family	Role in Vacuolar Membrane Fusion/ Interactions with Other Components
Vam3	Qa SNARE, Syntaxin homolog, originally classified as a vacuolar t-SNARE	Forms a complex (cis and trans) with the other SNAREs Nyv1, Vam7, Vti1; interacts with Vps33, an Sec1/Munc18 (SM) family member to direct the docking of multiple transport intermediates with the vacuole
Nyv1	R SNARE, Synaptobrevin homolog, originally classified as a vacuolar v-SNARE	Forms a complex (cis and trans) with the other SNAREs Vam3, Vam7, Vti1
Vam7	Qc SNARE, SNAP-25 homolog, originally classified as a vacuolar t-SNARE	Forms a complex (cis and trans) with the other SNAREs Vam3, Nyv1, Vam3; has a PX (Phox) domain with affinity for PI(3)P as its membrane anchor
Vti1	Qb SNARE, essential gene, originally classified as a vacuolar v-SNARE	Forms a complex (cis and trans) with the other SNAREs Vam3, Nyv1, Vam7
Ypt7	The vacuolar Rab family GTPase similar to mammalian Rab7; required on each partner vacuole in its GTP-bound state to mediate tethering and possibly docking	The GDP-bound form of Ypt7 is complexed within the cytosol and is recruited to the membrane with the help of GDF (GDI Displacement Factor) and via their prenylation by geranylgeranyl transferase II (GGTase II); vacuole-localized Ypt7 is activated to the GTP-bound form by its guanine nucleotide exchange factor (GEF), Vps39, a HOPS complex subunit. Ypt7-GTP specifically binds HOPS as its downstream effector. The GTPase-activating protein (GAP) Gyp7 stimulates the hydrolysis of GTP to GDP to inactivate Ypt7; Ypt7 is proposed to primarily contribute to the membrane affinity of HOPS, and through HOPS, of the soluble SNARE Vam7.
Vps39	Vacuole-specific subunit of the HOPS tethering complex, proposed GEF of the vacuolar Rab Ypt7	C-terminal of Vps39 binds the Vps C core complex through a C-terminal region of Vps11, has a partial RING motif; has a C-terminal Clathrin Heavy Chain Repeat; has each been shown to undergo homo-oligomerization in a yeast-two-hybrid assay
Vps41	Vacuole-specific subunit of the HOPS tethering complex	Has a C-terminal Clathrin Heavy Chain Repeat; has WD40 motif forming beta-propeller; phosphorylation of Vps41 by yeast casein kinase Yck3 switches its tethering function between endosome-vacuole fusion and AP-3 vesicle delivery to the vacuole; has each been shown to undergo homo-oligomerization in a yeast-two-hybrid assay; binds directly and selectively to Ypt7-GTP
Vps16	Conserved core subunit of the HOPS tethering complex	Required for Vps33 association with Vps11 and Vps18
Vps18	Conserved core subunit of the HOPS tethering complex	Has a C-terminal RING motif and a Clathrin Heavy Chain Repeat

Vps33	Conserved core subunit of the HOPS tethering complex	Belongs to the Sec1/Munc18 (SM) family of cofactors that are universally required for SNARE-mediated membrane fusion; proposed to regulate vacuolar fusion by binding the N-terminal Habc domain of Vam3
Sec18	Homohexameric AAA ATPase; homologous to mammalian N-ethylmaleimide-sensitive factor (NSF)	SNARE chaperone that disassembles postfusion cis-SNARE complexes; required for the priming step in homotypic vacuole fusion, vesicular transport between ER- Golgi-Plasma membranes, autophagosome-vacuole fusion.
Sec17	SNAP family member homologous to mammalian α -SNAP	Adaptor protein or co-chaperone to Sec18; stimulates the ATPase activity of Sec18; peripheral membrane protein required for the priming step in homotypic vacuole fusion, vesicular transport between ER- Golgi-Plasma membrane and autophagosome-vacuole fusion.

Structural organization of HOPS subunits is remarkably similar to that observed in other membrane-shaping multisubunit building blocks such as COPI, COPII, Clathrin and the Nuclear Pore Complex. Therefore, it is likely that HOPS complex might self-assemble into higher order structures on membranes in *cis* and/or *trans*. For example, in different yeast two-hybrid assays, Vps11 [72], Vps39 [79] and Vps41 [80] have each been shown to undergo homo-oligomerization, dependent in case of the latter two subunits, on the presence of CHCR domains.

Vps39 and Vps41 form a discrete complex-specific subassembly that functions in Rab recognition. The activities of this subassembly are coordinated with the core through contacts between the C-Terminal Domain (CTD) of Vps39 and the CTD of Vps11 [81]. The core subunits Vps16 and Vps33 also form a stable subassembly. Vps33 belongs to the Sec1-Munc18 (SM) family of SNARE-binding cofactors, which are universally required for SNARE-mediated membrane fusion, so Vps16 and Vps33 likely link the Rab signaling activities of HOPS to SNARE-mediated membrane fusion.

Vps41 has been shown to bind directly and selectively to Ypt7-GTP which explains how the HOPS holocomplex acts as the downstream effector of activated Ypt7 [82]. Vps39 was previously proposed to be the GEF associated with Ypt7 [74]. However, although Vps39 showed a lack of nucleotide specificity in Ypt7 binding, as might be expected for a GEF, in a more recent study, highly purified preparations of Vps39 failed to exhibit any nucleotide exchange activity in fluorescence and radioisotopic assays that readily detected the activities of other bona fide GEFs. Instead, the major Ypt7 GEF activity appeared to reside within the Ccz1/Mon1 complex [83]. The Vps39-Vps41 subcomplex is a physically and functionally integrated effector module containing two Ypt7-binding sites that reside within the N-terminal predicted β -propeller regions of Vps39 and Vps41 that physically interact with one another [81]. The HOPS Rab-recognition module contains one subunit, Vps41, that detects Ypt7-GTP and a second subunit, Vps39 that is insensitive to the nucleotide binding state of Ypt7. HOPS might therefore monitor not only the presence of Ypt7-GTP but also the ratio of Ypt7-GTP to Ypt7-GDP.

Vps11, particularly in its C-terminal region, forms a densely connected hub, interacting with Vps16, Vps18 and Vps39

[81]. Vps16 is required for Vps33 association with Vps11 and Vps18. Vps11 may be a simple structural scaffold or it could have a more dynamic role in linking Rab signaling to Vps-C outputs, including the SNARE machinery that mediates fusion at the vacuole. Biochemical as well as genetic analyses has revealed that the Vps11 CTD is a key integrator of Vps-C complex assembly, Rab signaling, and endolysosomal traffic. The RING/Zn²⁺ finger domains in different HOPS subunits seem to have distinct functions in endolysosomal trafficking. Mutants lacking the RING domain exhibited impaired CPY processing, limited CPY secretion from the cell and defects in ALP processing at various degrees. These phenotypes are diagnostic of defective docking or fusion at the vacuole. The severity of the trafficking defects observed in each Δ RING/Zn²⁺ finger mutant, from most severe to least, is as follows: vps18-826 Δ > vps11-926 Δ > vps39-979 Δ [81]. Importantly, it was proposed that these subunits might be capable of self-interaction and/or interactions with other subunits mediated through their RING domains.

SM proteins are required in all SNARE-dependent physiological fusion reactions. They bind individual SNAREs or SNARE complexes and regulate their assembly. Vam3 has been known to bind the SM protein Vps33 via its N-terminal Habc domain and the SNARE domain and this interaction was shown to be critical for the late stage of fusion pore opening [76]. This further depicts how the composition and architecture of the multisubunit HOPS complex can integrate various roles to support vacuolar tethering and docking.

In various studies employing either native yeast vacuoles or purified proteins, the HOPS complex has been shown to individually bind phosphoinositides (preferentially PI(3)P and PI(4,5)P₂), the PX domain of (and full length) Vam7, the SNARE domain of (and full length) Vam3, and Ypt7. These multifarious interactions of the HOPS complex are reminiscent of tethering factors that interact with proteins and lipids that can reside on same or different membranes. This suggests an important role of HOPS in determining a fusion site by enriching relevant factors and nucleating SNARE complex assembly [84]. The specific functions of the HOPS complex and the mechanisms by which it couples activated Ypt7 to SNARE complex assembly are unknown. However, the known interaction topology integrating genetic, biochemical and functional data allows

us to draw an interaction network of fusion factors illustrated in figure 12. This can serve as a starting point to pursue further investigations. Here, two-way arrows indicate inter-

component relationships while simple lines indicate intra-complex relationships.

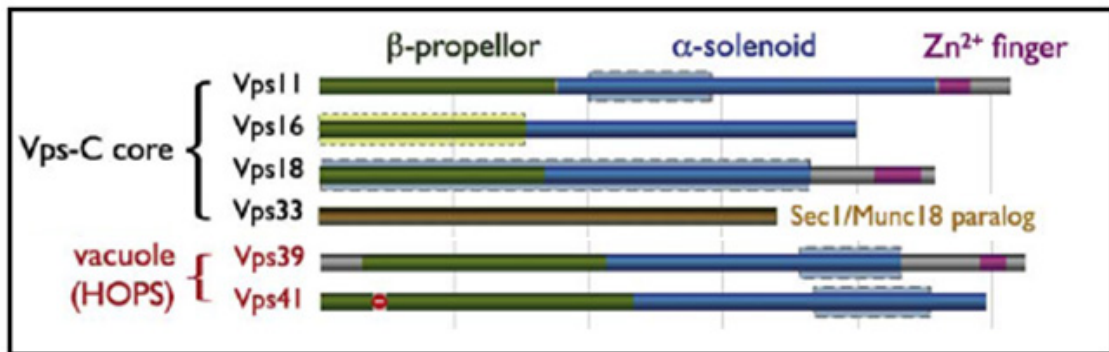


Figure 11: Subunit composition and domain architecture of the HOPS complex.

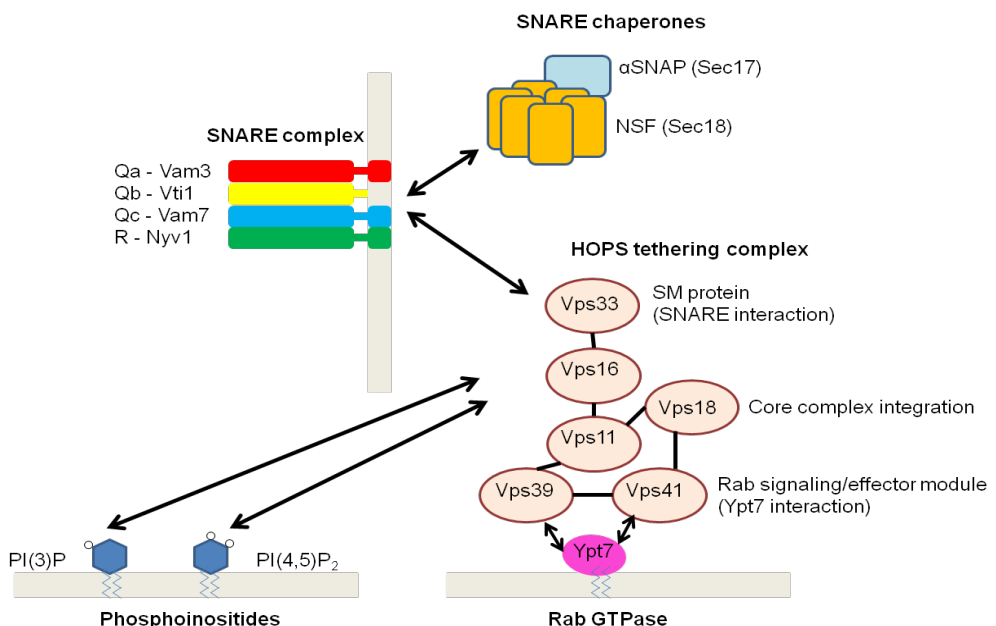


Figure 12: Known interactions among vacuole fusion components.

Comparisons with fusion reactions in other systems

Studies in budding yeast of the delivery of secretory vesicles to the plasma membrane at the bud tip have spearheaded our understanding of vesicular traffic. Secretory vesicles from the Golgi complex, bearing the Rab GTPase Sec4 and the v-SNAREs Snc1 and Snc2, are delivered to the bud tip secretion site, specified by Sec3 [85-87]. There, the multisubunit heterooctameric exocyst complex serves as the primary tethering agent. Exocyst holocomplex assembly occurs at the plasma membrane (and not on the secretory vesicle) via individual or sub-assemblies of subunits gathering from different sources, unlike the pre-formed

HOPS holocomplex [88,89]. The exocyst is an extended protein complex, 30 nm in length that localizes to the bud tip even when functions of SNAREs or Rab-like GTPases are compromised, whereas the t-SNAREs Sso1 and Sso2 are found distributed uniformly over the bud plasma membrane [4]. This physical and functional asymmetry of SNARE, GTPase, and tethering factor distribution between the secretory vesicle and plasma membrane is quite different from the situation in homotypic vacuole fusion. Although the recycling of Sec4 after vesicle fusion by GTP hydrolysis and extraction by its GDI Sec19 has been well documented [90], it remains unclear how the Snc1 and Snc2 v-SNAREs are recycled from the plasma membrane to presumably the

trans-Golgi. It is not yet known what primary landmark at the bud tip initiates exocyst assembly at this site. Whether there is a factor that prevents exocyst assembly on the secretory vesicles and subsequent homotypic fusion of these vesicles, is another question that remains to be resolved.

The brain has proven to be an excellent system for systematically isolating crucial trafficking components. It is well established that synaptic vesicles originating from endosomes form clusters at the active zone of the presynaptic plasma membrane [91]. Ca²⁺ flux triggers rapid exocytosis, which is followed by endocytosis and thus the synaptic vesicle machinery, is recycled [92]. Additionally, NSF and SNAPs were first purified from brain extract as factors which could support an intra-Golgi trafficking reaction [93-95], and syntaxin, synaptobrevin, and SNAP-25 were first identified as synaptic membrane proteins and later as SNAP receptors (SNAREs) by using brain extracts [10,14]. These SNAREs are cleaved by specific neurotoxins [12]. Cleavage is seen only when SNAREs are unpaired, and cleavage efficiently blocks Ca²⁺-triggered neurotransmission. Surprisingly, it has been shown that genetic or toxin-mediated removal of v- or t-SNAREs from Drosophila blocks neurotransmission but not the association of vesicles at the synapse [16]. Thus, it seems likely that synaptic vesicles clustered at the synapse are “tethered” but not yet SNARE paired. There is, however, no direct evidence as to when SNARE pairing in trans occurs at the synapse, and the roles of associated Rab GTPases and/or tethering complexes have remained obscure.

Synaptic vesicle fusion requires NSF, SNAP isoforms, and a preceding priming reaction which includes ATP-dependent phosphatidylinositol phosphorylation [96,97] and probably the same NSF- and ATP-dependent SNARE activation [98] as that occurring in homotypic vacuole fusion. Similar findings are reported for dense core granule exocytosis as well [99]. Because phosphatidylinositol phosphorylation is also a prerequisite for Sec17 release from vacuole membranes, these multiple priming reactions, which require ATP, may be very similar at the molecular level. The lack of an *in vitro* reaction of synaptic vesicle exocytosis has been an impediment, but one largely overcome by characterization of norepinephrine release from permeabilized neuroendocrine cells. Studies of this

release reaction have phenocopied all of the functional themes that have emerged in homotypic vacuole fusion, including the role of PI(4,5)P₂ and the action of ATP, NSF, and SNAP before the final act of Ca⁺⁺/calmodulin-triggered fusion [100-102].

There has been substantial study of precisely when SNAREs and NSF/SNAPs act in the release of synaptic vesicle contents at the presynaptic plasma membrane and how accompanying factors regulate their activity. Vacuole-to-vacuole fusion does not require any α -SNAP (yeast Sec17) after priming which occurs well before the SNAREs pair during docking. In cracked PC12 cell exocytosis, as in yeast vacuole fusion, NSF (yeast Sec18) dissociates from the SNARE complex after ATP hydrolysis but before calcium-triggered membrane fusion. On the other hand, for release of noradrenaline from perforated synaptosomes, NSF is required in a post-docking state for subsequent fusion [103]. Similar conclusions were drawn from studies of Drosophila NSF mutants which suggested that docked vesicles accumulate under non-permissive conditions [104]. Similarly, injection of tetanus toxin into squid giant synapses led to cleavage of uncomplexed synaptobrevin and a consequent accumulation of both docked and undocked vesicles [105]. These different observations in the vacuolar and synaptic systems could be explained if one considers that, at least in the yeast vacuole reaction, priming is a prerequisite for subsequent tethering through signaling by released Vam7 and HOPS to the Ypt7 tethering apparatus, whereas priming can happen after tethering of synaptic vesicles to the presynaptic plasma membrane, as for yeast ER-to-Golgi traffic.

The symmetrical requirement for a small GTPase on both partner membranes is shared by Ypt7 on yeast vacuoles [106-107] and Rab5 on early endosomes in mammalian cells [108]. However, neuronal Rab3 is largely localized to synaptic vesicles and is released during exocytosis [109-110]. Similarly, yeast Ypt1 seems to be required only on Golgi membranes to mediate a productive tethering with ER-derived vesicles *in vitro* [111]. Organelle identity, therefore, may not rest on a single class of proteins. Rather, each compartment may be specified by some combination of SNARE, Rab/Ypt protein and tethering factor at least.

Chapter 2

A HOPS Tethering Complex Dimer Catalyzes Trans-SNARE Complex Formation In Yeast Vacuolar Fusion

Chapter II

A HOPS Tethering Complex Dimer Catalyzes Trans-SNARE Complex Formation In Yeast Vacuolar Fusion

Portions of this work have been published in Kulkarni A, Alpadi K, Namjoshi S, Peters C (2012) A tethering complex dimer catalyzes trans-SNARE complex formation in intracellular membrane fusion, *Bioarchitecture*, 2(2): 59-69.

Introduction

Vesicular transport can be sectioned into a progression of interdependent subreactions that comprise vesicle budding, movement, priming, tethering, docking, lipid mixing and content mixing [3]. However, the precise protein interaction scheme underlying the evolution of priming through docking is still unresolved. I have exploited vacuoles purified from budding yeast as a model system to delineate specific protein interactions among SNARE, tether and Rab family members on the pathway to fusion.

Membrane fusion is a fundamental process marking the culmination of every vesicular trafficking route in the endomembrane system. Soluble N-ethylmaleimide sensitive factor Attachment protein receptors (SNAREs), are central players mediating the fusion of apposed lipid bilayers through the assembly of distinct trans-SNARE complexes. A trans-SNARE complex bridges two apposed membranes and is composed of a parallel four-helix bundle of the SNARE domain helices. Essential components of the yeast vacuolar fusion machinery include SNAREs - Vam3 (Q_a), Vti1 (Q_b), Vam7 (Q_c) and Nvy1 (R); the HOPS (HOMotypic fusion and vacuole Protein Sorting) tethering complex and the Rab GTPase Ypt7 [64]. HOPS is a highly conserved tethering complex operating within

the endolysosomal transport circuit. The HOPS complex is composed of six different subunits namely Vps11, Vps16, Vps18, Vps33, Vps39 and Vps41 [78]. By virtue of its modular structural architecture and multiple affinities toward small G proteins, SNAREs and lipids, the heterohexameric HOPS tethering complex is poised to link the recognition of membranes (via lipids/adaptors/small G proteins in general) with subsequent fusion (via SNAREs) through highly dynamic interactions with multiple sets of proteins. In the simplest sense, dimeric HOPS would create a highly stable platform capable of (i) binding activated Rab proteins, (ii) recruiting primed SNARE subcomplexes dependent on the action of Sec18/NSF (N-ethylmaleimide Sensitive Factor) and (iii) catalyzing the formation of a topologically restricted trans-SNARE complex, thus imparting additional specificity and fidelity to the process of membrane fusion. It is easy to visualize how a scaffold in the form of an oligomerized tethering complex would, by means of its size, reach over the distance between apposed membranes and, through multiple affinities, enhance the local concentration of fusion factors ultimately facilitating SNARE pairing in trans. The compatibility for fusion between two compartments is determined by a particular combination of SNAREs contributed by each membrane. As enumerated in table 2, four different SNAREs can be distributed over two membrane-bound compartments in eight non-redundant permutations as follows.

According to a previously accepted view, a specific combination of three Q-SNAREs from one membrane and one R-SNARE from the other were thought to interact in trans (current QaQbQc - R model as depicted in figure 13) bringing the membranes into close opposition to achieve fusion with much higher efficiency compared to other combinations [112,113]. This model was based on the fusion of synthetic proteoliposomes incorporating individual or preformed SNAREs.

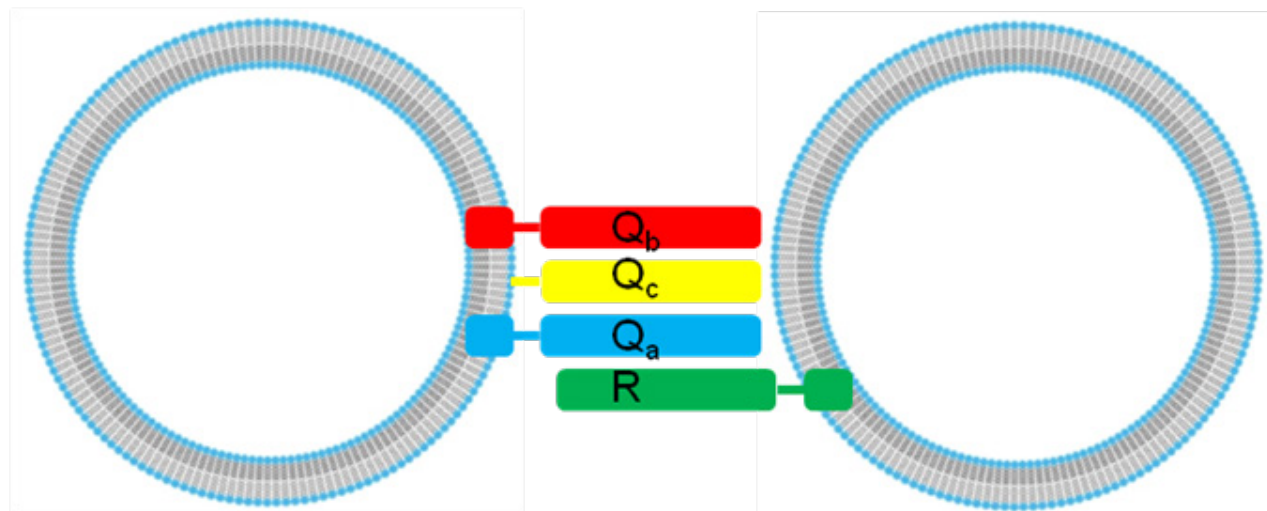


Figure 13: Previously accepted QaQbQc - R model of trans-SNARE complex formation.

However, depending on the conditions employed, other SNARE topologies can also become fusogenic as suggested by fusion experiments done with early endosomal SNAREs reconstituted into liposomes [114]. Yeast vacuole fusion is of homotypic architecture, meaning each fusion partner is exactly identical and possesses the same protein composition. It is not known what factors govern asymmetrical SNARE pairing in trans is,

given that both fusion partners possess exactly the same equipment in a homotypic scenario. Recent studies from my lab have indicated that an alternative QbQcR - Qa trans-SNARE distribution, depicted in figure 14, is biochemically distinguishable and functionally relevant for membrane fusion whereas no other trans-SNARE distribution was comparable in fusion efficiency [115].

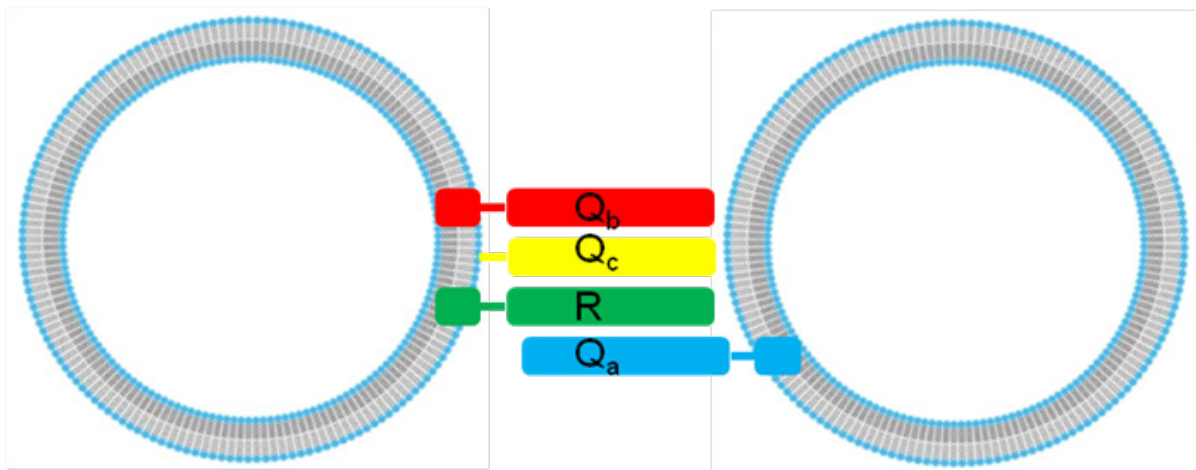


Figure 14: Currently proposed QbQcR - Qa model of trans-SNARE complex formation.

As compiled in table 3 compiled from [115], activity tests of vacuoles with diagnostic distributions of inactivating mutations over the two fusion partners confirm that this distribution accounts for a major share of the fusion activity.

Moreover, the generation of a stable QbQcR cis-SNARE

complex (on the same membrane) at a pre-tethering stage was observed, in contrast to an expected QaQbQc complex. As shown in **figure 15**, stability here is defined in terms of persistence of primed QbQcR or QaQbQc cis-complexes in the presence of ATP.

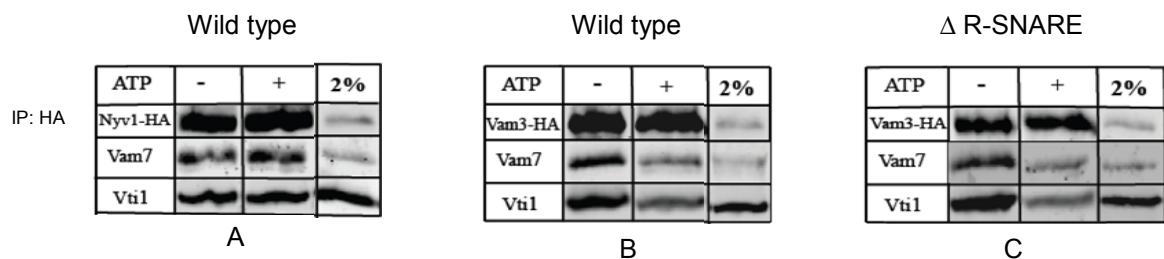


Figure 15: Existence of a stable QbQcR SNARE complex.

Vacuoles from wild type HA-tagged Nyv1 (A) and Vam3 (B) strains were incubated at 270C without or with 0.5M ATP in standard reaction buffer for 5 minutes and precipitated with immobilized HA antibodies. Precipitate was washed, resolved by SDS-PAGE and western blotting was performed using Vam7, Vti1 and HA antibodies. In (C) the same protocol was employed on vacuoles from Δ Nyv1 Vam3-HA strain.

Densitometric analysis (not shown) indicates more than 60% loss of co-precipitating Qb and Qc SNAREs as in

figure 15. The QaQbQc complex is as unstable in wild type vacuoles as in the R-SNARE knockout. This further confirms their instability as only QaQbQc cis-complexes can form in the R-SNARE knockout.

Importantly, this QbQcR SNARE complex was (i) sensitive to treatment of vacuoles with GDI that inactivates the Rab Ypt7, and (ii) absent on the tether-mutant vacuoles Ypt7-T22N and Δ Vps41 as evident in figure 16 adapted from [115].

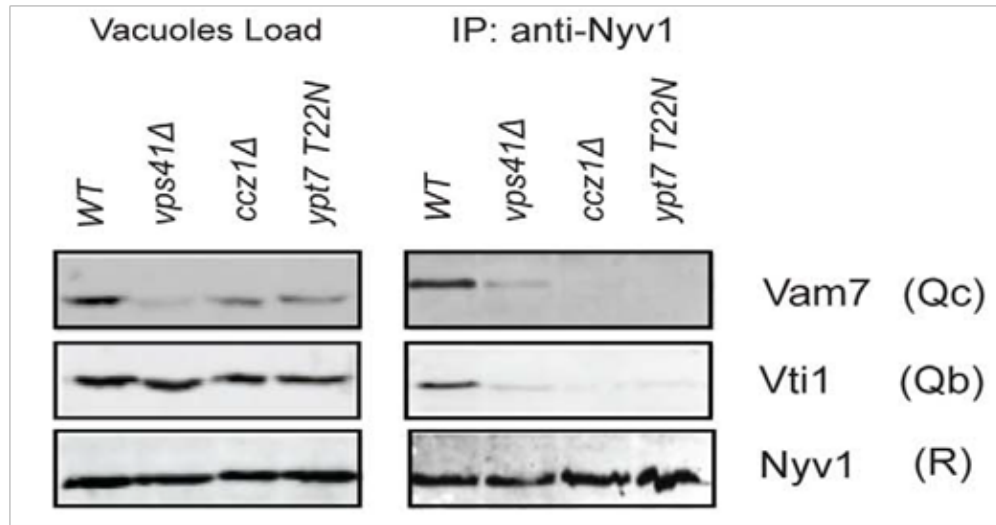


Figure 16: Presence of QbQcR complexes on tether mutant vacuoles assayed by immunoprecipitating the R SNARE Nyv1.

Table 2: Possible trans-SNARE pairing combinations.

Combination	Vesicle 1	Vesicle 2
2:2	Q_a, Q_b	Q_c, R
	Q_b, Q_c	Q_a, R
	Q_c, Q_a	Q_b, R
3:1	Q_a, Q_b, Q_c	R
	Q_a, Q_b, R	Q_c
	Q_b, Q_c, R	Q_a
4:0	Q_c, Q_a, R	Q_b
	Q_a, Q_b, Q_c, R	-

Table 3: Functional validation of trans-SNARE topology.

SNARE Distribution				Fusion Activity Prediction		Results	
Fusion partner 1		Fusion partner 2		$Q_b Q_c R - Q_a$ model	$Q_a Q_b Q_c - R$ model	Fusion observed	Prevalent model
Mutant	Functional	Mutant	Functional				
<i>vti1-1</i>	Q_a, Q_c, R	$\Delta nyv1$	Q_a, Q_b, Q_c	✗	✓	✗	$Q_b Q_c R - Q_a$
<i>vti1-1</i> $\Delta nyv1$	Q_a, Q_c	<i>WT</i>	Q_a, Q_b, Q_c, R	✓	✗	✓	$Q_b Q_c R - Q_a$
<i>vam3^{ls}</i> <i>vti1-1</i>	Q_c, R	<i>WT</i>	Q_a, Q_b, Q_c, R	✗	✓	✗	$Q_b Q_c R - Q_a$

The left panel depicts expression levels of SNAREs on purified wild type, $\Delta vps41$, $\Delta ccz1$ and *ypt7-T22N* vacuoles. The right panel shows precipitated QbQcR complexes from these vacuoles in the absence of ATP.

It is therefore likely that a preferred trans-SNARE topology is guided and stabilized by additional factors, potentially tethering complexes and Rab GTPases. It is hence worthwhile to know how this asymmetry in SNARE associations from opposing fusion partners is created to

Chapter 2

achieve the SNARE combination of QbQcR-Qa that has been shown to be physiologically the most fusogenic.

I hypothesize that the HOPS complex, through its dimerization, orchestrates this SNARE arrangement in a Ypt7-dependent manner. Therefore, I sought to obtain more evidence that might indicate a direct participation of the HOPS tethering complex and the Rab GTPase Ypt7 in coordinating the QbQcR-Qa trans-SNARE topology. I employed various approaches to investigate (i) whether the HOPS complex possesses any oligomerization tendencies and (ii) whether it is able to create an asymmetry in SNARE associations. First I resorted to gel filtration chromatography to detect if any higher-order oligomers of the entire HOPS complex processed from detergent extracts of purified yeast vacuoles exist and if so, determine their stability. Second, taking advantage of the fact that HOPS subunits contain complete or partial RING domains or Cysteine/Histidine-rich regions in general, I used a disulfide bridge dependent crosslinking strategy to ascertain if any multimerization of individual subunits occurs on native membranes. Most importantly, I used specific co-immunoprecipitation schemes involving differentially tagged versions of HOPS subunits and SNAREs to be able to categorically pinpoint HOPS-SNARE associations leading to trans-SNARE complex establishment. I propose a novel concept that specificity in eukaryotic intercompartmental communications and regulation over trans-SNARE pairing is imparted by tethering complex dimerization more robustly than just the specific occurrence of SNAREs.

Materials and Methods

Yeast strains

BJ3505 or DKY6281 are the yeast strains employed in all assays as indicated. Modifications in these strain backgrounds include chromosomal tagging or deletions of non-essential genes.

Vacuole purification

BJ3505 or DKY6281 yeast strains were grown in YPD at 30 °C at 150 rpm to OD₆₀₀ = 2 and harvested (3 min, 5,000g). Cell walls were hydrolyzed by lyticase, recombinantly expressed in *E. coli* RSB805 (provided by Dr Randy Schekman, Berkeley), and prepared from a periplasmic supernatant. Harvested cells were resuspended in reduction buffer (30mM Tris/HCl pH 8.9, 10 mM DTT) and incubated for 5 min at 30°C. After harvesting as described above, cells were resuspended in 15 ml digestion buffer (600 mM Sorbitol, 50mM K-phosphate pH 7.5 in YP medium and 0.1 mg/ml lyticase). After 20 min at 30 °C, cells were centrifuged (1 min, 5,800 rpm in JLA25.5 rotor). The spheroplasts were resuspended in 2.5 ml 15% Ficoll-400 in PS buffer (10mM PIPES/KOH pH 6.8, 200 mM Sorbitol) and 200 µl DEAE-Dextran (0.4 mg/ml in 15% Ficoll-400 in PS). After 90 sec of incubation at 30 °C, the cells were transferred to SW41 tubes and overlaid with steps of 8%, 4% and 0% Ficoll-400 in PS. Cells were centrifuged for 60-75 min at 2°C and 30,000 rpm in an SW41 rotor.

Content mixing assay

DKY6281 and BJ3505 vacuoles were adjusted to a protein concentration of 0.5 mg/ml and incubated in a volume of 30µl PS buffer (10mM PIPES/KOH pH 6.8, 200mM Sorbitol) with 120mM KCl, 0.5mM MnCl₂, 1mM DTT. Inhibitors or recombinant proteins, if any, were added before starting the fusion by addition of the ATP-regenerating system (0.25mg/ml creatine kinase, 20mM creatine phosphate, 500mM ATP, 500 mM MgCl₂). After 60 min at 27 °C, or on ice, 1ml of PS buffer was added, vacuoles were centrifuged (2 min, 20,000g, 4 °C) and resuspended in 500 µl developing buffer (10 mM MgCl₂, 0.2% TX-100, 250mM Tris/HCl pH 8.9, 1 mM p-nitrophenylphosphate). After 5 min at 27 °C, the reactions were stopped with 500µl 1M glycine pH 11.5 and the OD was measured at 400 nm.

Gel filtration

400µg of purified yeast vacuoles were solubilized in buffer containing 1% Triton X-100, 3 mM EDTA, 2mM DTT and 150mM or 600mM KCl. After centrifugation for 4 min at 20,000 g the supernatant was applied on a Superose 6 column and the collected fractions were inspected using SDS-PAGE and western blotting.

Cis-HOPS assay

The yeast strain Vps41-HA containing a Vps41-TAP plasmid was treated with 1 mM PMSF for the last one hour of its growth period prior to harvesting the cells. 1 mM PMSF was included in the digestion buffer and in 15% Ficoll-400 in PS buffer during vacuole preparation. 500µg of vacuoles purified from this strain were incubated in buffer containing 120 mM KCl, 500µM MnCl₂ for 15 min at 27 °C. The vacuoles were then centrifuged for 2 min at 20,000 g and subsequently solubilized in buffer containing 1% Triton X-100 and 120mM KCl. Vps41-TAP was precipitated using IgG/Sepharose beads (GE Healthcare) and co-precipitating proteins were analyzed employing SDS-PAGE and western blotting.

Crosslinking assay

500µg of yeast vacuoles were purified from Vps11-HA, Vps16-HA, Vps18-TAP, Vps33-HA, Vps39-HA and Vps41-HA strains. Vacuoles from each strain were incubated in buffer containing 120 mM KCl and 500µM MnCl₂ for 5 min at 27 °C. H₂O₂ was then added to a final concentration of 0.03% and the vacuoles were further incubated for 15 min at 27°C. After centrifugation for 2 min at 20000 g at 4 °C, the supernatant was discarded and the pellet was analyzed on non-reducing SDS-PAGE followed by western blotting.

Trans-SNARE assay

500µg of yeast vacuoles purified from Vam3-HA and Nyv1-VSV strains were mixed and incubated in PS buffer with 120mM KCl, 500µM MnCl₂ and 1 mM DTT for 5 min at 27 °C in the absence of ATP. The fusion reaction was started by adding ATP-regenerating system (0.25 mg/ml creatine kinase, 20 mM creatine phosphate, 500mM ATP,

500mM MgCl₂). After 5 min at 27 °C, the vacuoles were cooled down to 7°C and incubated further for 30 min at this temperature. Thereafter, 3mM EDTA was added and vacuoles were centrifuged for 2 min at 4 °C at 20,000 g and subsequently solubilized in buffer containing 0.5% Triton, 50mM KCl, 3mM EDTA, 3mM DTT in PS. Vam3-HA was precipitated using Protein G/anti-HA antibodies (Covance, mouse monoclonal) and co-precipitating proteins were analyzed employing SDS-PAGE and western blotting.

HOPS immunoprecipitations

500µg of yeast vacuoles purified from a ΔN-terminal Vam3 strain harboring Vps16-HA were mixed with 500µg of vacuoles harboring Nyv1-VSV or Ypt7-T22N or with wild type and incubated in PS buffer containing 120mM KCl, 500 µM MnCl₂ and ATP-regenerating system. After 15 min at 27 °C, vacuoles were centrifuged for 2 min at 20,000 g and subsequently solubilized in buffer containing 1% Triton X-100, 75mM KCl, 3mM EDTA and 2mM DTT. Vps16-HA was precipitated using Protein G/anti-HA antibodies (Covance, mouse monoclonal) and co-precipitating proteins were analyzed employing SDS-PAGE and western blotting.

Results

Fusion activity of SNARE, HOPS and Rab mutant vacuoles

To validate asymmetric SNARE participation from opposing

fusion partners as previously suggested in [116], I tested the fusion efficiency between combinations of wild type, ΔVam3 (Qa SNARE) and ΔNyv1 (R SNARE) vacuoles.

Vacuoles derived from wild type, ΔVam3 or ΔNyv1 (DKY and BJ) strains, were incubated in the combinations mentioned, under standard fusion conditions. Normalized OD400 values in the presence of ATP for five independent experiments are shown as mean±s.d.

As displayed in figure 17, the vacuole combination wild type/ΔVam3 (Qa SNARE) shows a strong fusion defect whereas wild type/ΔNyv1 (R SNARE) does not significantly affect vacuole fusion activity relative to wild type/wild type vacuole fusion. ΔVam3/ΔVam3 and ΔNyv1/ΔNyv1 vacuoles showed almost complete abolition of fusion efficiency. Although both Vam3 and Nyv1 are normally present on each vacuole in the homotypic scenario, Vam3 knockout and Nyv1 knockout vacuoles behave differently in their fusion outcomes when the partner vacuoles are wild type. This shows that the tendency to compensate for the absence of each of these SNAREs is not equivalent, or that additional factors have different propensities to interact with either of these SNAREs. I further analyzed the fusion outcomes of HOPS and Ypt7 mutants to corroborate the related evidence from [117], I found that deletion of individual HOPS subunits Vps11, Vps16, Vps33, Vps39 and Vps41 even on one fusion partner (the other being wild type) completely abolishes vacuole fusion activity, as plotted in figure 18.

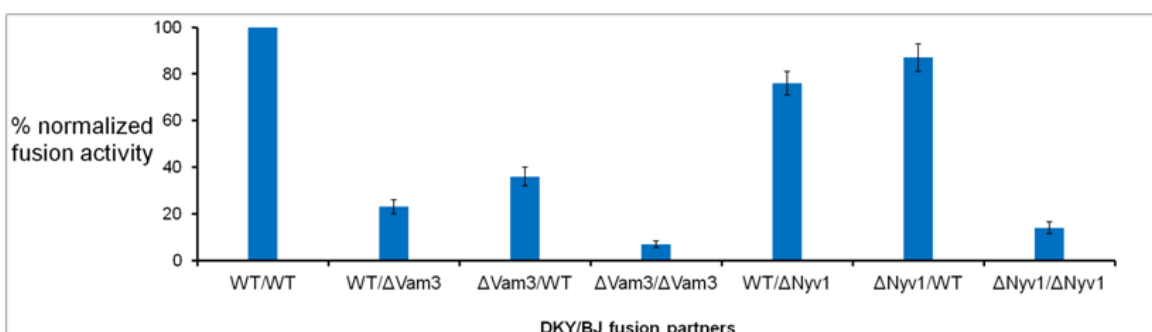


Figure 17: Fusion of Qa and R SNARE mutant vacuoles.

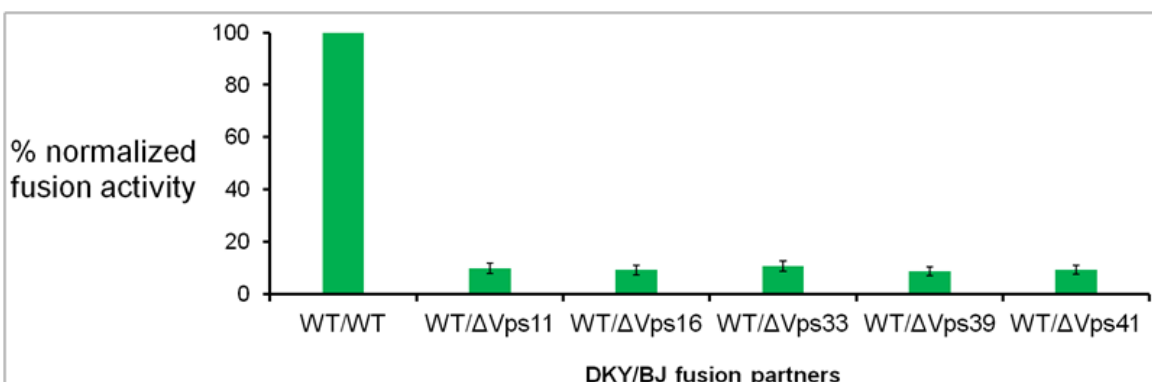


Figure 18: Fusion of HOPS complex mutant vacuoles.

Chapter 2

Vacuoles derived from wild type or HOPS subunit deletion strains were incubated in the combinations mentioned, under standard fusion conditions. Normalized OD₄₀₀ values in the presence of ATP for five independent experiments are shown as mean±s.d.

This implies that structural integrity of the entire HOPS complex on each fusion partner is necessary for its function in vacuolar fusion.

Furthermore, as depicted in figure 19, Ypt7-T22N vacuoles delivering a GDP-locked inactive form of the Rab7 homolog Ypt7 failed to fuse with wild type vacuoles, however vacuoles from Ypt7-Q68L providing a constitutively active GTP-bound form of Ypt7 do not significantly affect fusion with wild type vacuoles. Concomitantly, external addition of recombinant Rab GDI (GDP Dissociation Inhibitor) which inactivates Ypt7, inhibits the fusion of wild type vacuoles.

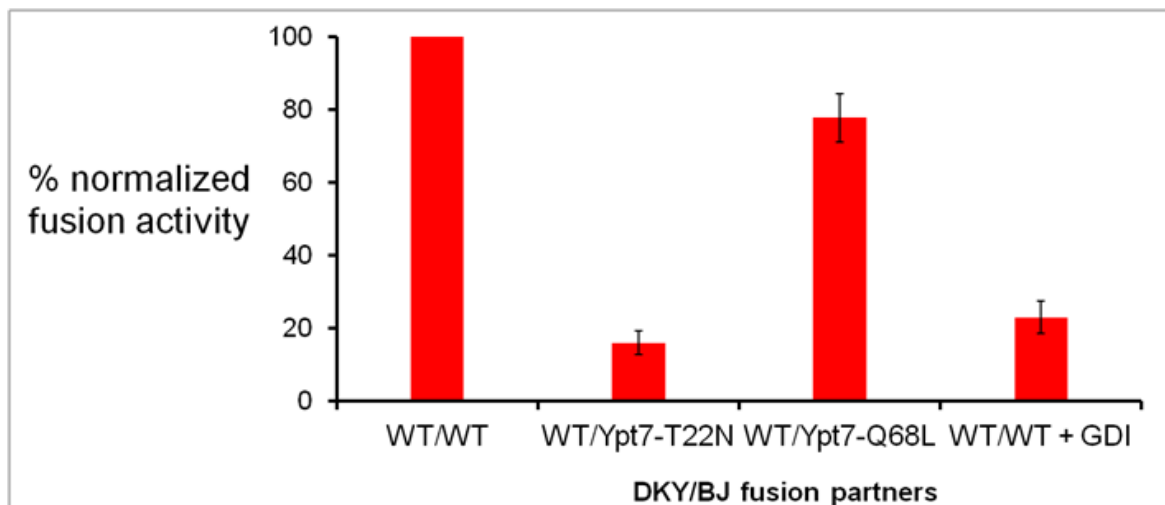


Figure 19: Fusion of Rab mutant vacuoles.

Vacuoles derived from wild type, Ypt7-T22N or Ypt7-Q68L strains, were incubated in the combinations mentioned, under standard fusion conditions. Normalized OD₄₀₀ values in the presence of ATP for five independent experiments are shown as mean±s.d.

Microscopic examination of deletion strains of the SNAREs Vam3 (Qa) [70][116] and Vam7 (Qc) [118] revealed that their vacuoles display aberrant morphology *in vivo*. Prominent vacuoles could not be observed in those cells. Instead, the cells accumulated numerous smaller, vacuole-like compartments. On the contrary, upon deletion of the SNARE Nvy1 (R), vacuolar morphology was completely normal and unaltered compared to that in wild type [116]. These *in vivo* observations of SNARE deletions further support their fusion outcomes *in vitro*. It is possible that other R SNAREs (such as Ykt6) are able to substitute for Nvy1 or that Vam3 is regulated differently or more tightly than Nvy1 in the catalysis of yeast vacuolar membrane fusion.

To test the impact of Rab and HOPS components *in vivo* I performed phenotypic characterization of vacuolar morphology by specifically labeling yeast vacuoles with the lipid binding fluorescent dye FM4-64. Logarithmic phase wild type yeast cells treated with FM-64 show discretely stained compartments readily identifiable as vacuoles. Figure 20 shows representative images of vacuolar

morphology observed in cell populations from HOPS and Rab mutant yeast strains.

Vacuoles in cells from the Ypt7-T22N and ΔVps41 strains were labeled with the dye FM4-64. Representative snapshots are shown. Red compartments represent labeled vacuoles. White scale bar at the top right in the merge image panel measures 2.5μm.

As shown in figure 21, I characterized different yeast strains by recording their fusion efficiency with the wild type, in order to rule out a total lack of fitness for proposed experiments.

Fusion of vacuoles harboring tagged HOPS subunits and tagged or truncated SNAREs was measured relative to wild type vacuoles.

Having replicated the individual importance of SNARE, tether and Rab proteins in yeast vacuolar fusion *in vitro* and *in vivo*, I proceeded to investigate whether there is an interdependence or connection among these factors in their ability to accomplish fusion.

HOPS is a dimeric complex on the surface of yeast vacuoles

A straightforward way to evaluate complex formation tendency of a protein or multiprotein complex is to perform gel filtration analysis. Vacuoles purified from wild type yeast cells were detergent extracted and the solubilizate was

run through a Superose 6 column able to resolve proteins within a molecular size range of 10-2,000 kDa. Fractions from gel filtration were analyzed by SDS-PAGE and immunoblotted by probing with antibodies raised against the HOPS subunit Vps39. The predicted molecular mass of the HOPS complex obtained by summing the masses of individual subunits is around 600 kDa. Remarkably however, we observed that HOPS predominantly migrates

at exactly double the expected molecular mass which is around 1,200kDa as depicted in figure 22 (top lane). Upon modifying the solubilization conditions by increasing the salt concentration beyond physiological levels HOPS was found to run at its predicted monomeric mass of 600kDa (figure 22 bottom lane). There is almost complete transposition of a dimeric population to a monomeric population of HOPS under high salt concentration.

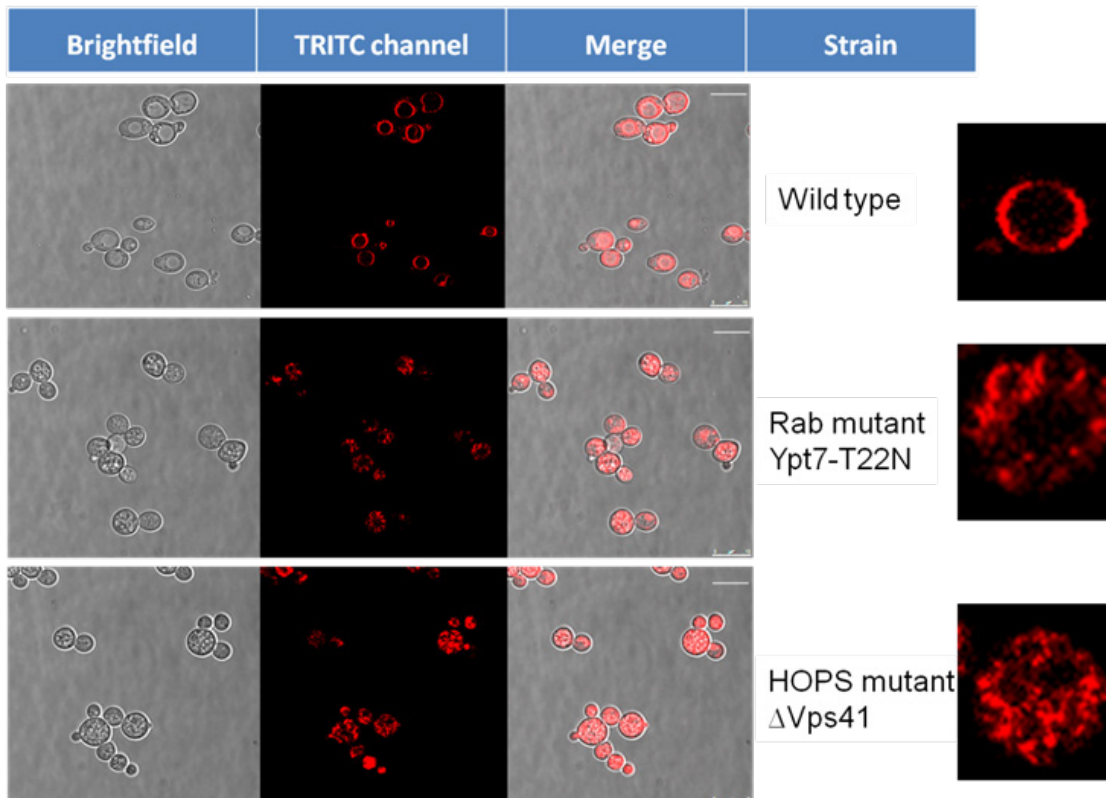


Figure 20: *In vivo* vacuolar morphology of Ypt7 and HOPS mutant strains.

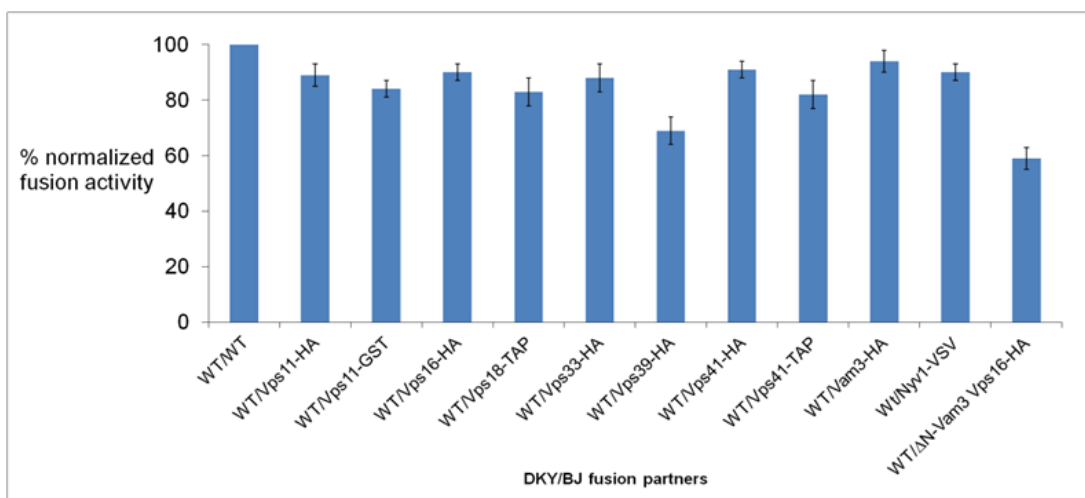


Figure 21: Functional analysis of vacuoles harboring various modified or epitope-tagged fusion components.

Chapter 2

Fractions 13-26 from Superose 6 gel filtration of solubilized vacuoles were inspected using SDS-PAGE followed by immunoblotting against Vps39. When vacuoles were processed at 150 mM KCl in the solubilization buffer, HOPS predominantly runs in fraction 16 (top lane). At 600 mM KCl, HOPS predominantly runs in fraction 21 (bottom lane). Arrows indicate approximate molecular weights. To further confirm whether the observed mobility shift corresponds to a true HOPS dimer or involves other binding partners, I

co-expressed the HOPS subunit Vps41, as two differently tagged versions in the same strain-Vps41-HA through its native chromosomal locus and Vps41-TAP through an extrachromosomal plasmid source. It is to be noted that any interaction between identical subunits carrying different epitope tags cannot originate from intra-complex binding but rather signifies interaction between two different HOPS complexes.

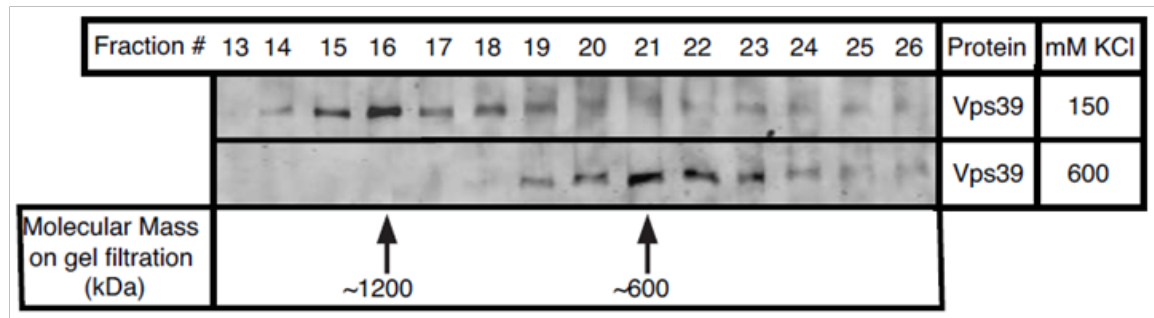


Figure 22: Gel filtration analysis of purified yeast vacuoles.

As shown in figure 23 (top panel), I assayed for HOPS complex dimerization by IgG pull down of Vps41-TAP and probing for any co-precipitating Vps41-HA and ascertained holocomplex precipitation by probing for Vps39 since these

are known to be the HOPS-specific subunits. Relative co-precipitation efficiencies of Vps41-HA and Vps39, plotted in **figure 23 (bottom panel)**, indicate that HOPS quantitatively forms a dimer in this assay.

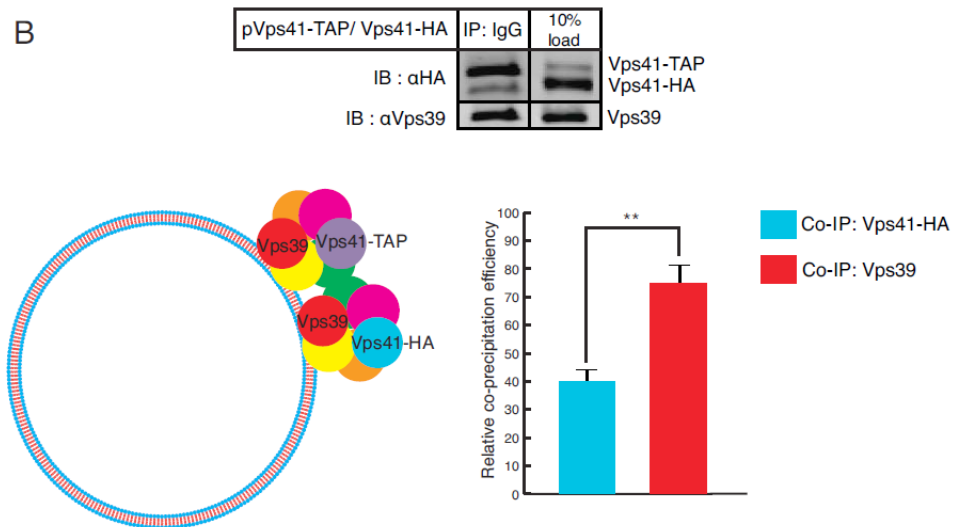


Figure 23: Cis-HOPS complexes assayed by differently tagged Vps41.

Vacuoles from the Vps41-HA strain harboring a Vps41-TAP plasmid were processed as described in Materials and Methods. After IgG pull down of Vps41-TAP, co-precipitating proteins were analyzed by SDS-PAGE and western blotting. In the top panel, the left lane shows precipitated Vps41-TAP, co-precipitating Vps41-HA and Vps39 and the right

lane displays corresponding protein inputs. The bottom panel depicts relative co-precipitation efficiencies of Vps41-HA and Vps39 quantified by Odyssey densitometry and normalized from three independent experiments. Vps39 is consistently found to co-precipitate at approximately twice the efficiency of that of Vps41-HA ($p < 0.01$).

HOPS dimerizes in cis via Vps11

The HOPS subunits Vps11, Vps39 and Vps41 have previously been reported to interact with themselves in different yeast two-hybrid analyses. Also Vps11 and Vps18 have been proposed to potentially multimerize via their C-terminal RING domains, which are susceptible to oxidation. I therefore devised a chemical crosslinking strategy in which disulfide bridges are formed between Cysteine residues when treated with hydrogen peroxide. Vacuoles harboring HA tagged versions of individual HOPS subunits were incubated with and without 0.03% H₂O₂ under standard fusion conditions and then subjected to non-reducing SDS-PAGE followed by immunoblotting

with anti-HA antibody. As indicated in figure 24, a higher band corresponding to a disulfide crosslinked product appears exclusively in the case of Vps11 (figure 24, lane 2) among all of the HOPS subunits suggesting a role of the Cysteine-rich RING domain of Vps11 in mediating its homooligomerization.

Vacuoles harboring HA or TAP tagged versions of all HOPS subunits were incubated under standard fusion conditions with or without 0.03% H₂O₂, centrifuged and analyzed on non-reducing SDS-PAGE followed by western blotting with anti-HA antibody. Lanes 1-12 show the effect of peroxide treatment on each HOPS subunit labeled below. Only Vps11 shows a crosslinked product marked by the arrow (lane 2).

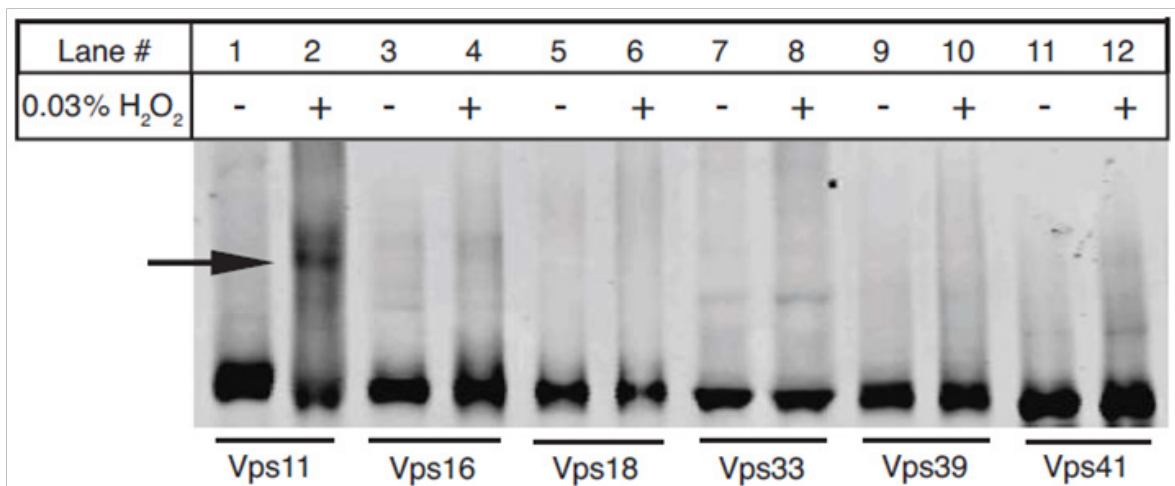


Figure 24: Chemical crosslinking of HOPS subunits.

To deduce the order of oligomerization of Vps11, I employed the same protocol on a GST-tagged version of Vps11 (Vps11-GST~145 kDa) along with the HA-tagged version of Vps11 (Vps11-HA~120 kDa). It is expected that addition of another tag differing in size will alter the apparent mobility of Vps11 on SDS-PAGE. I compared the molecular mass shifts between crosslinked and non-crosslinked proteins from vacuoles harboring Vps11-HA and Vps11-GST individually and observed that the crosslinked product in each case runs at exactly double the molecular mass of the non-crosslinked one confirming that Vps11 forms a homodimer (~240 kDa for Vps11HA/Vps11-HA and ~290 for Vps11-GST/Vps11-GST) as shown in figure 25 (lanes 1-4). Interestingly, upon crosslinking Vps11-HA and Vps11-GST together in a mixture, I did not observe any intermediate crosslinked product corresponding to Vps11-HA/Vps11-GST interaction (~265 kDa) (figure 25, lanes 5 and 6). This implies that there is only a preferred cis-interaction occurring between Vps11 molecules on apposed native membranes since no intermixing between the differently tagged Vps11 populations is seen. Trans-interactions, if any, cannot be detected at this level of sensitivity.

Cross-linking of vacuoles harboring C-terminal 6HA or GST/3HA tags on Vps11 was done as described in 2A.

Molecular weights in kDa are as marked. Vps11-HA (~120 kDa, lane 1) forms a higher molecular weight crosslinked product (~240 kDa, lane 2). Similarly Vps11-GST (~145 kDa, lane 3) forms a crosslinked product (~290 kDa, lane 4). A mixture of Vps11-HA and Vps11-GST (lane 5) shows two crosslinked products (~240 and 290 kDa, lane 6) identical to those observed in lanes 2 and 4, but no intermediate band.

To further verify whether the HOPS complex in general dimerizes in a trans configuration, I looked at inter-vacuolar HOPS interactions by employing Vps39-HA and non-tagged Vps39 versions. Vacuoles from the Vps39-HA strain and those from the wild type strain were mixed and incubated with or without ATP, solubilized and immunoprecipitated against the HA epitope (figure 26, lanes 1 and 2). Additionally, vacuoles from these two strains were separately solubilized and the solubilizates were then mixed to control for interactions forming in the immunoprecipitation buffer (figure 26, lane 3). The precipitates were separated on SDS-PAGE and immunoblotted using anti-Vps39 antibody. As depicted in figure 26, there is no significant increase in Vps39 co-precipitation efficiency over background levels proving the absence of any trans-HOPS dimers.

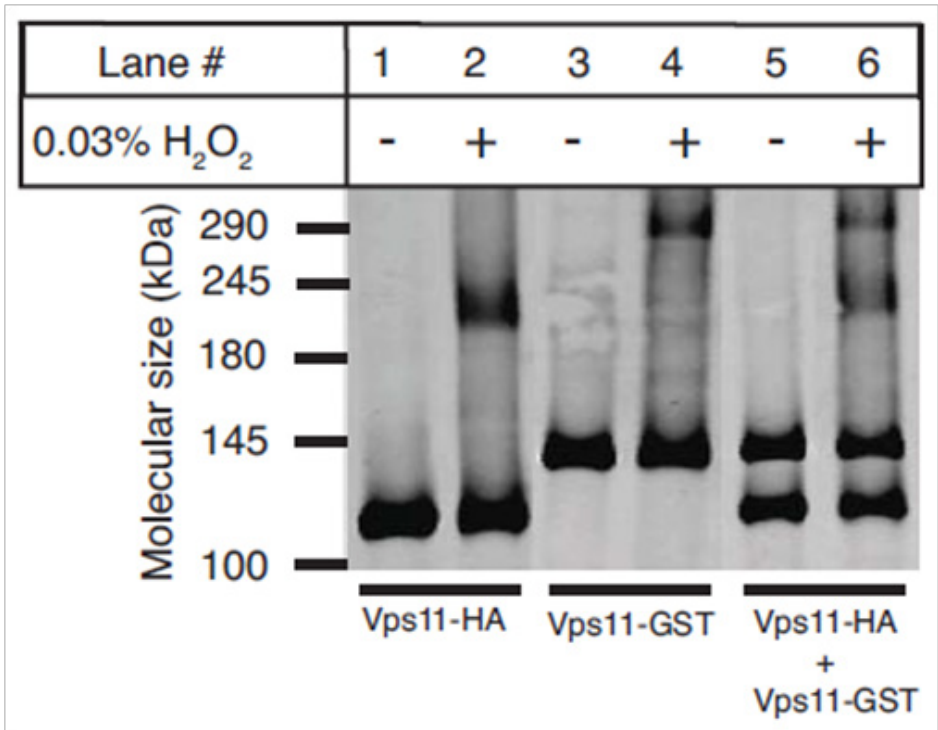


Figure 25: Chemical crosslinking of Vps11-HA and Vps11-GST.

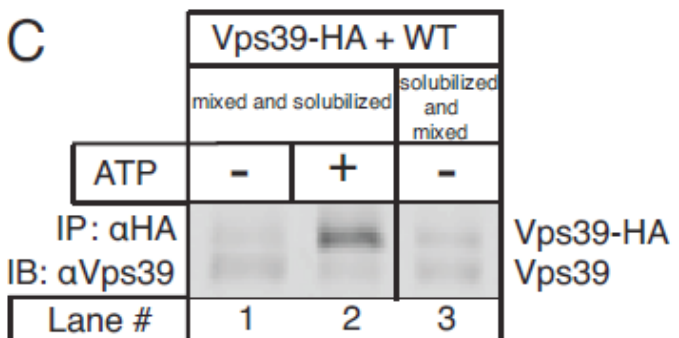


Figure 26: Test for trans-HOPS complexes assayed by Vps39 variants.

Vacuoles from Vps39-HA and wild type strains were processed as described in Materials and Methods. Vps39-HA was precipitated using anti-HA antibody and co-precipitating Vps39 was analyzed using SDS-PAGE and western blotting. Interactions between Vps39-HA and non-tagged Vps39 from the two fusion partners include those observed in the absence of ATP (lane 1), in the presence of ATP (lane 2) and in the solubilization buffer (lane 3).

HOPS catalyzes a Rab GTPase-dependent trans Qa-QbQcR SNARE complex establishment

Previous work from my lab had demonstrated that the ATPase Sec18/NSF creates an activated QbQcR cis-SNARE pool that serves as an acceptor subcomplex for the single Qa SNARE originating from the opposite membrane

[115]. It was shown that the HOPS complex and the Rab GTPase Ypt7 are necessary to maintain a stable QbQcR cis-SNARE subcomplex. Also we know that functional Ypt7 is necessary on each partner for successful homotypic vacuolar fusion [106]. This led me to inquire whether Ypt7 is involved in stabilizing trans-SNARE pairing. I used two approaches to alter Ypt7 and hence study its role on trans-SNARE complex establishment-(1) the Ypt7-T22N point mutant strain which delivers a GDP-locked inactive form of Ypt7 and (2) recombinant GDI (GDP dissociation inhibitor) which extracts Ypt7 from its membrane-bound form and thereby inactivates it. Trans-SNARE complexes are generated upon addition of ATP to purified vacuoles. Differential tagging of peptides allows us to distinguish interactions occurring on the same (cis) membrane

from those on opposing (trans) membranes. I adjusted the experimental conditions to be able to capture only trans-SNARE complexes and eliminate the possibility of obtaining any post-fusion cis-SNARE complexes. First I assayed for trans-SNARE complex formation between Vam3 (Qa) and Nyv1 (R) using differently tagged versions of these SNAREs. As displayed in **figure 27**, Vam3-HA vacuoles from the wild type strain were mixed with Nyv1-VSV vacuoles from either the wild type or the Ypt7-T22N point mutant strain and incubated with or without ATP. The

vacuole mixtures were solubilized and immunoprecipitated against the HA epitope. The precipitate was resolved on SDS-PAGE and western blotting using the indicated antibodies was performed to analyze the extent of trans-interactions. A clear trans-SNARE signal is observed in the presence of ATP where Nyv1 (R) from the wild type strain significantly co-precipitates with Vam3 (Qa) compared with that in absence of ATP (lanes 1 and 2). In contrast, Nyv1 (R) from the Ypt7-T22N strain is unable to form a trans-SNARE complex with Vam3 (Qa) (lanes 3 and 4).

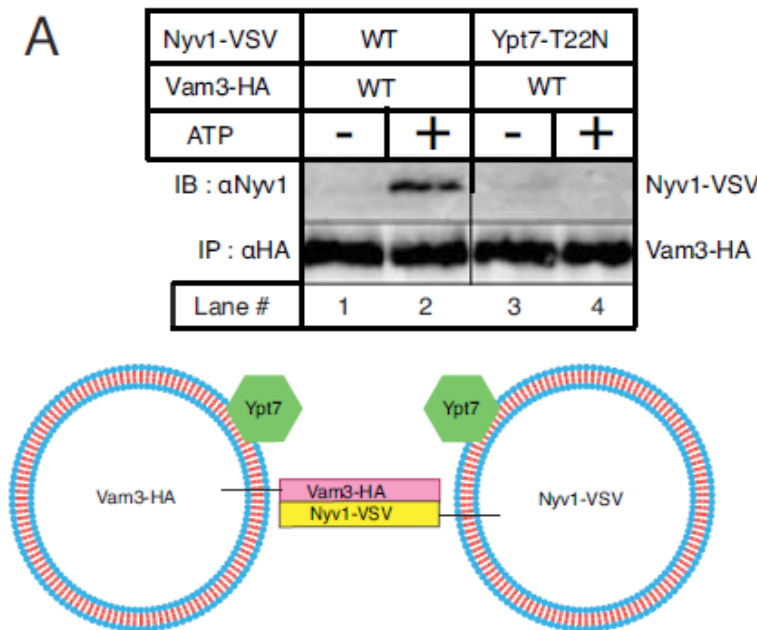


Figure 27: Trans-SNARE complexes assayed by tagged SNAREs.

Vam3-HA vacuoles from the wild type strain were mixed with Nyv1-VSV vacuoles from either the wild type strain (lanes 1 and 2) or the Ypt7-T22N strain (lanes 3 and 4) and incubated with or without ATP under standard fusion conditions. Vam3-HA was precipitated using Protein-G/anti-HA antibody and co-precipitating Nyv1-VSV was detected by SDS-PAGE and western blotting with antiNyv1 antibody. A trans-SNARE complex is observed only in the presence of ATP when both partners are wild type (lane 2) but not in a Rab mutant background for one of the partners (lane 4).

To further address the issue of requirement of Rab function on each fusion partner, I resorted to the following co-immunoprecipitation strategies involving HOPS, SNARE and Rab variants. As represented in figure 28, vacuoles were purified from the Vps16-HA strain deleted for the N-terminal region of Vam3, and mixed with vacuoles from either the wild type or the Ypt7-T22N strain. This combination allows us to make a distinction between the Qa SNAREs arriving from apposed fusion partners since full-length Vam3 runs higher on SDS-PAGE than its truncated form. It is known that the N-terminal truncation of Vam3 in both fusion

partners still permits complete trans-SNARE complex formation [76]. Therefore, it is justifiable to use this strain, although its fusion efficiency is not exactly comparable to wild type. The vacuole mixture mentioned before was solubilized and immunoprecipitated against the HA epitope. The precipitate was separated on SDS-PAGE and blotted against the indicated antibodies. I observed that Vam3 (Qa) originating from the wild type background co-precipitates significantly with Vps16-HA in an ATP-dependent manner recapitulating a classical trans-SNARE signal (lanes 1 and 2). Remarkably however, no Vam3 (Qa) from the Ypt7-T22N background is able to co-precipitate with Vps16-HA (lanes 3 and 4). Taken together, these results suggest that small G proteins are necessary for trans-SNARE formation on both fusion partners-one delivering a QbQcR SNARE subcomplex and the other delivering the Qa SNARE.

Vacuoles from the Δ N-terminal Vam3 strain harboring Vps16-HA were mixed with vacuoles from either the wild type strain (lanes 1 and 2) or the Ypt7-T22N strain (lanes 3 and 4) and incubated with or without ATP under standard fusion conditions. Vps16-HA was precipitated using

Chapter 2

Protein-G/anti-HA antibody and co-precipitating Vam3 was detected by SDS-PAGE and western blotting with antiVam3 antibody. Vam3 (trans-Qa SNARE) co-precipitates with Vps16-HA only in presence of ATP when both partners are

wild type (lane 2) but not in a Rab mutant background for one of the partners (lane 4). Lanes 5-8 show corresponding protein inputs.

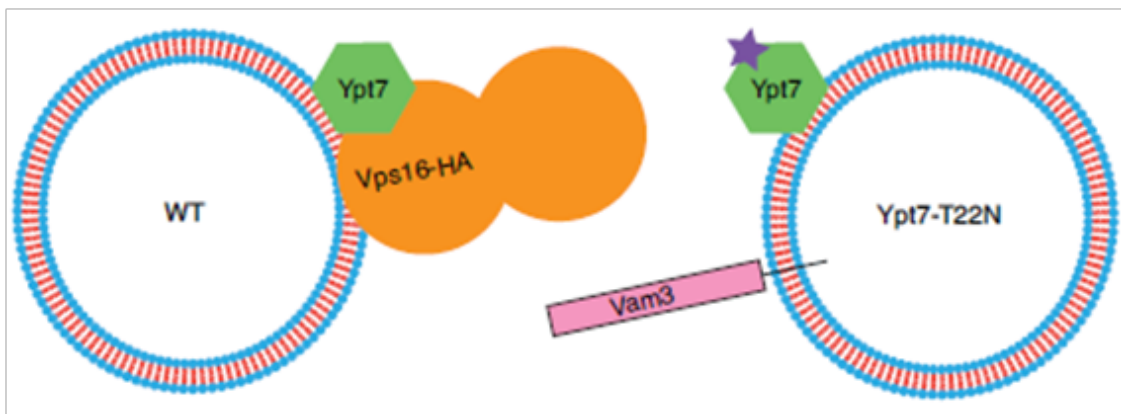
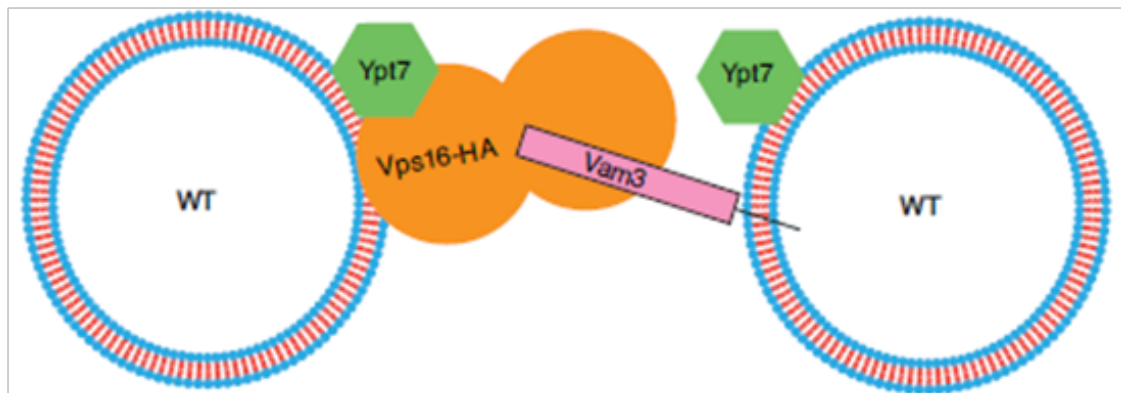
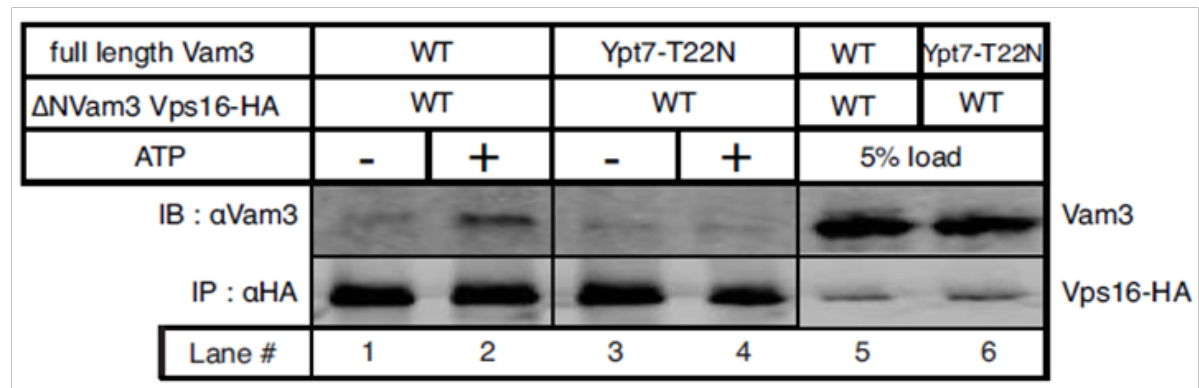


Figure 28: Trans-HOPS/Qa SNARE interactions.

To be able to assess HOPS-SNARE topology more completely, I used vacuoles from the Vps16-HA strain deleted for the N-terminal region of Vam3 in combination with vacuoles from the Nyv1-VSV strain. This permits us to distinguish Qa and R SNAREs originating from each fusion partner. Also, using GDI as a Ypt7 inactivating

agent it is simultaneously possible to assay for Rab protein requirement for the process. As illustrated in figure 29, vacuoles from the two strains mentioned above were mixed and incubated in the presence of ATP only or both ATP and GDI, solubilized and immunoprecipitated against the HA epitope. The precipitate was resolved on SDS-PAGE and

analyzed by western blotting using the indicated antibodies. In the presence of ATP, Vps16-HA preferentially interacts with Nyv1 in cis and with full length Vam3 in trans (lane 1). The co-precipitation efficiencies of both these SNAREs diminish significantly in the presence of GDI (lane 2).

Vacuoles from the DN-terminal Vam3 strain harboring Vps16-HA were mixed with vacuoles from the Nyv1-VSV strain and incubated with ATP alone (lane 1) or both ATP and GDI (lane 2) under standard fusion conditions. Vps16-HA was precipitated using Protein-G/anti-HA antibody and co-precipitating SNAREs were analyzed by SDS-PAGE and western blotting against the indicated proteins. Full length

Vam3 (trans Qa SNARE) and Nyv1 (cis R SNARE) co-precipitate with Vps16-HA in an ATP-dependent manner as. Lane 3 shows corresponding protein inputs.

It is worthwhile to note that the reciprocal Qa (truncated Vam3) and R (Nyv1-VSV) SNAREs are not detectable in the HOPS precipitation indicating selective recruitment of SNAREs to the HOPS complex in preparation for trans-SNARE complex formation. These results, in conjunction with previous studies describing the existence of a stable QbQcR cis-SNARE subcomplex, lead to a model of HOPS dimer-mediated assembly of a QbQcR-Qa trans-SNARE complex.

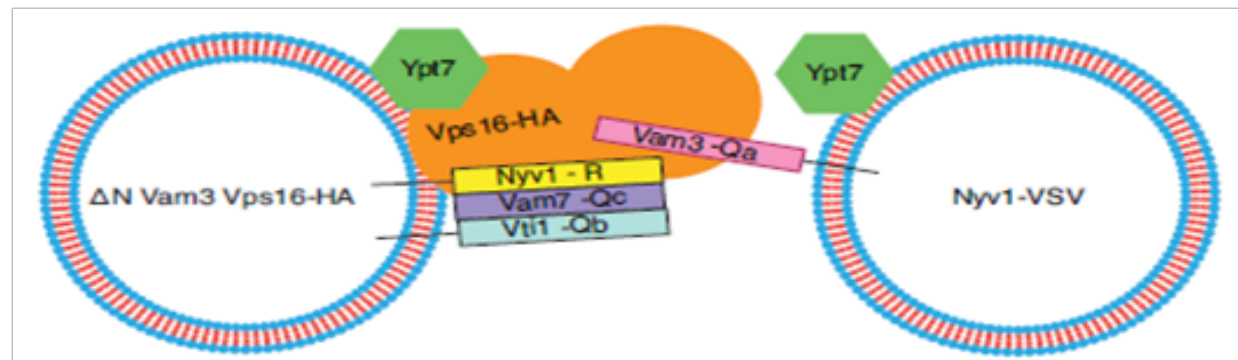
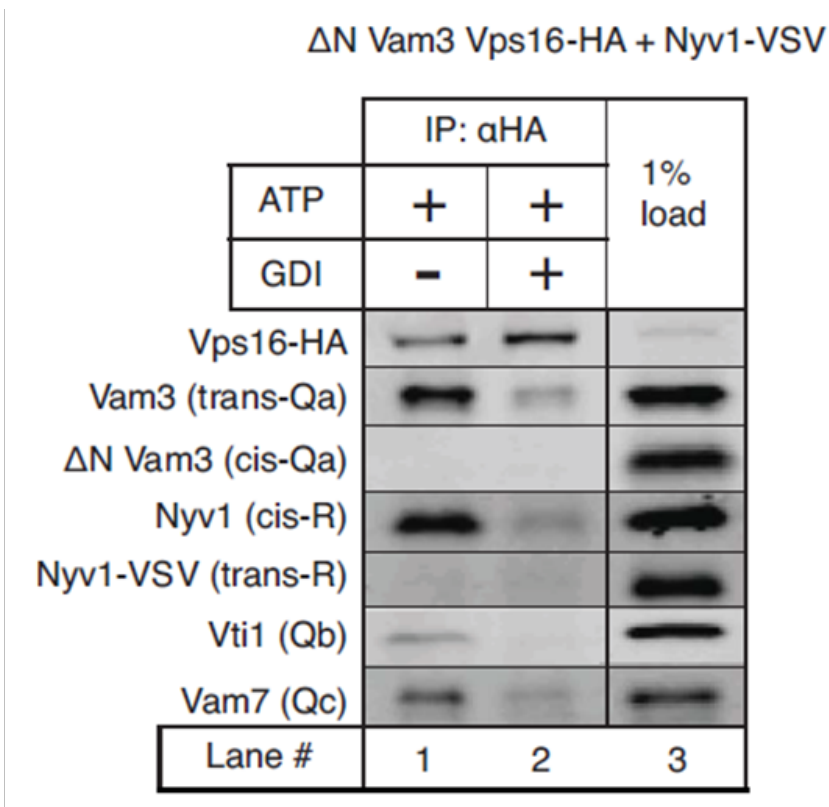


Figure 29: HOPS-SNARE topology.

Chapter 2

Discussion

It has been reported that there is promiscuity and diversity in SNARE-SNARE associations [5,7,119,120]. Unrestricted pairing of SNAREs by random chance in a cell where continuous membrane flux is required between dynamically evolving compartments would create tremendous disturbances in overall homeostasis, including inappropriate cargo delivery and premature protein turnover to cite a few. This makes the pathway leading to trans-SNARE complex formation a critical target for regulation.

SNARE-driven membrane fusion serves different functions at different locations in a cell, ranging from neurotransmitter release to phagosome maturation. The kinetics of each fusion event must therefore be adjusted by local factors and trans-SNARE distribution influences their fusion efficiency as we have demonstrated in our previous functional studies. Also, figure 27 implies that mere existence of SNAREs on opposing membranes is not sufficient for the formation of trans-SNARE complexes. Hence, orientation of the relevant SNARE topology at the appropriate location in a cell becomes an important aspect to be governed by additional factors. The requirement for SNAREs to function as the sole determinants of fusion specificity is not absolutely critical since a number of factors, by virtue of their size, abundance or localization, can see each other upstream of trans-SNARE pairing. Faithful membrane fusion would require one or more agents to exercise stringent control over and dictate specific channelization of SNARE molecules entering into trans-complexes. Based on this study, the dimeric HOPS tethering complex and the activated Rab GTPase Ypt7 appear as prime candidates having an intrinsic or acquired capability to perform this job.

Various lines of evidence seem to support my general idea that control over trans-SNARE complex formation occurs through collaborative action of tethers and Rabs, and that interactions among different tethering factors and the corresponding Rab proteins sets up the stage for SNARE-driven fusion. In the context of physiological membranes the vesicle tethering protein p115 was biochemically shown to selectively catalyze the assembly of Gos28 (v-SNARE) and syntaxin5 (t-SNARE) during NSF-driven Golgi reassembly. The syntaxin binding SM(Sec1/Munc18) family member Sly1 also coprecipitated in this complex [34]. Another study demonstrated a Rab1-mediated recruitment of p115 to COPII vesicles on which the cis-complex of cognate v-SNAREs was stabilized [31]. In these reports, however, trans-SNARE complex formation and topology were not explicitly assayed. Studies on heterotypic fusion involving ER-derived COPII vesicles and the Golgi hint toward a QbQcR-Qa trans-SNARE distribution with the Qa SNARE acting from the Golgi membrane although each membrane contains the full complement of SNAREs [121]. The asymmetry in SNARE function was suggested to be caused by an asymmetric requirement for functional Rab GTPase Ypt1 and the SM family protein Sly1 specifically on the Golgi compartment suggesting a possible role of these factors in contributing to fusion specificity.

Purified HOPS, when added to SNARE-reconstituted proteoliposomes, was recently shown to accelerate their fusion [122] and HOPS was proposed to be the direct agent of tethering, but evidence for a pathway of HOPS-mediated trans-SNARE complex formation is lacking. It was shown using a liposome-based system that an endosomal Rab GTPase can dimerize in trans with itself to tether membranes [123]. However, in contrast to typical multisubunit or elongated coiled-coil tethering factors, the scope for small G proteins to function as tethering agents solely by themselves appears rather limited by their overall size and surface area available for orchestrating multifarious sequential interactions. Studies involving purified SNAREs, HOPS and Rabs reconstituted into synthetic liposomes do provide critical clues about probable functions of these fusion elements along with mechanistic insights [123-125]. However, to be able to firmly establish and extrapolate fundamental mechanisms underlying membrane fusion, evidence from model systems incorporating physiological membranes is essential.

Studies on rat liver Golgi membranes have shown that the coiled-coil tether Golgin-84 on COPI vesicles interacts with the cis-Golgi localized heterooctameric COG (conserved oligomeric Golgi) complex through its Cog7 subunit and it was suggested that this tether-tether interaction in trans may aid SNARE complex formation [125]. EEA1 (early endosomal antigen 1), the rod-like coiled coil tether functioning on endosomes was shown to form a parallel coiled coil dimer [126]. Importantly, EEA1 (both recombinant and that derived from rat brain) can be crosslinked to yield a product with double the molecular mass of the monomer. It contains an N-terminal Zinc finger, a C-terminal PI(3)P binding FYVE domain and two binding sites for a GTP-bound form of Rab5-one at the N-terminal and other at the C-terminal. It was postulated in this study that the EEA1 dimer was likely to link Rab5-enriched compartments to each other. TRAPP II is a tethering complex composed of ten different subunits localized at the Golgi network. Native TRAPP II purified from yeast was found to exist predominantly in dimeric form as judged by the 2-fold symmetry apparent in negatively stained electron micrographs [127]. Also gel filtration studies have shown that TRAPP II elutes at approximately twice the value of molecular masses of its individual components [128]. However, it remains to be determined whether this TRAPP II dimer is able to link native membranes via interactions with Rab GTPases or SNAREs.

Experiments on HOPS subunits implicate Vps39 and Vps41 in Rab recognition and emphasize that Vps11 functions as a platform for HOPS complex assembly with its C-terminal RING domain being functionally critical for traffic to the vacuole [81]. A recent advance illustrated the cryo-EM structure of the HOPS complex stating that HOPS is a flexible, seahorse-like structure, 28-35 nm long, and was not found to exist as a dimer [129]. To account for previously reported interactions and modes of action of HOPS, it was suggested that HOPS could oscillate between different conformations that bring its head (Vps41, Vps33) and tail (Vps39) subunits closer or farther to accommodate binding

partners, especially Ypt7 and SNAREs. We conceptualize that a HOPS dimer assimilating this behavior can indeed sequentially stabilize a QbQcR cis-SNARE complex (likely on one HOPS complex in the dimer); execute, in concert with Ypt7 from trans, long-range membrane recognition and tethering over tens of nanometers (likely through Vps39/Vps41 on the partner HOPS complex in the dimer); followed by topologically regulated QbQcR-Qa trans-SNARE complex assembly (likely through Vps33).

According to the homotypic model depicted in figure 30, a fusion reaction starts out with identical fusion partners each possessing a full complement of the tetrameric cis-SNARE complex. Upon Sec18/NSF-induced activation of SNAREs in the presence of ATP, a HOPS dimer, accompanied by activated Ypt7 in cis, coordinates a stable QbQcR cis-SNARE complex having displaced the Qa SNARE.

The HOPS dimer recognizes activated Ypt7 in trans and incorporates the single Qa SNARE from the apposed fusion partner ultimately catalyzing Rab-dependent assembly of a QbQcR-Qa trans-SNARE complex.

Each fusion partner (vacuole) is exactly identical and possesses similar fusion machinery including four vacuolar SNAREs, a HOPS dimer and Ypt7. In the presence of ATP, the HOPS dimer along with Ypt7 in cis coordinates a QbQcR acceptor subcomplex having displaced the Qa SNARE. A HOPS dimer on one fusion partner (left) recognizes activated Ypt7 on the opposing fusion partner (right) and incorporates the single Qa SNARE from the opposing partner. Ultimately a HOPS dimer-dependent QbQcR-Qa trans-SNARE complex is assembled. HOPS subunits are color coded throughout.

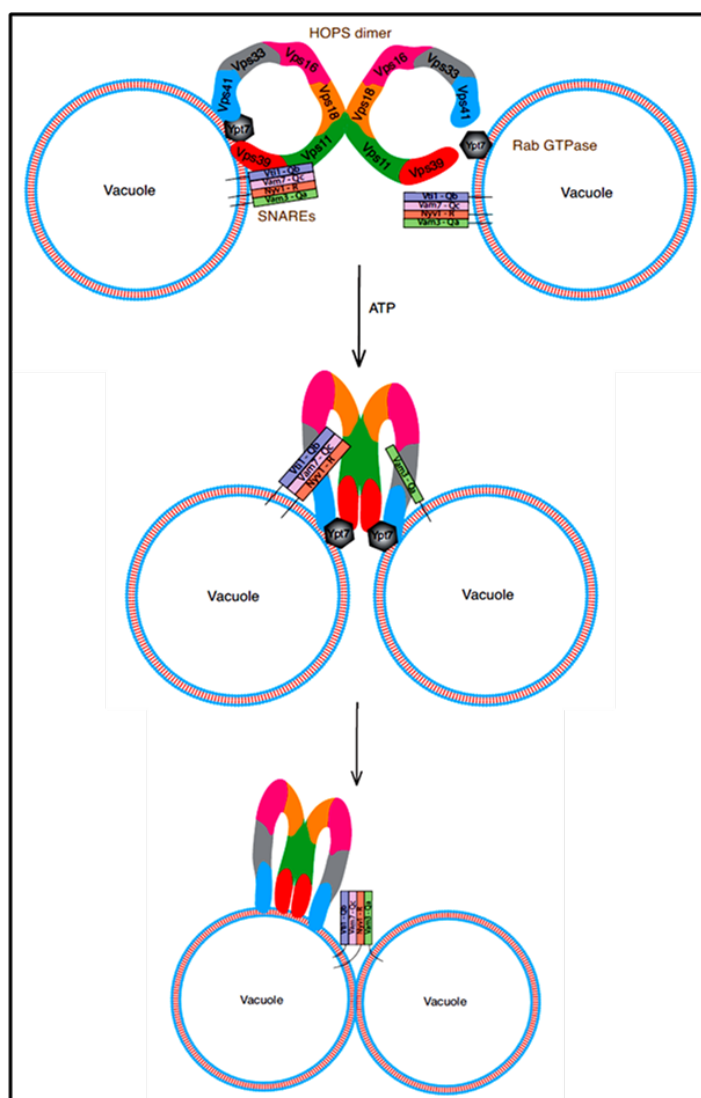


Figure 30: Working model for trans-SNARE complex establishment in homotypic fusion.

Similarly a model explaining trans-SNARE complex formation in a more general heterotypic scenario can be proposed as shown in figure 31. Each fusion partner possesses its own distinct fusion machinery consisting of SNAREs, tethering factors and Rab proteins. Here, initial recognition of apposed membranes is likely to occur through interaction between their cognate tethering complexes in trans. Functional Rab proteins are required

on both membranes for the heterogeneous tether dimer to be able to coordinate trans-SNARE complex assembly. Since the tethers and Rabs are already dissimilar on each fusion partner as opposed to homotypic fusion, asymmetry in SNARE pairing becomes intrinsic. Eventually the tether dimer organizes a QbQcR-Qa trans-SNARE complex leading to fusion.

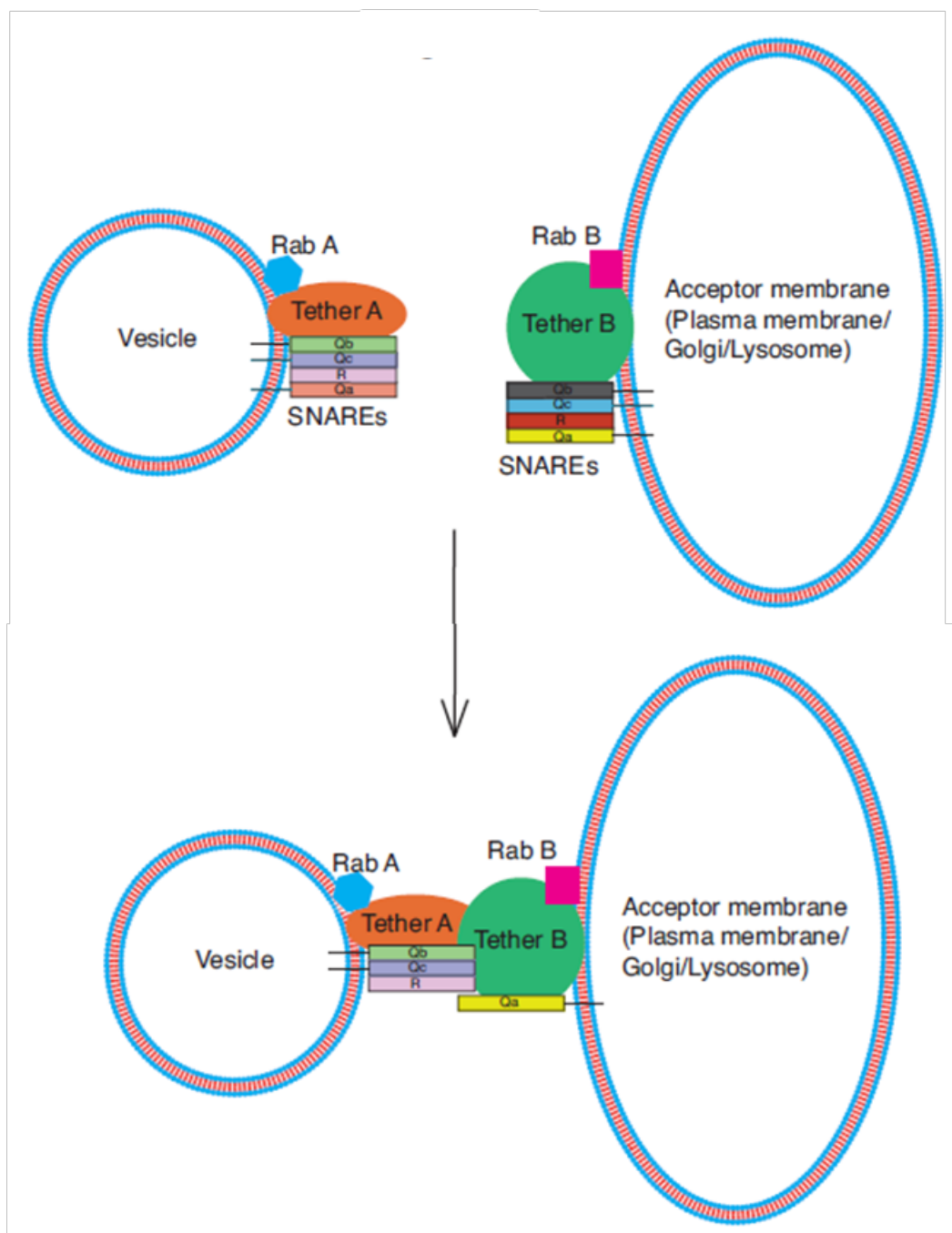


Figure 31: Proposed model for trans-SNARE complex establishment in heterotypic fusion.

Each fusion partner possesses its own distinct set of fusion factors. Initial recognition between the non-identical fusion partners (vesicle and plasma membrane for example) is likely to occur through interaction between their cognate tethering complexes. This heterogeneous tether dimer catalyzes the formation of a QbQcR-Qa trans-SNARE complex in the presence of functional Rab GTPases on each partner.

Altogether my results suggest that both recognition of the appropriate fusion partner as well as coordination of a preferred trans-SNARE topology by a common Rab GTPase-dependent tether-tether scaffold may be a general mechanism that leads to homotypic and heterotypic fusion events.

Chapter 3

**The dynamin homolog Vps1 promotes
the transition from hemifusion to content
mixing in yeast vacuolar fusion**

Chapter III

The dynamin homolog Vps1 promotes the transition from hemifusion to content mixing in yeast vacuolar fusion

Portions of this work have been published in Kulkarni A, Alpadi K, Sirupangi T, Peters C (2014) A dynamin homolog promotes the transition from hemifusion to content mixing in intracellular membrane fusion. *Traffic*, doi: 10.1111/tra.12156.

Introduction

SNARE proteins are central players mediating membrane fusion reactions and are hence crucial for diverse functions including synaptic transmission/endocrine secretion involving vesicle fusion with the plasma membrane and subsequent release of neurotransmitter/hormone, as well as organelle maturation associated with immune responses, apoptosis and cell division. Fusion in the endomembrane system occurs between cognate sets of v- (vesicular or R) and t- (target or Qa, Qb and Qc) SNAREs [21]. The trans-SNARE complex is a four-helix bundle composed of a complementary set of zippered SNAREs from opposing membrane compartments and is a pre-requisite for membrane fusion. Subsequently, a hemifused state is formed in which only outer leaflets of lipid bilayers merge but inner leaflets remain separated [130]. Lipid bilayer destabilization during docking and lipid mixing leads to opening and enlargement of a fusion pore resulting in content mixing. Inadequate accessibility of stable SNARE complexes has impeded the determination of their interactions with potential regulatory factors and in conjunction, the counting of SNAREs needed for membrane fusion. Achieving appropriate fusion levels satisfying the functional demand makes SNARE proteins and trans-SNARE pairing important target elements for regulatory factors. Determining the number of SNARE complexes needed for fusion therefore becomes a crucial question.

Involvement of the core fission component dynamin and related proteins in exocytosis and other fusion reactions has only been recently explored and is awaiting mechanistic explanations [68, 130-132]. Dynamin is typically known to polymerize into rings and form collar-like constrictions of membranes [43]. This results in membrane deformation leading to the hemifused state from the opposite direction compared to that in fusion. The yeast dynamin homolog Vps1 (Vacuolar Protein Sorting 1) is a dynamin-related protein involved in vesicle trafficking along the secretory and endocytic pathways converging at the vacuolar compartment [133]. Vps1 consists of an N terminal GTPase domain, a middle domain and a C terminal GTPase Effector/Assembly Domain (GED) [42]. It was suggested that Vps1 exercises control over the fusion reaction likely because a population of the t-SNARE Vam3 was observed to comigrate with a high molecular weight complex containing Vps1 [70]. I was therefore curious to investigate whether the oligomerization of Vps1 is somehow able to determine t-SNARE availability

at the fusion site. The implication of the dynamin homolog Vps1 in controlling late stages in yeast vacuole fusion will provide a new insight into the regulation of SNARE complex assembly and lipid bilayer merger. It is indeed intriguing to learn how Vps1 contributes as a SNARE channelizing agent to accomplish fusion.

Materials and Methods

Yeast strains: BJ3505 or DKY6281 yeast strains used in this study carried the Δ vps1 background and were transformed with plasmid encoding either vps1 wild type or mutants. Vps1 alleles were expressed from the plasmid with the backbone pRS416.

Vacuole purification: BJ3505 or DKY6281 yeast strains were grown in YPD at 30 °C at 150 rpm to OD600 = 2 and harvested (3 min, 5,000 g). Cell walls were hydrolyzed by lyticase, recombinantly expressed in E. coli RSB805 (provided by Dr Randy Schekman, Berkeley), and prepared from a periplasmic supernatant. Harvested cells were resuspended in reduction buffer (30 mM Tris/HCl pH 8.9, 10 mM DTT) and incubated for 5 min at 30°C. After harvesting as described above, cells were resuspended in 15 ml digestion buffer (600 mM Sorbitol, 50 mM K-phosphate pH 7.5 in YP medium and 0.1 mg/ml lyticase). After 20 min at 30 °C, cells were centrifuged (1 min, 5,800 rpm in JLA25.5 rotor). The spheroplasts were resuspended in 2.5 ml 15% Ficoll-400 in PS buffer (10 mM PIPES/KOH pH 6.8, 200 mM Sorbitol) and 200 μ l DEAE-Dextran (0.4 mg/ml in 15% Ficoll-400 in PS). After 90 sec of incubation at 30°C, the cells were transferred to SW41 tubes and overlaid with steps of 8%, 4% and 0% Ficoll-400 in PS. Cells were centrifuged for 60-75 min at 2 °C and 30,000 rpm in an SW41 rotor.

Content mixing assay: DKY6281 and BJ3505 vacuoles were adjusted to a protein concentration of 0.5 mg/ml and incubated in a volume of 30 μ l PS buffer (10 mM PIPES/KOH pH 6.8, 200 mM Sorbitol) with 120 mM KCl, 0.5 mM MnCl₂, 1mM DTT. Inhibitors or recombinant proteins, if any, were added before starting the fusion by addition of the ATP-regenerating system (0.25 mg/ml creatine kinase, 20 mM creatine phosphate, 500mM ATP, 500 mM MgCl₂). After 60 min at 27 °C, or on ice, 1ml of PS buffer was added, vacuoles were centrifuged (2 min, 20,000g, 4 °C) and resuspended in 500 μ l developing buffer (10 mM MgCl₂, 0.2% TX-100, 250 mM Tris/HCl pH 8.9, 1 mM p-nitrophenylphosphate). After 5 min at 27 °C, the reactions were stopped with 500 μ l 1M glycine pH 11.5 and the OD was measured at 400 nm.

Rh-PE labeling of vacuoles: Rhodamine labeled 1,2-dihexadecanoyl-sn-glycero-3-phosphoethanolamine (Rh-PE, Molecular Probes) does not readily dissolve in DMSO. I added 1.25 ml of analytical grade DMSO (Sigma-Aldrich, D8418) per 5mg Rh-PE (3mM solution) and incubated the preparation (1h, 37 °C) under occasional vortexing. Once Rh-PE had completely dissolved, 80- μ l aliquots were prepared and stored in 1.5 ml tubes at -20 °C. Rh-PE aliquots were thawed and shaken at 37 °C and 1,400 r.p.m. for 20 min. Rh-PE aliquots were centrifuged (15 min at room temperature, 13,100g) to pellet

Chapter 3

aggregated Rh-PE. The supernatant was used immediately for labeling. A total of 560 μ g of freshly prepared vacuoles were equilibrated to 32 °C in 800 μ l PS buffer (10mM PIPES/KOH pH6.8, 200mM Sorbitol) in 1.5 ml tubes for approximately 40 sec at 500r.p.m. 60 μ l of the Rh-PE solution was withdrawn, carefully avoiding the pelleted Rh-PE, and added to the equilibrated vacuoles in a drop-wise fashion under gentle vortexing. The tube was incubated in a water bath at 27 °C for 30 s. A total of 500 μ l of PS buffer with 15% (w/v) Ficoll (pre-warmed to 27 °C) was added, the suspension was gently mixed and transferred to a siliconized 2 ml tube (pre-cooled on ice). For pipetting, 1 ml Gilson tips were cut open in order to minimize shear forces on the vacuolar membranes. Vacuoles were overlaid with 200 μ l of PS buffer containing 4% (w/v) Ficoll (27 °C) and 500 μ l PS buffer containing 0% (w/v) Ficoll (27 °C). The gradient was centrifuged (5 min, 3 °C, 11,700g, swingout rotor) with slow acceleration and deceleration. Stained vacuoles were recovered from the 0%/4% Ficoll interface.

Lipid mixing assay: BJ3505 vacuole fusion reactions with a volume of 180 μ l and a final vacuole concentration of 0.25 mg/ml were set up as follows: 120 μ l vacuole mastermix in PS buffer was supplemented with 0.3 mM MnCl₂ and 110 mM KCl. Inhibitors or recombinant proteins, if any, were premixed in 60 μ l PS with 110 mM KCl and 0.3 mM MnCl₂. A total of 60 μ l inhibitor mix were added to 120 μ l vacuole mastermix, supplemented with 9.5 μ l of 20X ATP-regenerating system and gently vortexed. 100 μ l reaction mix was pipetted into non-coated black 96-well plates pre-cooled to 0 °C. Air bubbles were avoided by not completely ejecting the suspension from the tips. The microtitre plate was pre-treated immediately before use with 5% (w/v) skim-milk powder in water (1 h). The plate was washed, dried and cooled on ice. Fluorescence change was measured with a FlexStation3 fluorescent microplate reader (Molecular Devices) at 27 °C, at wavelengths of 538 nm excitation and 585 nm emission. Measurements were taken every 2 min for a total time of 30 min, yielding fluorescence values at the onset (F_0) and during the reaction (F_t). After completion of the reaction, 100 μ l of PS with 1% (w/v) Triton X-100 was added. Fluorescence was followed for 10 min, taking measurements every 30 sec. The 20 measurements, which showed a small decrease, were averaged to yield fluorescence after infinite dilution (F_{TX-100}). The relative fluorescence change $\Delta F/F_{TX-100} = (F_t - F_0)/F_{TX-100}$ was calculated for every time point t. F_{TX-100} was invariant over time; that is, F_{TX-100} values were comparable when Triton X-100 was added before or after the fusion reaction. Therefore, F_{TX-100} taken at the end of the fusion reaction was used as a reference for all time points.

Trans-SNARE assay: Vacuoles were adjusted to a protein concentration of 0.5 mg/ml. The total volume of one assay was 1 ml containing equal amounts of the two fusion partners in PS buffer with 125 mM KCl, 0.5 mM MnCl₂ and 1 mM DTT. Mixed vacuoles were incubated for 5 min at 27 °C in the absence of ATP. The fusion reaction was started by adding ATP-regenerating system (0.25 mg/ml creatine kinase, 20 mM creatine phosphate, 500 mM ATP, 500 mM

MgCl₂). After 30 min at 27 °C, the vacuoles were centrifuged for 2 min at 4 °C at 20,000g. The pellet was resuspended in 1.5 ml solubilization buffer (1% Triton, 50 mM KCl, 3 mM EDTA, and 1 mM DTT in PS). After centrifugation for 4 min at 4 °C (20,000g), the supernatant was incubated with 30 μ l Protein G beads (Roche) and 15 μ g anti-HA antibody (Covance, mouse monoclonal) for 1 h at 4 °C with gentle shaking. The Protein G beads were washed three times with 50 mM KCl, 0.25% Triton, 3 mM DTT and 3 mM EDTA in PS buffer, and incubated for 5 min at 60 °C in 2X reducing SDS sample buffer.

HOPS precipitation assay: Vacuoles were isolated from BJ3505 wild type and Vps1 mutant strains harboring Vps11-HA. Subsequently, the vacuoles were solubilized in buffer containing 100 mM KCl, 500 mM MnCl₂ and 1% Triton X-100. The samples were centrifuged at 20,000g for 10 min, and 10 μ g of anti-HA antibody (Covance) and Protein G beads were added to the solubilize. After incubation for 1 h at 4 °C with end-to-end rotation, the samples were centrifuged for 1 min and the beads were washed twice with solubilization buffer. SDS sample buffer was added to the beads and incubated at 90 °C for 2 min. The eluted proteins were separated by SDS-PAGE and analyzed by western blotting with the indicated antibodies.

Sec17 immunodepletion protocol: Vacuoles were isolated from BJ3505 wild type and Vps1 mutant strains. Vacuoles in PS buffer containing 100 mM KCl and 500 mM MnCl₂ were solubilized with 0.5% Triton X-100. The samples were exposed without centrifugation to 15 μ g of anti-Sec17 antibody and Protein G beads. After incubation for 1 h at 4 °C with end-to-end rotation, the samples were centrifuged for 1 min to remove anti-Sec17 bound material. Fresh protein G beads were then added to remove traces of anti-Sec17 and its bound content from solubilized vacuoles. The samples were centrifuged for 1 min and the supernatant was analyzed by SDS-PAGE followed by western blotting using anti-Vam3 antibody.

Vam3 precipitation assay: Vacuoles were isolated from BJ3505 wild type and Vps1 mutant strains. Vacuoles in PS buffer were solubilized in buffer containing 100 mM KCl, 500 mM MnCl₂, 0.25% Triton X-100 and 10% Glycerol. The samples were centrifuged at 20,000g for 10 min, and 10 μ g of anti-Vam3 antibody and Protein A beads were added to the solubilize. After incubation for 1 h at 4 °C with end-to-end rotation, the samples were centrifuged for 1 min and the beads were washed twice with solubilization buffer. SDS sample buffer was added to the beads and incubated at 90 °C for 2 min. The eluted proteins were separated by SDS-PAGE and analyzed by western blotting with the indicated antibodies.

Protein expression and purification: His-tagged Vps1 (wild type and mutants) was expressed in SoluBL21 cells (Genlantis) by induction with 1 mM IPTG for 6 hours at 30 °C for wild type and for 48 hours at 25 °C for mutants. Pelleted cells were resuspended in buffer (20 mM HEPES, 500 mM NaCl, pH 7.4), and the protein was purified using Protino Ni-TED resin (Macherey-Nagel) packed in a column (Thermo

Scientific). Vps1 was concentrated and buffer exchanged in a centrifugal filter device (Amicon Ultra, Millipore) into PS buffer. Approximately 10 mg for wild type and 0.5 mg for mutants was obtained from 1 liter of cell culture.

FM4-64 labeling of vacuoles *in vivo*

BJ3505 cells from the different Vps1 strains were grown to logarithmic phase in YPD. They were treated with 10 μ M FM4-64 (Invitrogen) for 30 min at 30 °C and subsequently chased for another 90 minutes. The cells were washed with fresh YPD, resuspended and mounted on a glass slide in sterile water.

Microscopy

Images were taken from a Leica TCS SP5 confocal microscope using an argon laser and at 60X magnification

through the TRITC channel. Images were exported as TIFF files.

Results

Vps1 mutations employed in this study

Crystal structures of mammalian dynamin1 and human dynamin1-like protein DNM1L have identified interfaces in the GED that are critical for self-oligomerization. I utilized the available crystal structure of mammalian dynamin [49] as a template to create mutations in Vps1. Importantly, yeast Vps1 can model mammalian dynamin reasonably well since they share ~45% overall sequence homology and >70% sequence homology within known dynamin oligomerization interfaces. Figure 32 shows shared features among dynamin family members.



Figure 32A: Structure and sequence comparisons among dynamin family members. Homology-based structural model comparing bacterial dynamin and yeast Vps1 (both as monomers).

dDynamin	651	ETIRNLVDSYMKIVTKTTRDMVPKAIMMLI	INNAKDFINGELLAHLYASGDQAQMMEESAESATRREE	718
ceDynamin	654	ETIRNLVDSYMRRIITKTIKDLVPKAVMHLIVNQTGEFMKDELLAHLYQCGDTDALMEESQIEAQKREE		721
mDynamin	660	ETIRNLVDSYMAIVNKTVRDLMPKTIMHLMNNNTKEFIFSELLANLYSCGDQNTLMEESAEQAQRRE		727
yeastVps1	619	EVIKLILLSSYFSIVKRTIADIIPKALMLKLIVKSKTDIQKVILLEKLYGKQDIEELTKENDITIQRRE		686

Figure 32B: Sequence alignment of yeast Vps1 (GED residues 619-686) with dynamin family members.

The following image depicts an alignment of the known crystal structure of bacterial dynamin shown in pink and the predicted structure of yeast Vps1 shown in grey, with a portion of the GED of Vps1 highlighted in the yellow box. The residues Y628, K642 and I649 are situated within this region.

Organisms include *Drosophila melanogaster* (dDynamin), *Caenorhabditis elegans* (ceDynamin) and *Rattus norvegicus/Homo sapiens* (mDynamin). Residues conserved across multiple species and chosen for mutation are highlighted in green.

Chapter 3

The mammalian dynamin crystal structure revealed conserved residues in the GED (i) making critical hydrogen bonds that hold the oligomer together - these include mammalian dynamin K863 (homologous to yeast Vps1 K642) and mammalian dynamin Y669 (homologous to yeast Vps1 Y628) and (ii) likely to participate in hydrophobic interactions that promote self-assembly - for example, mammalian dynamin I690 (homologous to yeast Vps1 I649). The I649K Vps1 mutant was chosen based upon its plasma membrane invagination defects during endocytosis and was characterized as a polymerization-deficient mutant [67]. It is important to note that mammalian dynamin I690 is located at an oligomerization interface different from mammalian dynamin K683 and Y669. These two groups of amino acid residues also mediate oligomerization by different means - either through hydrophobic interactions or hydrogen bonding. Hence certain phenotypic differences may be expected between these two groups. The homologous residues in yeast Vps1 were mutated to other amino acids to potentially disrupt the hydrogen bonding or hydrophobic interactions between Vps1 monomers at that position. Hence the Vps1 mutants created were K642L (Leucine introduces a neutral residue and removes the original positive charge of Lysine 642) and Y628F (replacement with Phenylalanine removes the hydrogen bond forming phenolic -OH group from Tyrosine 628), in addition to

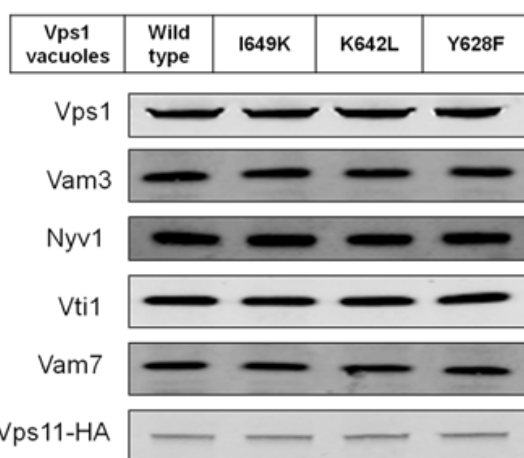
I649K (Lysine adds a positive charge and decreases the hydrophobicity at yeast Vps1 Isoleucine 649 and thereby aims to disrupt any hydrophobic interaction that I649 likely mediates). The Vps1 mutants used in this study therefore are: I649K, K642L and Y628F. I measured the effect of these single-point Vps1 mutations on (i) sequential stages in the vacuole fusion cascade, (ii) Vps1 oligomerization capacity and (iii) binding affinity and complex formation with the t-SNARE Vam3.

Specific point mutations in the Dynamin homolog Vps1 affect critical intermediates in yeast vacuolar membrane fusion

The most straightforward way to assess the involvement of a particular player in the fusion of yeast vacuoles is to study the effect of its deletion or mutation on one or both fusion partners in a colorimetric ATP-driven content mixing assay [63]. This assay depends upon the maturation of a reporter enzyme, Alkaline Phosphatase. The Vps1 mutant vacuoles were tested for protein levels and reporter enzyme activity at the outset (figure 33) and were comparable to wild type levels.

In general, each Vps1 mutation impaired vacuolar content mixing (figure 34).

A



B

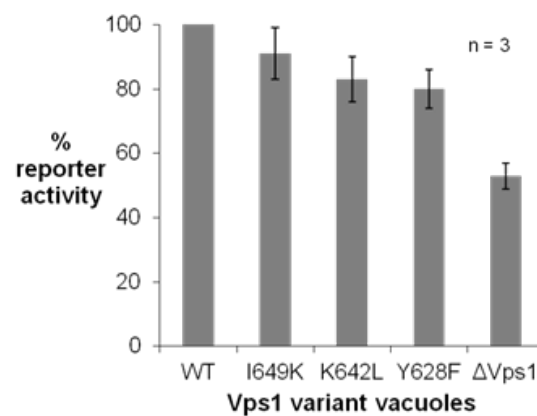


Figure 33: Comparison of protein levels and reporter activity among Vps1 wild type and mutant vacuoles.

- Vacuoles were purified from Vps1 variant strains, resuspended in PS buffer (20 mM Sorbitol, 10 mM PIPES pH 6.8) and resolved on SDS-PAGE. Western blot analysis was then performed to compare protein levels of Vps1, Vam3, Nyv1, Vam7, Vti1 and Vps11.
- To control for reporter enzyme (Alkaline phosphatase) activity, fusion reactions were carried out in the presence of TX-100.

I649K Vps1 vacuoles displayed ~30% fusion activity while K642L and Y628F Vps1 vacuoles showed almost no fusion relative to wild type Vps1 vacuoles. If a fusion defect is observed it is possible to locate the exact cause of the defect by sequentially assaying the stages upstream of content mixing, specifically lipid mixing and trans-SNARE complex formation.

There is an established hemifusion assay that measures the rate and extent of lipid mixing between the outer leaflets of fusing vacuoles [130]. Lipid mixing was measured using Rhodamine-Phosphoethanolamine (Rh-PE) labeled and unlabeled vacuoles prepared from each Vps1 strain. Rh-PE on labeled vacuoles is present in a self-quenching concentration and only emits weak fluorescence. When

mixed with unlabeled vacuoles, Rh-PE disperses from labeled to unlabeled membranes and is dequenched leading to rise in fluorescence emission, as illustrated in figure 35.

Vps1 mutant vacuoles surprisingly exhibited substantial (~55%) lipid mixing relative to wild type vacuoles (figure 36).

Vacuoles were isolated from the Δ Vps1 BJ strain

reconstituted with plasmid expressing either wild type Vps1 or Vps1 mutants I649K, K642L or Y628F. A population of the vacuoles was labeled with Rh-PE and incubated with the unlabeled population under standard hemifusion conditions. Normalized relative fluorescence units were plotted versus time for three independent experiments and are shown as mean \pm s.d.

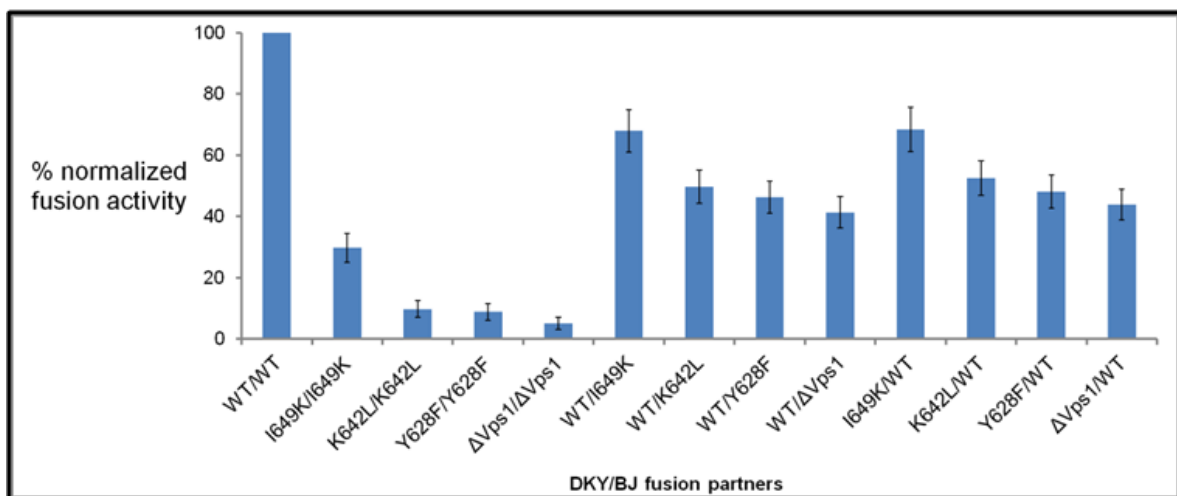


Figure 34: Vps1 single-point mutants impair vacuolar content mixing.

Vacuoles derived from Δ Vps1 (DKY and BJ) strains, reconstituted with plasmid expressing either wild type Vps1 or Vps1 mutants I649K, K642L or Y628F, were incubated in the combinations mentioned, under standard fusion conditions. Normalized OD400 values in the presence of ATP for five independent experiments are shown as mean \pm s.d.

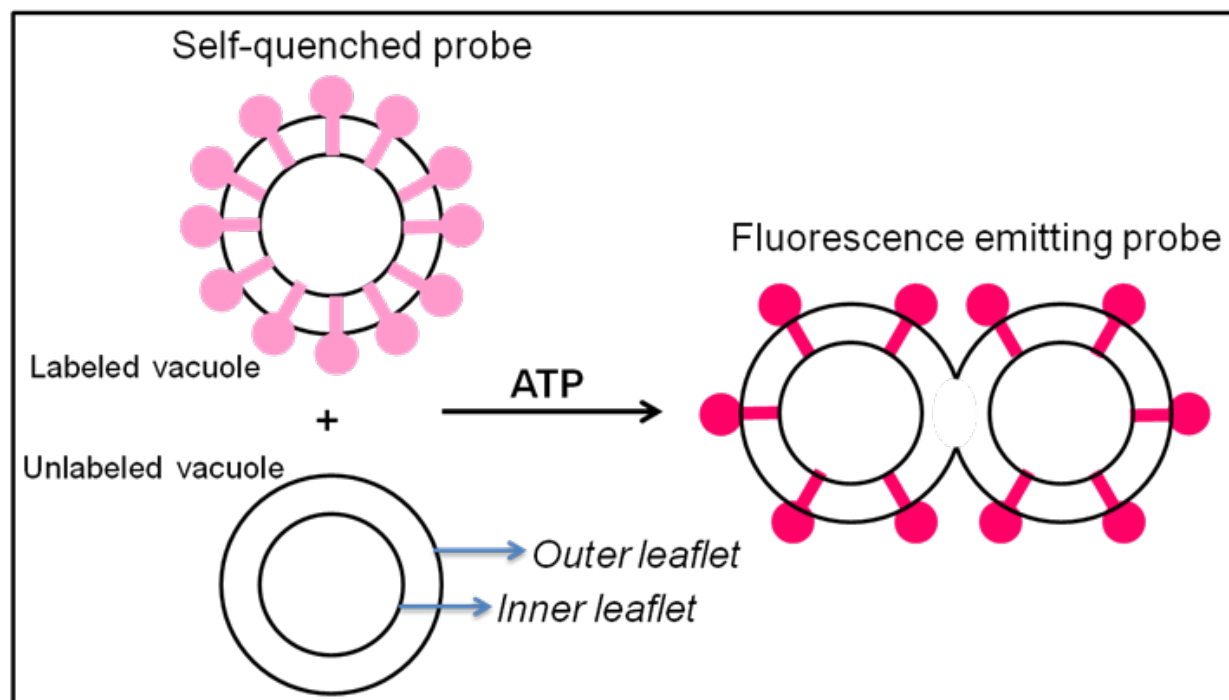


Figure 35: Principle of the vacuolar lipid mixing (hemifusion) assay.

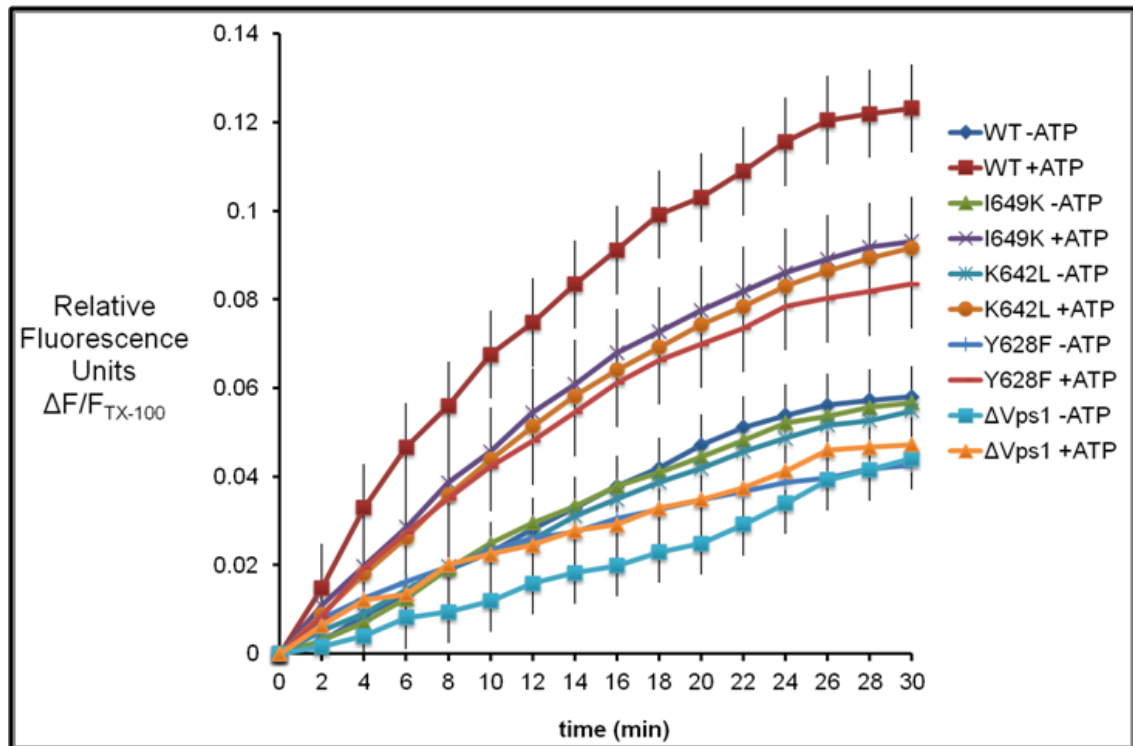
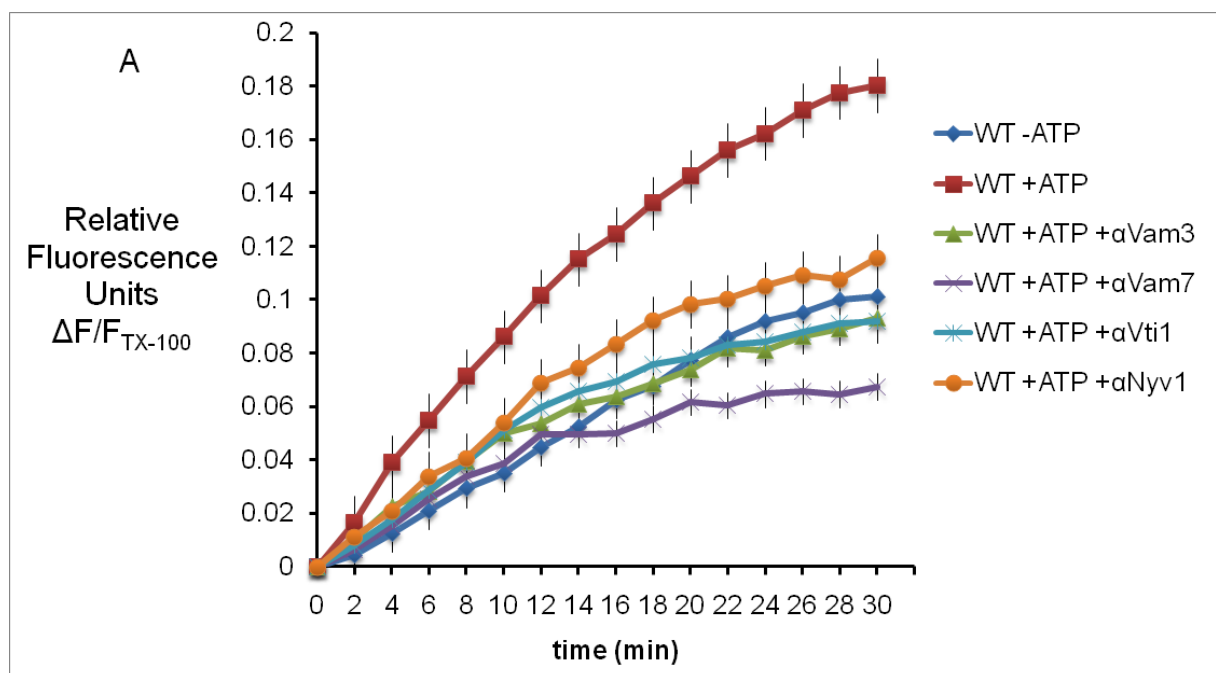
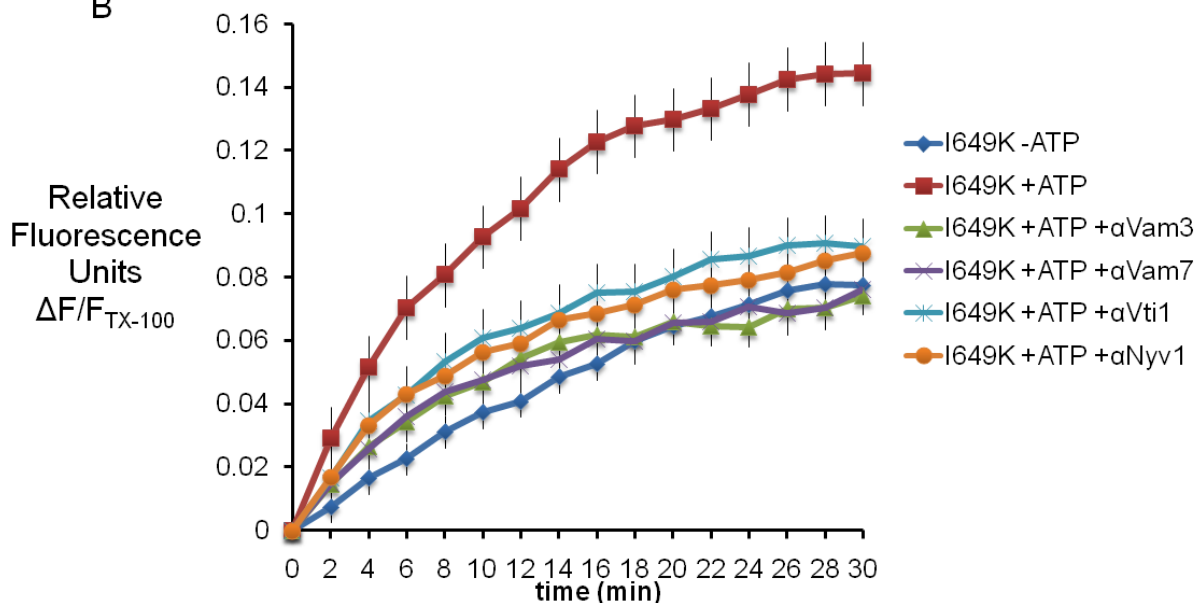
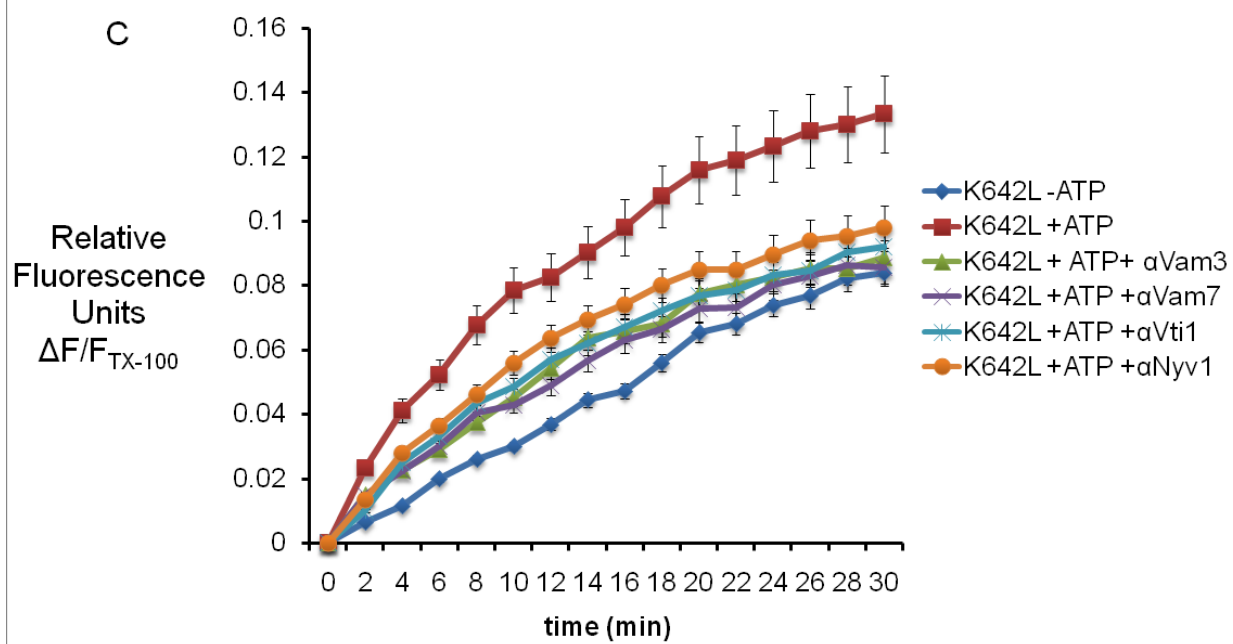


Figure 36: Vps1 mutants exhibit substantial vacuolar lipid mixing.

Vacuoles employed in the hemifusion assay were treated with antibodies against all four vacuolar SNAREs and were found to abolish any lipid mixing since they are expected bind to and therefore block the respective SNARE domain

(figure 37A-D). It was thus confirmed that hemifusion in these mutants was a true intermediate along the authentic SNARE-driven fusion pathway.



B**C**

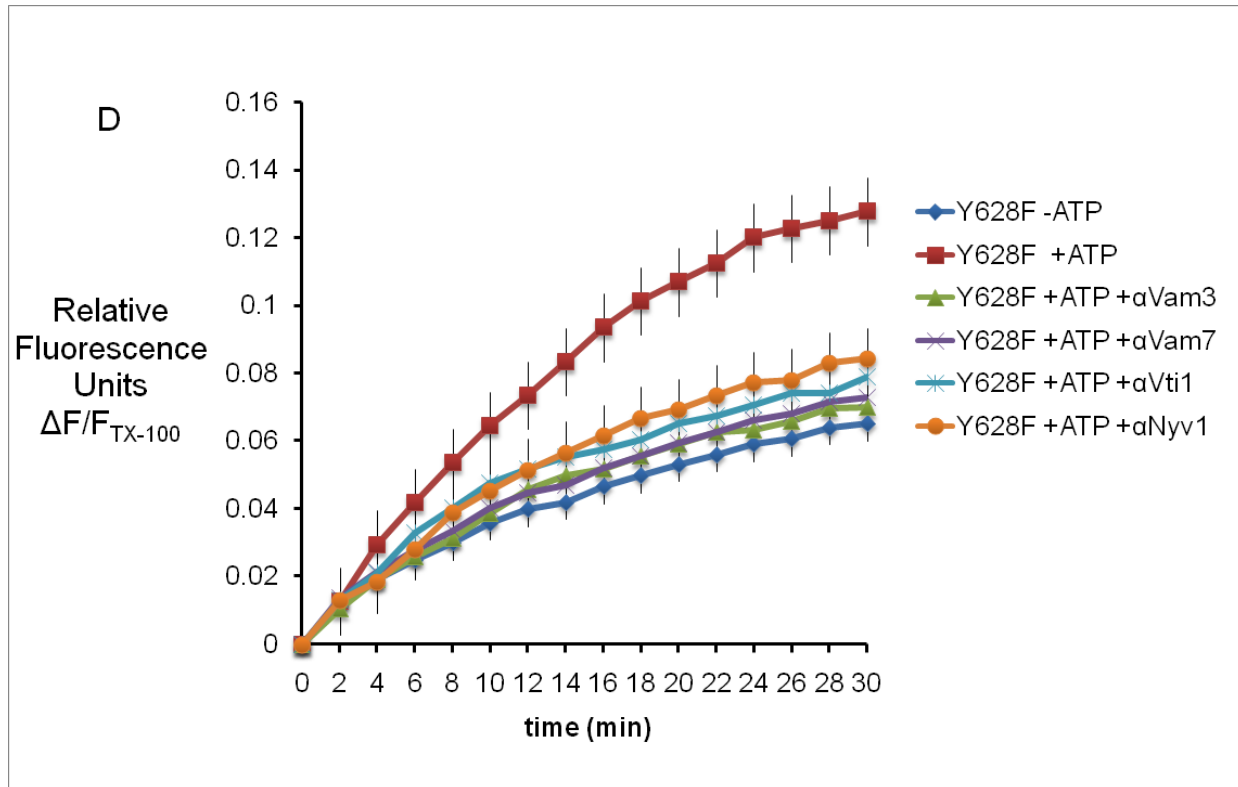


Figure 37: Lipid mixing of Vps1 wild type and mutant vacuoles upon SNARE antibody treatment.

Vacuoles were isolated from the Δ Vps1 BJ strain reconstituted with plasmid expressing either (A) wild type Vps1 or Vps1 mutants (B) I649K, (C) K642L or (D) Y628F.

A population of the vacuoles was labeled with Rh-PE and incubated with the unlabeled population under standard hemifusion conditions. Normalized relative fluorescence units were plotted versus time for three independent experiments and are shown as mean \pm s.d. Prior to addition of ATP, the vacuole mixture was incubated with antibodies to Vam3, Vam7, Vti1 and Nvy1. Treatment with each antibody diminished the extent of lipid mixing.

Subsequently, trans-SNARE complex formation was assayed between differentially tagged SNAREs originating from two fusion partners in the background of each Vps1 variant: one partner with the v-SNARE Nvy1 (R) harboring a VSV tag and the other partner with the t-SNARE Vam3 (Qa) harboring an HA tag. Upon addition of ATP to a mixture of wild type vacuoles a classical trans-SNARE signal is observed in the form of co-precipitating Nvy1-VSV when Vam3-HA is immunoprecipitated (figure 38). This signal vanishes in the presence of GDI (GDP Dissociation Inhibitor), a Rab GTPase inactivator. Only limited trans-SNARE complex assembly (25-50% relative to wild type, from densitometric analysis) was detected in the background of each Vps1 mutation (figure 38). It may be mentioned that Rab GTPases cycle between GDP and GTP bound states that in turn affect their interactions with lipids and proteins. For membrane fusion, Rab-GDP is the inactive, cytosolic form whereas Rab-GTP is the membrane-anchored active

form. It is known that yeast vacuolar fusion is inactivated when the Rab7 homolog Ypt7 is extracted from the vacuolar membrane by GDI.

Vacuoles from wild type or Vps1 mutant strains harboring the tagged SNAREs Vam3-HA or Nvy1-VSV were isolated and mixed together in the presence or absence of ATP, detergent extracted using 1% Triton X-100 and immunoprecipitated using anti-HA antibody. GDI (GDP Dissociation Inhibitor) is a Rab protein inactivator. It inhibits trans-SNARE complex formation and is used as a negative control. Western blot analysis was performed using monoclonal anti-HA antibody to detect precipitated Vam3-HA and polyclonal anti-Nvy1 antibody to detect co-precipitating Nvy1-VSV and quantified by densitometric analysis of three independent experiments.

The local clustering of SNAREs at the HOPS tethering complex is believed to represent a valid fusion site [134]. Association of the Syntaxin-like vacuolar t-SNARE Vam3 with the HOPS tethering complex on isolated vacuoles was analyzed by immunoprecipitation the HOPS subunit Vps11-HA from vacuolar extracts and probing for co-precipitating Vam3. This association was reduced to 40-60% (figure 39) of wild type in the Vps1 mutants suggesting that Vps1 could in fact be involved in building up the local SNARE density at the fusion site.

Vacuoles from wild type or Vps1 mutant strains harboring the tagged HOPS tethering complex subunit Vps11-HA were isolated and incubated in the presence of ATP, detergent extracted using 1% Triton X-100 and immunoprecipitated using anti-HA antibody. Western blot analysis was performed using anti-HA to detect precipitated Vps11-HA and anti-Vam3 to detect co-precipitating Vam3 and quantified by densitometric analysis of three independent experiments.

As displayed in figure 39, the Vam3 pool connected to the HOPS tethering complex which is the relevant pool

engaging in trans-SNARE formation is decreased in the Vps1 mutants. Previous work from my lab has demonstrated that this Vam3 pool is mutually exclusive from the Sec17 associated Vam3 present in a cis-SNARE complex which is unchanged even on Vps1 knockout vacuoles [134]. I therefore immunodepleted Sec17 from vacuolar extracts of Vps1 wild type and mutant vacuoles (figure 40) and probed the supernatant for Sec17-unbound Vam3 by western blot analysis. I found that residual Vam3 is free, but in reduced amounts (30-55%) on Vps1 mutant vacuoles relative to Vps1 wild type vacuoles.

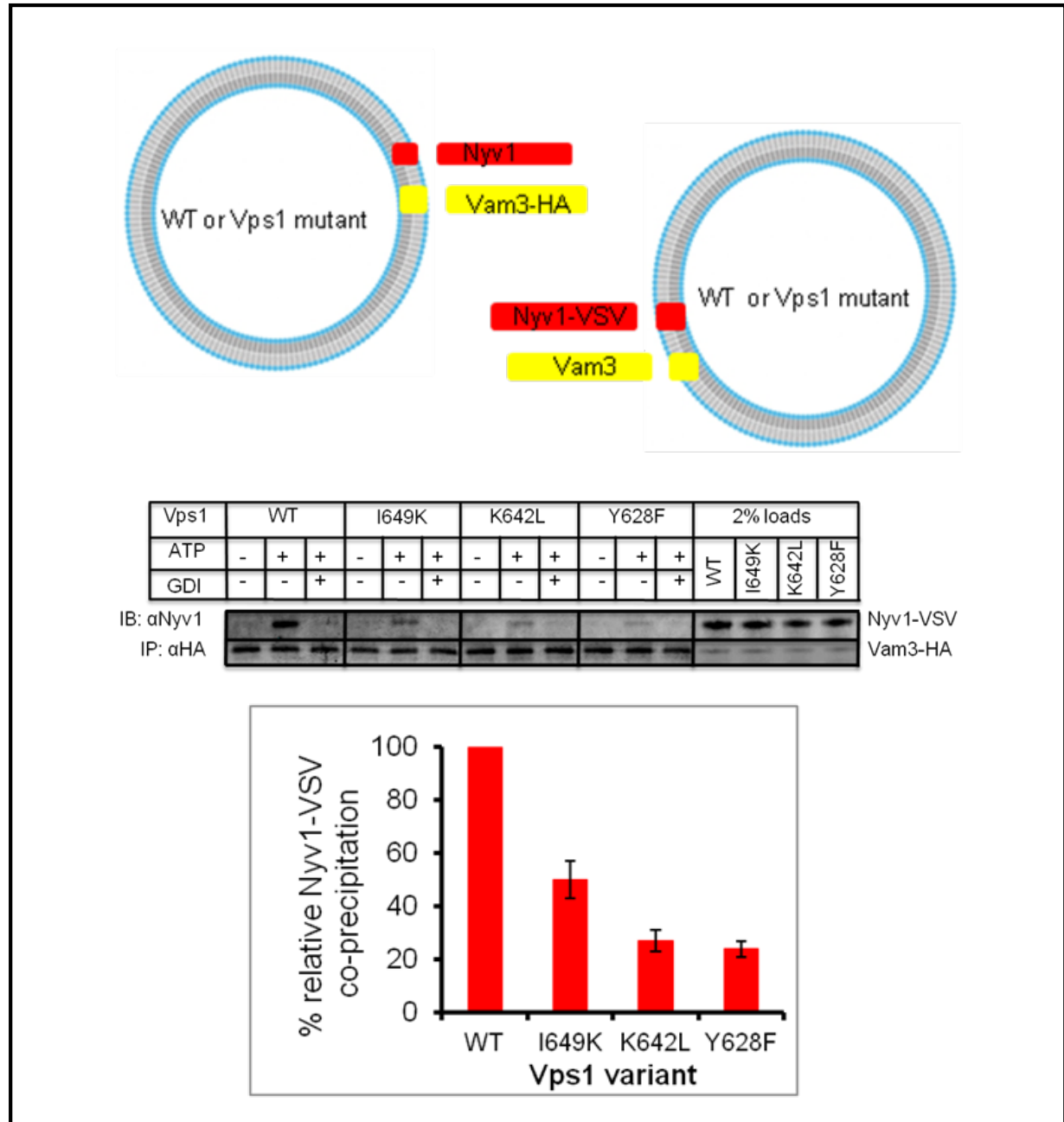


Figure 38: Vps1 mutant vacuoles demonstrate limited trans-SNARE complex formation.

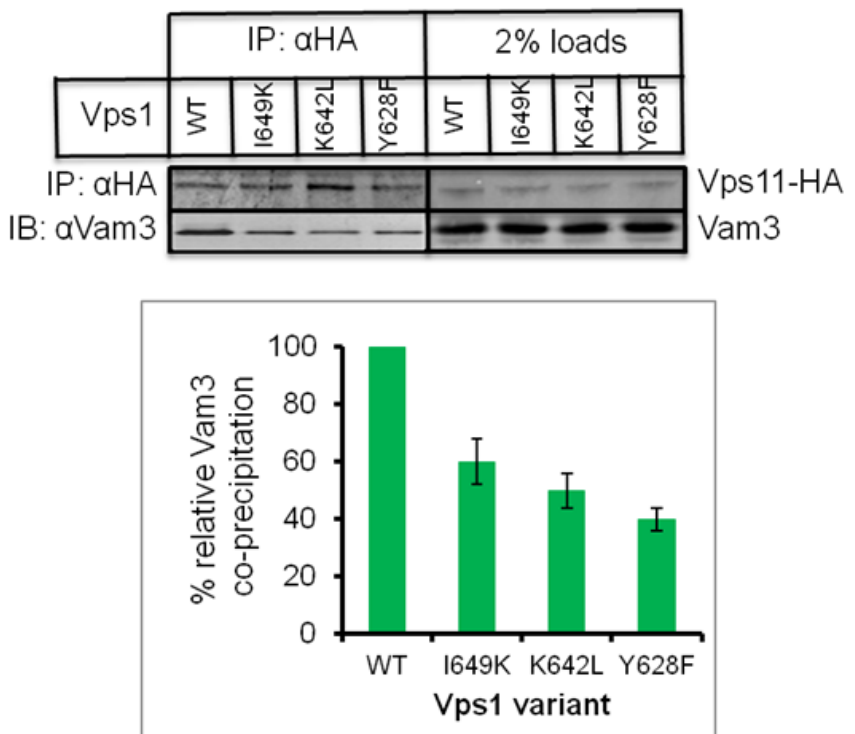


Figure 39: HOPS-Vam3 association on the vacuole is reduced in Vps1 mutants.

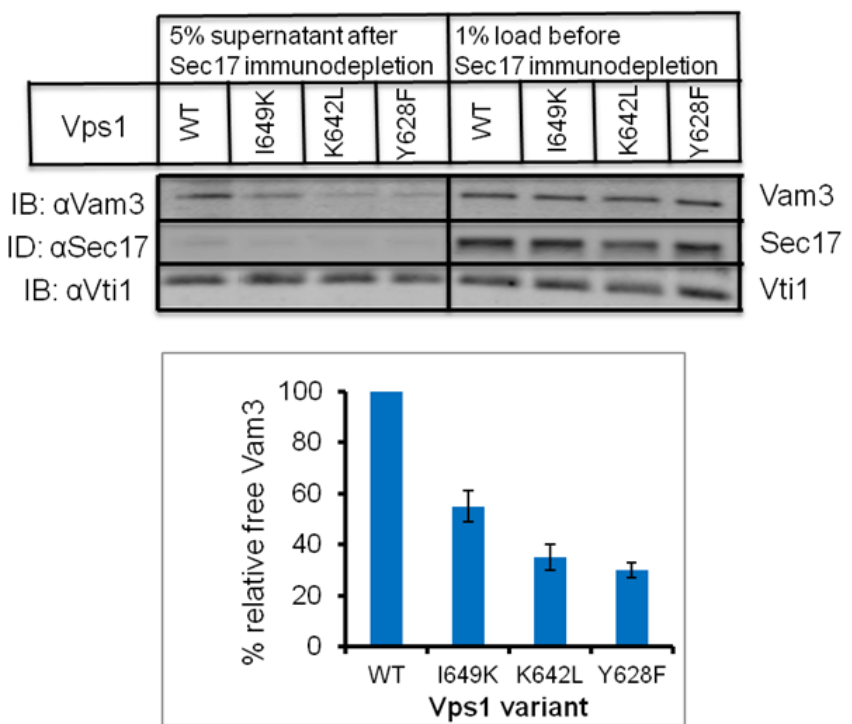


Figure 40: Sec17 immunodepletion reveals differences among Vps1 variants in the free Vam3 pool outside of cis-SNARE complexes on the vacuole.

Vacuoles from wild type or Vps1 mutant strains were purified, detergent extracted using 1% Triton X-100 and immunoprecipitated using anti-Sec17 antibody. Anti-Sec17-bound content was removed and the Sec17 depleted supernatant fraction was analyzed by western blotting. Polyclonal anti-Vam3 antibody was used to detect free Vam3 present in the Sec17-depleted fraction. Signal intensities were quantified by densitometric analysis of three independent experiments.

The level of free Vam3 (Sec17-unbound, not in a cis-SNARE complex) in the mutants corresponds to the relative amounts of Vam3 associated with the HOPS tethering complex (figure 39) and the trans-SNARE production efficiency (figure 38) in those mutants. From figure 40, it must also be noted that Vti1, a highly abundant vacuolar SNARE residing mostly outside of the cis-SNARE complex, remains relatively unchanged in the Sec17 depleted fraction across the Vps1 variants. This further signifies a Vam3-specific effect of the Vps1 mutations.

These data demonstrate that Vps1 has an influence on the

amount of trans-SNAREs and the amount of t-SNAREs connected to the HOPS tethering complex. This correlates to the requirement of a certain threshold of SNARE density on the HOPS complex and trans-SNAREs at the fusion site to overcome the barrier from hemifusion to content mixing. It was therefore essential to examine whether this impact of specific Vps1 mutations on fusion-related events relates to the potential of those mutations to alter its self-assembly behavior.

Vps1 mutants are polymerization-deficient

The polymerization behavior of these Vps1 mutants was evaluated to ascertain the basis of their fusion defects. Based on a sedimentation assay [67], the pellet and supernatant fractions after ultracentrifugation of recombinant Vps1 proteins were probed by SDS-PAGE followed by western blotting using anti-Vps1 antibody. Each of the Vps1 mutants was characterized as polymerization-deficient since there was no appreciable partitioning of Vps1 into the pellet fraction from the mutants relative to wild type Vps1 (figure 41).

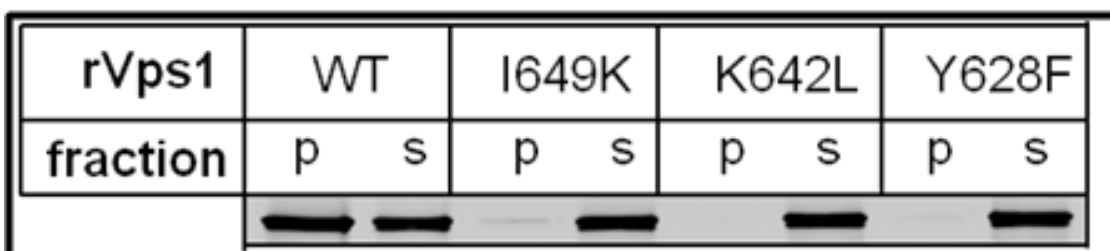


Figure 41: Vps1 mutants are polymerization-deficient.

25 μ M purified recombinant Vps1 variants were subjected to ultracentrifugation at 250,000g for 20 minutes at 30°C. Entire pellet (p) fraction and 10% of supernatant (s) fraction from the processing of each Vps1 variant were resolved by SDS-PAGE. Western blot analysis was performed using anti-Vps1 antibody.

Furthermore, to assess the oligomer formation capacity of Vps1, recombinant proteins under physiological salt concentration (150 mM KCl) were crosslinked with Disuccinimidyl glutarate (DSG) and the cross-linking pattern was analyzed by SDS-PAGE followed by western blotting using anti-Vps1 antibody.

Under the chosen conditions, wild type Vps1 was crosslinked to dimeric and higher order oligomers indicated by the arrow (figure 42), whereas I649K Vps1 predominantly formed only a dimer. Cross linked K642L and Y628F Vps1 were present entirely in the monomeric state itself, similar to the non-crosslinked protein (figure 42).

Figure 43 depicts the crosslinking pattern of Vps1 observed on Vps1 wild type and mutant vacuoles. Vacuoles were treated with two different concentrations (200 μ M and 400 μ M) of the crosslinker DSG. Vps1 on wild type vacuoles forms discrete higher order crosslinked products indicated by the arrow. In contrast, under the same conditions, Vps1 on I649K, K642L and Y628F mutant vacuoles does not form higher order complexes with the same efficiency as that observed in the wild type, indicating a

general oligomerization defect of Vps1 on native vacuolar membranes.

These results clarify that a building block larger than a dimer, likely a tetramer, is at least necessary for Vps1 to polymerize. The decrease in trans-SNARE complex formation efficiency in the Vps1 mutants remarkably corresponds to the loss of Vps1 polymerization capacity.

Analysis of Vam3-Vps1 complexes

Reduction in Vps1-mediated Vam3 binding to the HOPS tethering complex in the Vps1 mutant vacuoles could also be due to loss of affinity between Vam3 and Vps1 itself, and not entirely and solely due to loss of self-assembly capacity of Vps1 in the mutants. To quantify the binding affinity between recombinant Vam3 and each Vps1 variant, the K_d of the interaction between GST-Vam3 (full length or SNARE domain only) and Vps1-His6 was measured by biolayer interferometry using the Octet Red 96 instrument (ForteBio Inc.). None of the Vps1 mutants showed any statistically significant difference ($p < 0.05$) in binding affinity to Vam3 relative to wild type Vps1 (Table 4).

Chapter 3

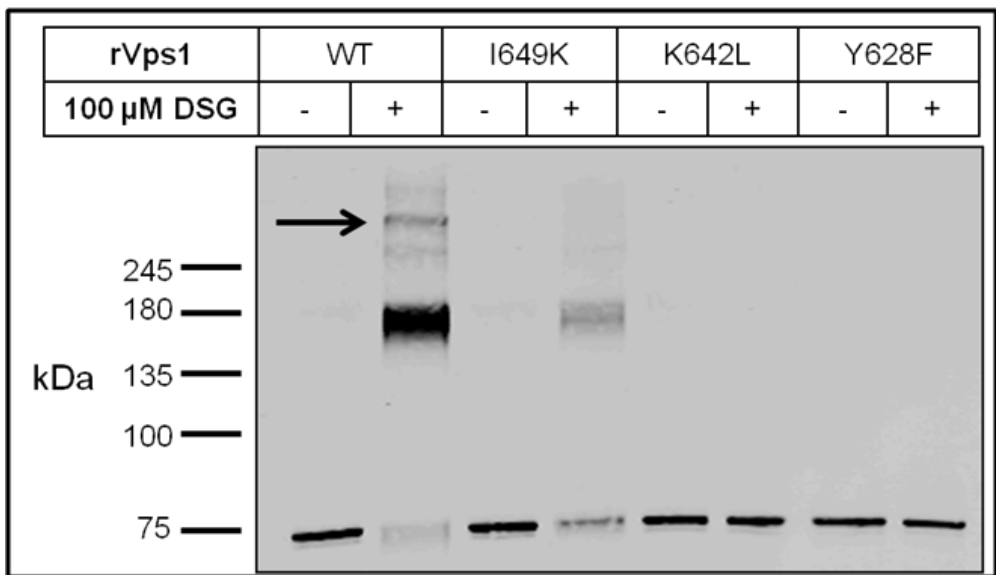


Figure 42: Chemical crosslinking of recombinant Vps1 variants.

Purified recombinant Vps1 variants were incubated with 100 mM DSG at 27°C for 15 min, quenched with 100 mM Tris-HCl pH 8, resolved by reducing SDS-PAGE and probed with anti-Vps1 antibody.

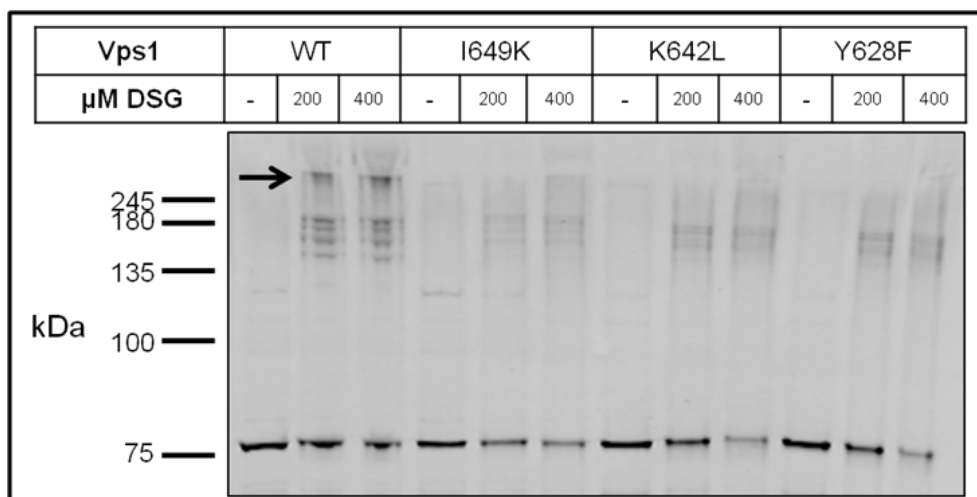


Figure 43: Chemical crosslinking of Vps1 on vacuolar membranes.

Purified Vps1 wild type or mutant vacuoles containing 150 mM KCl and 500 μ M MnCl₂ were incubated with 200 and 400 μ M DSG at 27°C for 30 min, subjected to Methanol-Chloroform extraction and the pelleted material was resuspended in sample buffer, resolved by reducing SDS-PAGE and probed with anti-Vps1 antibody.

Table 4: Vps1-Vam3 Kd values.

Vps1	K_d -Full Length Vam3 (μ m)	K_d -SNARE domain Vam3 (μ m)
Wild type	0.33 ± 0.03	0.36 ± 0.02
I649K	0.32 ± 0.01	0.33 ± 0.03
K642L	0.18 ± 0.02	0.29 ± 0.02
Y628F	0.35 ± 0.03	0.34 ± 0.03

Binding affinity between recombinant Vam3 (full length and SNARE domain) and Vps1 variants was measured by biolayer interferometry using Octet Red 96 Instrument (ForteBio Inc.)

This protein-protein interaction study showed that each Vps1 variant, irrespective of its self-assembly behavior, binds the SNARE domain of Vam3 with approximately identical affinity. To further confirm this result in the context of vacuolar membranes, I immunoprecipitated Vam3 from Vps1 wild type or mutant vacuolar extracts and probed for co-precipitating Vps1. As displayed in figure 44, in assembly-incompetent Vps1 mutants in which monomers or dimers of Vps1 predominate, the amount of Vps1 co-precipitating with Vam3 was reduced relative to that in wild type Vps1. This is expected because, although Vps1 variants have fairly identical binding affinity to Vam3, the absolute amount of Vps1 that co-precipitates with Vam3

decreases with their capacity to oligomerize.

Vacuoles from wild type or Vps1 mutant strains were isolated and detergent extracted using 0.25% Triton X-100 and immunoprecipitated using anti-Vam3 antibody. Western blot analysis was performed using anti-Vam3 to detect precipitated Vam3 and anti-Vps1 to detect co-precipitating Vps1 and quantified by densitometric analysis of three independent experiments.

This result explicitly demonstrates the existence of a Vam3-Vps1 complex on vacuolar membranes and assesses the effects of the Vps1 self-assembly mutants on this complex formation.

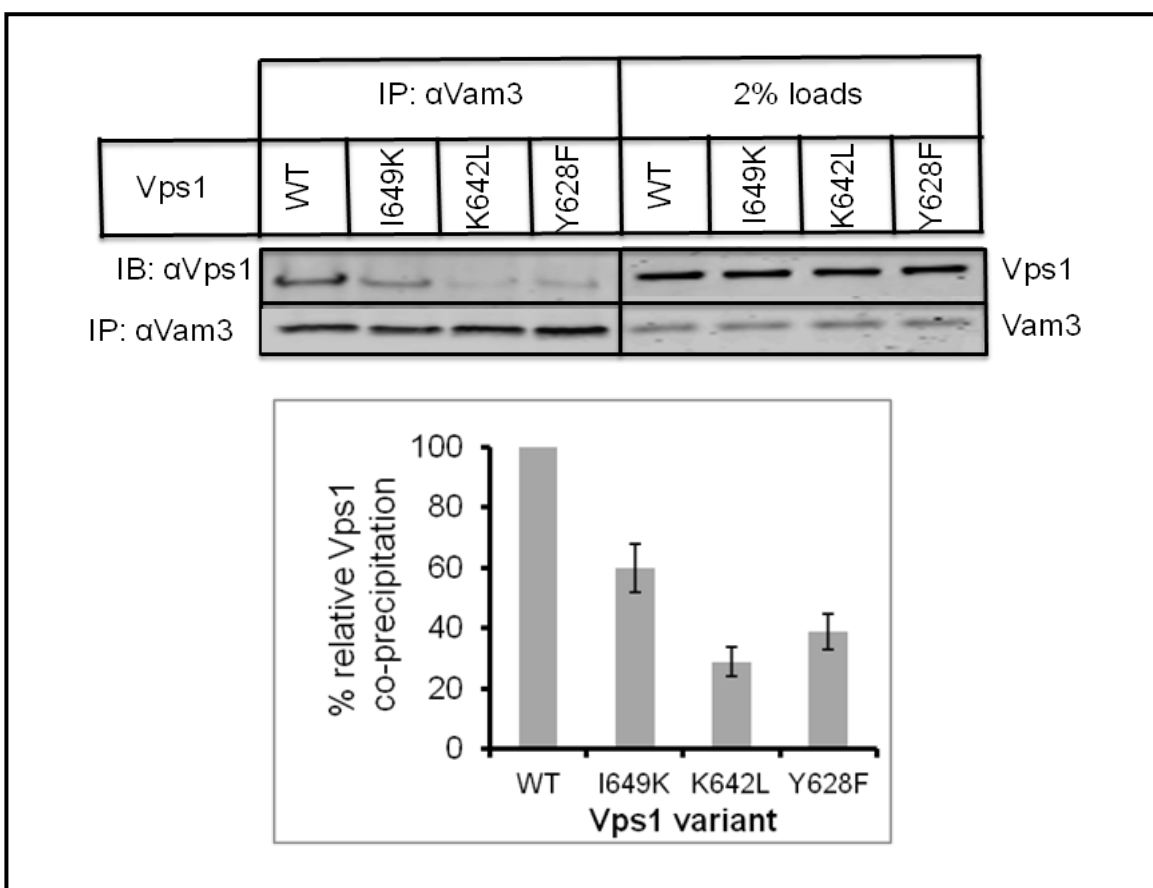


Figure 44: Absolute amount of Vps1 in Vam3-Vps1 complexes on the vacuole decreases in Vps1 mutants.

Functional evidence of Vps1 involvement in membrane fusion

A prediction from the Vam3-Vps1 binding affinity values would be that each Vps1 variant would exhibit equal potency to inhibit fusion of wild type vacuoles when added as a purified recombinant protein (figure 45) externally in the fusion assay, since each of them binds with approximately identical affinity to the SNARE domain of Vam3, sequester it out and would hence block it from entering into trans-SNARE complexes, which are the pre-requisite for fusion.

Therefore each recombinant Vps1 variant was titrated in a fusion reaction of wild type vacuoles to directly demonstrate its influence on content mixing. Each Vps1 mutant showed a concentration-dependent trend of fusion inhibition very similar to wild type Vps1 (figure 46).

In a standard fusion reaction of wild type vacuoles, recombinant Vps1 variants were titrated in a range of 0.6 - 6 µM and fusion activity was measured. Normalized OD400 values were plotted versus Vps1 concentration for three independent experiments and are shown as mean±s.d.

Chapter 3

Accordingly, treatment of wild type vacuoles with excess of recombinant Vps1 variants (4 μ M) was also found to block their hemifusion (figure 47) and trans-SNARE complex formation (figure 48) similar to their fusion inhibition.

In a standard hemifusion reaction of wild type vacuoles, 4 μ M recombinant Vps1 variants were added and hemifusion activity was measured. Normalized relative fluorescence units were plotted versus time for three independent experiments and are shown as mean \pm s.d.

Wild type vacuoles harboring the tagged SNAREs Vam3-HA or Nyv1-VSV were isolated, mixed together and incubated with 4 μ M recombinant Vps1 variants in the presence of ATP, detergent extracted using 1% Triton X-100 and immunoprecipitated using anti-HA antibody. Western blot analysis was performed using anti-HA to detect precipitated Vam3-HA and anti-Nyv1 to detect co-precipitating Nyv1-VSV.

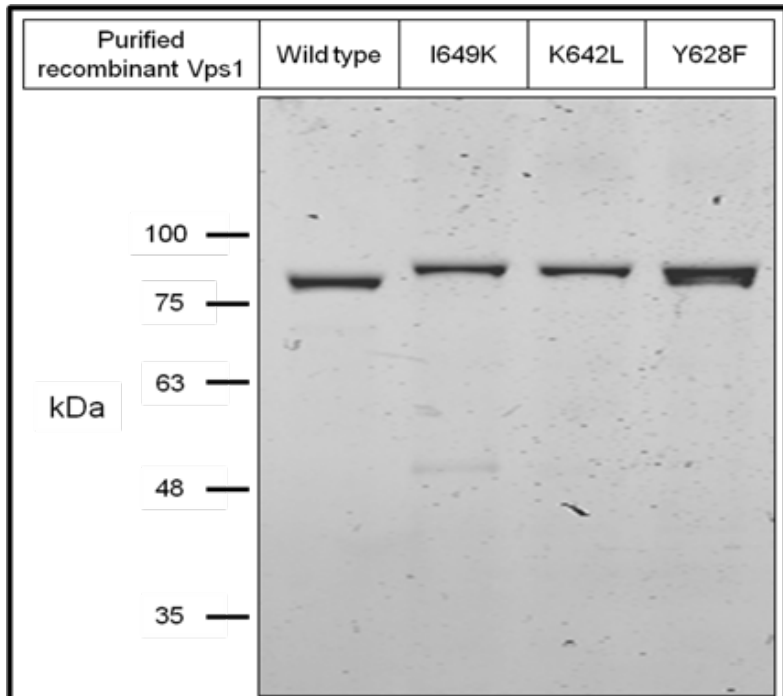


Figure 45: Coomassie staining of purified recombinant Vps1 variants.

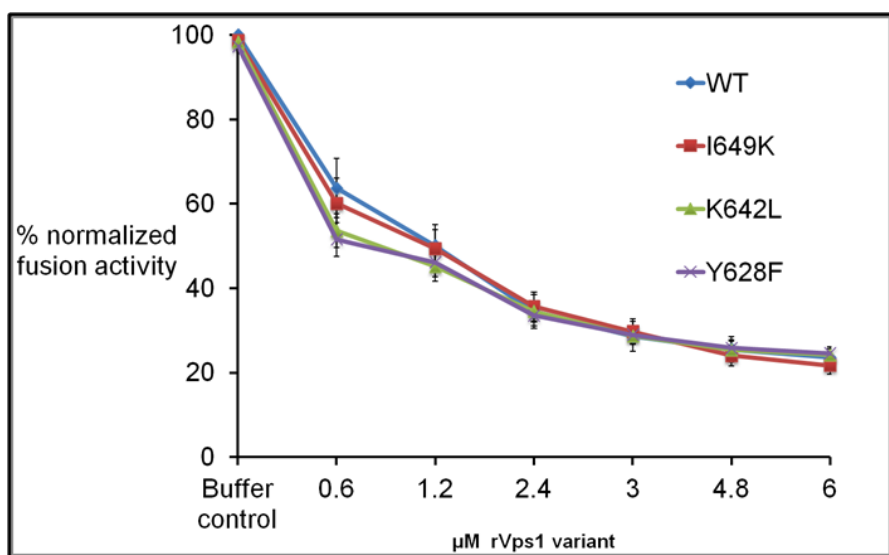


Figure 46: Recombinant Vps1 variants inhibit vacuolar fusion.

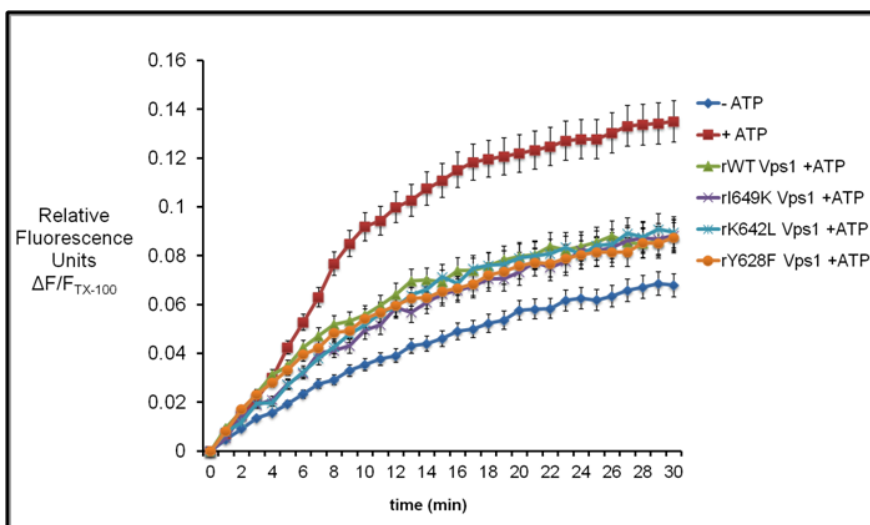


Figure 47: Recombinant Vps1 variants inhibit wild type vacuolar hemifusion.



Figure 48: Recombinant Vps1 variants inhibit trans-SNARE complex formation between wild type vacuoles.

Significance of Vps1 mutations in live cells

To analyze the impact of Vps1 mutations *in vivo* I performed phenotypic characterization of vacuolar morphology by specifically labeling yeast vacuoles with the lipid binding fluorescent dye FM4-64. Logarithmic phase yeast cells treated with FM-64 show discretely stained compartments

readily identifiable as vacuoles. Figure 49A (a-e) shows representative images of vacuolar morphology observed in cell populations from Vps1 wild type, I649K, K642L, Y628F and knockout strains. Figure 49B illustrates a quantification of the range of number of clear, round vacuoles or small, dispersed vesicles observed in each cell counted across cell populations from the different strains.

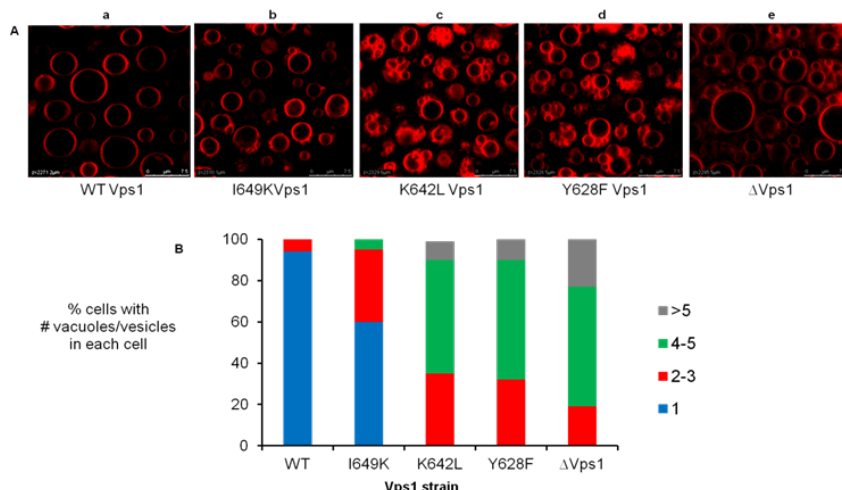


Figure 49: *In vivo* vacuolar morphology of Vps1 variants.

Vacuoles in cells from the different Vps1 strains: wild type, I649K, K642L, Y628F and knockout were labeled with the dye FM4-64. One hundred cells were counted randomly in each experiment. Representative snapshots are shown in panel (A). Red compartments represent labeled vacuoles. White scale bar at the bottom right in each image panel measures 7.5 μ m. (B). The percentage of cells showing the range of number of vacuoles/ vesicles per cell was plotted for each Vps1 strain. Values are averaged from three independent experiments.

Overall, the *in vivo* observations reflect the degree of vacuolar fusion defects measured *in vitro* (figure 32). There is a decrease in number of cells with a single vacuole with no surrounding vacuoles or vesicles: Vps1 wild type >> I649K > K642L ~ Y628F > Vps1 knockout and concomitant increase in number of unfused small vacuoles or vesicles per cell: Vps1 wild type << I649K < K642L ~ Y628F < Vps1 knockout. This seems to correspond to the inability of Vps1 mutants to overcome the hemifusion-content mixing barrier leading to a certain probability of vacuolar fusion *in vivo*.

Discussion

An important outcome of this study was the identification of graded loss-of-function Vps1 mutants that were a great asset to evaluate the Vps1-driven regulation of trans-SNARE formation since the mutants were able to provide different basal thresholds of SNARE complexes, as opposed to the Vps1 total knockout, which produces no trans-SNARE complexes. Altogether the results explain how accumulation of SNARE molecules at the fusion site, measured in terms of trans-SNARE complex formation and Vam3 recruitment to the HOPS complex, is directly connected to the polymerization capacity of Vps1. This translates into a critical barrier of local SNARE concentration that must be overcome to achieve fusion. These results

suggest that Vps1 is able to regulate SNARE density at the fusion site through its polymerization and Vam3 binding properties and thereby accomplishes the transition from docking to hemifusion to content mixing in yeast vacuolar fusion. Several studies attempting to measure the number of SNARE complexes catalyzing membrane fusion have generated estimates ranging between 1 and 15 depending upon the conditions chosen [135-137]. These findings support the general view derived from both synthetically reconstituted and physiological model systems that multiple SNARE complexes are required for fusion [138-140]. Although numerous helical rungs of dynamin promoting membrane fission have been widely observed, a recent study demonstrated that catalysis by dynamin via smaller, transient subunits, in fact, favors reversible hemifission or alternatively, hemifusion [141].

In an attempt to rescue the fusion of Vps1 mutant vacuoles, I employed various strategies. As displayed in figure 50, overexpression of Vam3 (10 fold over endogenous levels) on Vps1 wild type or mutant vacuoles did not lead to bypass of Vps1 block of fusion activity. In fact, over expression of Vam3 on each wild type fusion partner actually led to fusion inhibition. Since there is limited amount of Vps1 on the vacuole, over expressing Vam3 will create more single Vam3 associated with the HOPS complex but not connected to Vps1. This results in a K642L or Y628F Vps1 mutant-like phenotype. Recombinant Vam7 known to stimulate fusion of non-canonical SNARE combinations and Chlorpromazine, an amphipathic small molecule known to decrease the force required for membrane deformation and increase negative membrane curvature, were used as additional tools to potentially bypass Vps1 requirement in fusion [142]. Recombinant wild type Vps1 was also tested for its ability to restore the fusion of Vps1 mutant vacuoles. However, none of these approaches resulted in any rescue of fusion activity of the Vps1 mutants.

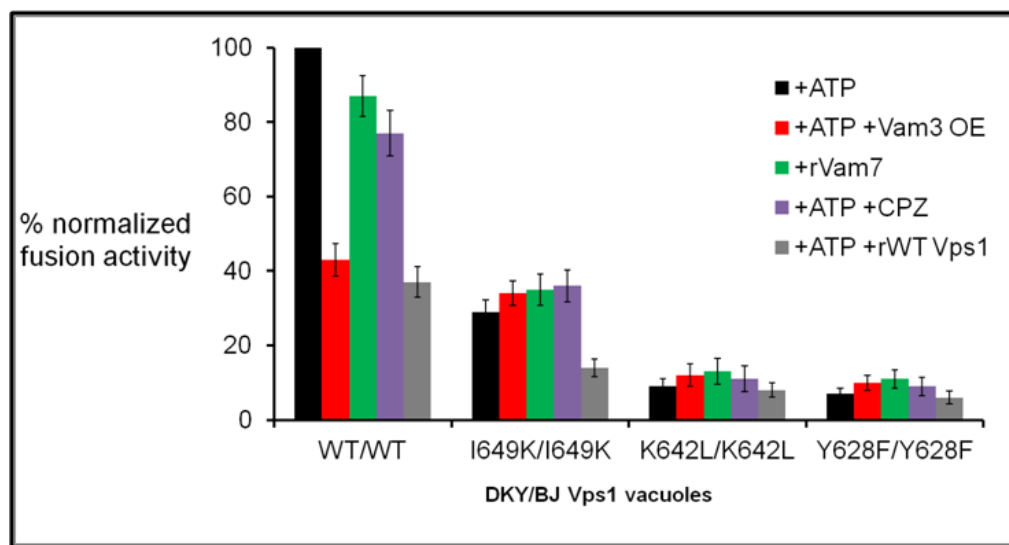


Figure 50: Strategies to rescue fusion defects of Vps1 mutant vacuoles.

Standard fusion reactions of Vps1 wild type or mutant vacuoles were set up in the presence of following agents: red bars indicating 10-fold Vam3 over expression on each fusion partner, green bars indicating addition of 100nM recombinant Vam7, purple bars indicating addition of 150 μ M Chlorpromazine and grey bars indicating addition of 4 μ M recombinant wild type Vps1. Normalized OD400 values were plotted for three independent experiments and are shown as mean \pm s.d.

I suggest that Vps1, through its oligomerization and SNARE domain binding, coordinates the HOPS tethering complex-associated pool of Vam3 and thereby the trans-SNARE complexes at the fusion site. My observations seem to fit this hypothesis since various strategies to surpass the hemifusion-fusion barrier still prove inadequate to activate fusion of the assembly-incompetent Vps1 mutant vacuoles as they are anyway unable to accumulate the threshold level of SNAREs at the fusion site. In the case of assembly-incompetent Vps1 mutations, local SNARE density since the beginning itself is below the threshold for fusion. It is likely that excess of SNAREs or altered physical properties of the lipid bilayer might re-establish the SNARE zippering process in the presence of threshold levels of even non-canonical SNARE combinations more efficiently than that in the case of Vps1 mutants having lowered SNARE density at the fusion site. In order to re-establish the lacking Vam3-HOPS complexes on Vps1 mutant vacuoles, recombinant wild type Vps1 (rWT Vps1) has to displace the other vacuolar SNAREs from Vam3 in the cis-SNARE complexes

and allow the N-terminus of Vam3 to reconnect to the HOPS complex. Since this process includes the interaction of rWT Vps1 with the SNARE domain of Vam3, fusion remains blocked due to inaccessibility of the Vam3 SNARE domain, quite similar to our wild type experiments, where rWT Vps1 inhibits vacuolar fusion (figure 46). This means that the re-establishment of the HOPS-Vam3 pool by rWT Vps1 as a prerequisite for successful fusion is counteracted by the blockage of the Vam3 SNARE domain. Therefore, I expect rWT Vps1 to always show inhibitory effects on vacuolar fusion.

Visualized at the molecular scale, as represented in figure 51, wild type Vps1 in its native polymeric state binds Vam3 and brings together multiple SNARE complexes satisfying or exceeding the local threshold of SNAREs necessary and sufficient for complete fusion. In contrast, in assembly-incompetent Vps1 mutants, this threshold SNARE abundance is not attained. This is not because of reduced Vam3 binding to Vps1, but is linked to the self-assembly capacity of Vps1. Vps1 in these polymerization-defective mutants is unable to gather sufficient Vam3 molecules for complete fusion and the process is stalled at the hemifused state. K642L, Y628F and I649K Vps1 would likely bring in fewer SNARE molecules at the fusion site, which are still sufficient for hemifusion but below the threshold for complete fusion. In comparison, there is no HOPS-associated Vam3 fraction on Vps1 knockout vacuoles, which are therefore unable to deliver any t-SNAREs at the fusion site.

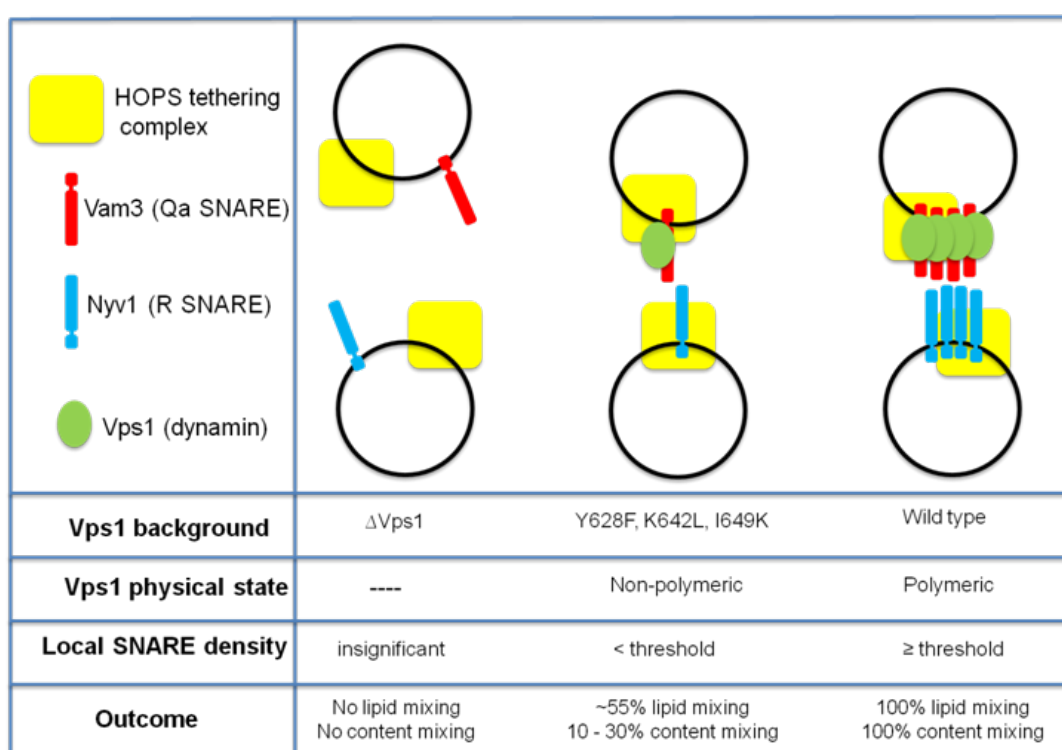


Figure 51: Schematic representation of Vps1 function in SNARE-mediated fusion.

Chapter 3

Formation and maintenance of a concentrated reservoir of SNAREs, dependent on contributions from associated protein and lipid sources, has been established as one of the provisions that define a docking site and promote fusion. t-SNAREs or Syntaxins in particular have been the target of various mechanisms regulating their molecular conformations and distributions in preparation for fusion. Multiple copies of syntaxin were proposed to line the fusion pore in Ca⁺⁺/Synaptotagmin-triggered exocytosis [143]. Various biochemical studies have demonstrated that self-oligomerization, binding to t-SNAREs and membrane association of Synaptotagmin may be critical in mediating vesicle docking and for coupling Ca⁺⁺ influx to fusion during exocytosis [144].

Although Vps1 belongs to the family of Dynamin-related proteins differing from Classical Dynamin in the sense that DRPs lack a PH domain and a Proline/Arginine Rich Domain present additionally in classical dynamins, the Vps1 single-point mutants employed in this study were derived from the crystal structure of mammalian dynamin and the residues involved have been known to be evolutionarily conserved from yeast to mammals. The striking sequence homology of Vps1 with mammalian dynamin at specific alpha helices forming an oligomerization interface, coupled with our results suggest that Vps1-like control of membrane fusion is likely to occur via Dynamin in specialized adaptations such as synaptic transmission in higher eukaryotes. Furthermore, the existence of Dynamin-Syntaxin complexes on secretory granules in adrenal chromaffin cells indicates that dynamin may participate in coupling exocytosis and endocytosis in other systems as well [145].

Components such as tethering factors and Rab GTPases have been well known to coordinate SNARE-mediated fusion [146]. Numerous additional proteins may regulate the rate, extent and location of assembly and in turn the number of SNARE complexes either by directly occluding the SNARE motif of Syntaxin (e.g. Dynamin, Tomosyn, Amisyn, Syntaphilin) or by preventing full zippering of the SNARE complex (e.g. Sec1, Unc18, Complexin).

The HOPS tethering complex subunit Vps33, which is a t-SNARE binding SM (Sec1/Munc18) family member, has been shown to promote pore opening during the hemifusion-fusion transition [76]. Vps33 mutants having weaker Vam3 interactions employed in that study permitted wild type-like trans-SNARE pairing. Assembly-incompetent Vps1 mutants, having identical Vam3 interactions but reduced Vam3-HOPS associations relative to wild type Vps1 used in our study, allowed only limited trans-SNARE assembly. Together these key results suggest that Vps1 coordinates a SNARE density of fusogenic potential prior to SNARE recruitment to the HOPS complex. This event must be situated upstream of HOPS function in promoting the hemifusion-fusion transition. The HOPS complex most likely pushes the hemifused state through to content mixing with the already existing number of trans-SNAREs but it is Vps1 that builds up the local SNARE concentration.

Compelling evidence indicating a role of dynamin in exocytosis has recently emerged. Dynamin was shown to regulate terminal stages in the fusion of lytic granules with the plasma membrane during the cytotoxic response of natural killer cells [131]. Similarly, it was reported that siRNA knockdown of dynamin led to marked decrease in glucose-stimulated insulin secretion from insulin granules of β cells [68]. Interestingly, a study on a bacterial dynamin-like protein stated its involvement in mediating nucleotide-independent membrane fusion [132]. Additionally, the mechanochemical properties of dynamin or dynamin-related proteins have been suggested to contribute to fusion pore dynamics during exocytosis [69-147]. My finding extends the repertoire of dynamin function in SNARE-mediated fusion, which is of great prominence since it might provide a molecular understanding of the control of (i) reversible fusion pore opening and reclosure implicated in kiss-and-run fusion in synaptic transmission and (ii) fusion-fission equilibrium in intracellular membrane trafficking and exo-endocytotic cycles [148].

Chapter 4

Summary, Significance, Outlook and Future Goals

Chapter IV

Summary, Significance, Outlook and Future Goals

Summary

Despite the ubiquitous occurrence of membrane fusion events, the underlying molecular mechanisms are little understood. Through studies on native yeast vacuoles representing a physiologically relevant model system to investigate membrane fusion mechanisms, I have reported a new finding that a HOPS tethering complex dimer catalyzes Rab/Ypt7-dependent formation of a topologically preferred QbQcR-Qa trans-SNARE complex. Further, I have been able to propose a novel concept that the yeast dynamin homolog Vps1, through its self-oligomerization and specific binding to the Qa SNARE domain, promotes the hemifusion-content mixing transition in yeast vacuole fusion by increasing the number of trans-SNAREs.

Significance and outlook

Membrane fusion has an overwhelming impact on the living world. The fusion of sperm and egg membranes marks the beginning of life. Intracellular membrane fusion enables molecular transport within every cell throughout life. Virus-cell membrane fusion may signify the end of life.

If membrane recognition in general does occur through assembly of a tether-Rab-SNARE platform as demonstrated in chapter II, it would provide a functionally non-redundant mechanism to ensure the fidelity of fusion and suppress incorrect SNARE-mediated fusion between any two membranes. This is important because, for example, in pancreatic acinar cells, inappropriate delivery of cargo can lead to mistaken lysosomal maturation of trypsinogen to trypsin causing pancreatitis [149]. Since the elementary machinery and mechanism is conserved among all SNARE-mediated fusion events in general, this prototype from homotypic fusion can be extended to propose a model for heterotypic scenarios occurring more widely and garnering more therapeutic attention, for example in vesicle-plasma membrane fusion in the case of synaptic transmission or hormonal secretion. In heterotypic fusion, the same tether could act both upstream and downstream of Rab activation or multiple tethers may participate in the reaction. The Rab-GTP may recruit other tethers that promote or assemble trans-SNARE pairs. My results indicate that the requirements for specific SNARE proteins in intracellular membrane fusion are less stringent than appreciated and suggest that combinatorial mechanisms using upstream-targeting elements along with SNARE proteins are required to maintain an essential level of compartmental organization.

Phenotypic characterization of mutations in the zebrafish homolog of Vps39 represent human multisystemic disorders which are known to affect skin pigmentation, vision, internal organs like the liver and the immune system [150]. In Drosophila, loss of function mutations in

homologs of Vps18, Vps33 and Vps41 lead to abnormality in the formation of lysosome-like pigment granules in the eye [151]. The mutant of Arabidopsis Vps16 (*vacuoleless*) exhibiting aberrant vacuolar morphogenesis leads to embryonic lethality [152]. Knockdown of HOPS genes in *C. elegans* led to accumulation of apoptotic-cell-containing phagosomes indicating an arrest of their maturation and impaired lysosomal degradation [153]. Evidence from diverse model systems show that components of the HOPS complex, which are highly conserved in multiple species [154], are likely to share myriad essential cellular roles ranging from regulation of membrane traffic to mRNA stability. Mutations in mammalian Rab7 have been known to be associated with the development of Charcot Marie Tooth disease in humans [155]. Similarly, insufficiencies in the SNAREs Syntaxin1 and SNAP25 are one of the causative agents of Type 2 Diabetes. Also, depletion of specific COG subunits has been implicated in cases of Congenital disorder of Glycosylation [156].

SNARE-SNARE associations are diverse in terms of kinetic and thermodynamic stability and subcellular localization. There is hence a need for additional agents to exercise stringent control over and dictate specific channelization of SNARE molecules entering into trans-complexes on the path to fusion. Due to their amphiphilic nature, the Qa, Qb, Qc and R SNARE domains can also associate in other combinations that result in four-helix helical bundles that are thermodynamically less stable than core QaQbQcR complexes. Particularly noteworthy are the complexes that are formed by the neuronal SNAREs. These include a Qaaaa complex (an antiparallel four-helix bundle [157]), a Qabab complex (a parallel four-helix bundle [158]), a Qaabbc complex (a parallel four-helix bundle with some disordered regions [159,160]) and, surprisingly, an antiparallel QabcR complex [120]. These complexes might not have the correct membrane topology or they might not contribute sufficient energy to drive membrane fusion. They therefore do not lie on the authentic fusion pathway and probably represent unproductive 'off-pathway' subreactions, and may require upstream and/or downstream proofreading by additional factors.

Different combinations of SNAREs were found to form complexes with the Qa SNARE Sed5, which were required for multiple routes in ER-Golgi and intra-Golgi vesicular traffic [161]. The apparent promiscuity of SNARE-SNARE interactions, together with the requirement for some SNAREs in more than one trafficking step, supports the view that the specificity of vesicle fusion events cannot be explained solely on the basis of SNARE pairing. Another study demonstrated that both cognate and non-cognate SNARE complexes, formed among SNAREs that would never see each other in any characterized trafficking pathway yet, are very similar with respect to their biophysical properties, assembly, and disassembly [7], suggesting that specificity of membrane fusion in intracellular membrane traffic cannot be simply attributed to the intrinsic specificity of SNARE

pairing. There have been reports that even SNARE-Rab interactions at times prove non-cooperative to specify the target membrane [162], hinting towards the need for tighter regulation of vesicle targeting and cargo delivery to the correct subcellular location. Concomitant action of tether scaffolds, Rab proteins and SNAREs seems to provide a relatively effective, reliable and robust way to achieve overall membrane recognition and fusion specificity.

Furthermore, direct interaction between SNAREs and dynamin family members has now been observed in more than one model system [134,145]. This suggests that the interaction between the fission and fusion machineries may be more generally exploited by the cell as a target for adjusting organelle size and morphology and hence is a physiologically relevant regulatory mechanism. A recent study demonstrated that the physiology of exo-endocytic cycles of synaptic vesicles is likely to be influenced by phosphorylation and nitration of specific tyrosine residues in Dynamin1 [163]. These modifications were suggested to regulate dynamin function via control of its self-assembly. For instance, presence of putative modification sites within the Vam3 binding region of Vps1 can shed light on the regulatory framework underlying intracellular fusion-fission control. Dynamin regulation is complex. Since various post-translational modifications of dynamin have been described as either functionally activating or inhibitory for dynamin recruitment to or association/dissociation with its binding partners at the site of action, it is critical to understand whether Vps1 binding to and/or release from Vam3 depends on such modifications. In the model presented in chapter III, it is implicit that Vps1 binds Vam3 and disengages its SNARE domain from participating in trans-SNARE complex formation and thereby silences fusion when fission is triggered. Release of Vps1 from Vam3, perhaps in response to a certain modification or any other unknown signal, makes the SNARE domain of Vam3 available to engage in fusion. This explains how fusion and fission activities are kept from overlapping and futile cycles are prevented. It would be important to know the domain of Vps1 that is engaged in binding the SNARE domain of Vam3, to further search for potentially conserved SNARE-binding dynamin regions in other systems where controlling the stability of dynamin-SNARE interactions would provide a method to achieve fusion-fission control.

Understanding in more detail how the fusion and fission machineries work together to achieve efficient lipid bilayer merge and to control organelle identity will have a deep impact on many disease-relevant topics. Dynamins are indispensable for synaptic vesicle recycling and therefore extremely important for sustained neurotransmission. Dynamin1 depletion in hippocampal neurons has been considered as a potential mechanism for early and irreversible cognitive decline in Alzheimer's Disease [164]. Mutations in dynamin and related proteins have been linked to at least two human diseases - centronuclear myopathy

(CNM) and Charcot-Marie-Tooth (CMT) disease [165,165]. These hereditary disorders are characterized by motor and sensory neuropathies and affect more than 1 in 3,000 people in the general population. Frameshift and missense mutations in OPA1, a gene encoding a mitochondrial dynamin-related protein, have been found to segregate with dominant optic atrophy having a population frequency of 1 in 50000 [167]. There is progressive loss in visual acuity leading, in many cases, to legal blindness.

Given the tendency of dynamin family members to form oligomers, it has been hypothesized that many of the OPA1 mutations are dominant-negative alleles that reduce the activity of the remaining wild-type allele, leading to the autosomal-dominant pattern of inheritance. Kidney podocytes and their foot processes maintain the ultrafiltration barrier and prevent urinary protein loss found in proteinuria. It has been demonstrated that dynamin is essential for podocyte function [168]. During proteinuric kidney disease, induction of cytoplasmic cathepsin L leads to cleavage of dynamin at an evolutionarily conserved site, resulting in reorganization of the podocyte actin cytoskeleton causing proteinuria. Dynamin mutants that lack the cathepsin L site, or render the cathepsin L site inaccessible through dynamin self-assembly, are resistant to cathepsin L cleavage. When delivered into mice, these mutants restored podocyte function and resolved proteinuria [168]. Therefore, studies investigating assembly-dependent functions of dynamin are vital. All these examples highlight the clinical burden associated with dynamin-related perturbations, thus enforcing in-depth analysis of dynamin-driven fundamental biochemical reactions.

Dynamins have been implicated as a class of regulatory proteins, acting either on SNAREs or SNARE-interacting proteins in different types of fusion processes. Among them are regulated exocytosis in neuroendocrine cells [169-171], sperm acrosomal reaction [172], cell-to-cell fusion [173], and fusion of a virus with the host cell [174]. Dynamin-2 has been shown to associate with secretory granules in chromaffin cells via its interaction with Syntaxin [145] and Synaptophysin [170]. In mammalian sperm, dynamin-2 associates with the SNARE regulatory protein complexin I, where it favors membrane fusion events during acrosomal exocytosis [175]. In chromaffin cell exocytosis, dynamin-1 was reported to accelerate fusion pore expansion in a GTPase activity-dependent fashion [169]. In comparison, the GTPase activity of dynamin-2 was said to be required at a stage preceding fusion pore expansion but following hemifusion during the fusion of myoblasts to form multinucleated myotubes [173]. Taken together, these findings indicate a pleiotropic role of dynamin in membrane fusion. Although dynamin does not seem to induce membrane fusion by itself, it seems to act during or after a hemifusion state. The underlying mechanism probably relies on dynamin's ability to sense membrane curvature and remodel membranes.

In kiss-and-run fusion occurring at the synapse, docked or even hemifused vesicles carrying neurotransmitter show transient opening of a fusion pore, release of contents into the synapse and immediate reclosure of the fusion pore without full dilation [176]. It is worthwhile to note that the hemifused state immediately precedes the reversible kiss-and-run fusion event. Factors controlling the hemifusion-fusion transition that have been identified from studies on yeast vacuoles would therefore be ideally poised to regulate the hotly discussed kiss-and-run mechanism of fusion pore opening and reclosure. The kiss-and-run debate is important to be resolved since in principle it can better explain rapid vesicle recycling and increased synaptic strength, hence providing a highly efficient mechanism for sustained neurotransmission.

The yeast vacuole resembling the mammalian lysosome is the major digestive organelle involved in protein processing and turnover. There is intense debate over how this organelle maintains its size and identity. Both endocytic and secretory pathways converge at the lysosome culminating in transfer of cargo to the lysosome through direct fusion with endosomes, phagosomes or ER/Golgi-derived vesicles. Interestingly, it has been speculated that this fusion can be transient (kiss-and-run) or complete (forming a hybrid organelle) [177]. Homotypic fusion of yeast vacuoles recapitulated in our content mixing assay is not reversible. To be able to resolve reversible kiss-and-run fusion, it would be necessary to move one immediate step beyond the hemifused state characterized in yeast vacuole fusion, and record fusion pore dynamics at fruit fly neuromuscular junctions or visualize the real-time heterotypic fusion of fluorescently labeled lysosomes/endosomes with phagosomes in living worms using the dynamin homologs (and corresponding mutants) in each organism. Kiss-and-run is a highly rapid and efficient mode of fusion that conserves energy and resources, and can recover compartments with greater fidelity. Importantly, its outcomes seem to be therapeutically relevant. For example, restricting complete fusion and making a provision for regulated kiss-and-run was found to be necessary for phagolysosome biogenesis and maturation which is an essential component in the acquisition of microbicidal and anti-parasitic properties in macrophages [178].

Conclusion

In conclusion, I will state that our understanding of how various factors cooperate to establish and maintain a subcellular compartment is still evolving. We will truly appreciate organelle identity when we can reconstitute these factors to program new compartments at will.

Future Goals

I have described a few immediate specific aims in order to acquire more complete visual, quantitative and functional understanding of roles of various membrane fusion components. Through cryo-electron microscopic immunolabeling it is possible to obtain ultra structural information in terms of localization, abundance and symmetry of factors enriched at fusion sites between purified yeast vacuoles *in vitro* while comparing wild type and various over expressors or mutants. Primary antibodies against HOPS tethering complex subunits, the Rab GTPase Ypt7 and the dynamin homolog Vps1 would be employed in this experimental scheme to detect these proteins directly or through epitope tags attached to them. To demonstrate the general applicability of yeast vacuole fusion principles to fusion reactions in other organisms, it is important to analyze the behavior, in terms of efficiency of content mixing, lipid mixing, trans-SNARE complex formation and vacuolar morphology, of knockout yeast vacuoles reconstituted with homologs of SNAREs, HOPS subunits, Ypt7 and Vps1 from higher eukaryotes and their mutants. It can be expected that such heterologous expression of related fusion components in yeast will at least partially restore fusion events and that specific mutations will mimic the observations in yeast. Another insightful experiment would be to dissect the GTP hydrolysis and self-assembly activities of Vps1 for their requirement in vacuolar fusion. GTP hydrolysis mutants will be tested for fusion, hemifusion, trans-SNARE complex formation and HOPS-Vam3 association in the initial screening.

GTPase activity of Vps1 variant vacuoles and recombinant protein variants can be compared using the established Malachite Green Phosphate assay. This will address the question whether Vps1 supplies an additional enzymatic activity besides a structural role during the transition from hemifusion to content mixing in yeast vacuolar fusion. Moreover, since the region(s) of Vps1 that bind to Vam3 are unknown, it is necessary to map individual domains of Vps1 while testing their interactions with the SNARE domain of Vam3. Determining the precise interacting regions between these two proteins will help to elucidate how Vps1 controls Vam3 activity and further how this binding and release can exercise fusion-fission control. Biolayer interferometry, which will give binding affinity (K_d) values, and yeast two-hybrid assays can be employed for this purpose. Lastly, mass spectrometric analysis can probe different post-translational modifications in Vps1. It will be interesting to examine whether activating or suppressing them (either constitutively or conditionally through genetic/chemical perturbations) influences vacuolar fusion and/or fission.

References

References

1. Penzlin H (2009) The riddle of “life,” a biologist’s critical view. *Naturwissenschaften* 96(1): 1-23.
2. Alberts B, Johnson A, Lewis J Raff, M Roberts, K Walter P (2008) Molecular Biology of the Cell. (5th edn), Taylor & Francis Group, UK, pp. 1392.
3. Cai H, Reinisch K, Ferro-Novick S (2007) Coats, tethers, Rabs, and SNAREs work together to mediate the intracellular destination of a transport vesicle. *Dev Cell* 12(5): 671-682.
4. Brennwald P, Kearns B, Champion K, Keränen S, Bankaitis V, et al. (1994) Sec9 is a SNAP-25-like component of a yeast SNARE complex that may be the effector of Sec4 function in exocytosis. *Cell* 79(2): 245-258.
5. Wendler F, Tooze S (2001) Syntaxin 6: the promiscuous behaviour of a SNARE protein. *Traffic* 2(9): 606-611.
6. Yang B, Gonzalez L, Prekeris R, Steegmaier M, Advani RJ, et al. (1999) SNARE interactions are not selective. Implications for membrane fusion specificity. *J Biol Chem* 274(9): 5649-5653.
7. Fasshauer D, Antonin W, Margittai M, Pabst S, Jahn R (1999) Mixed and non-cognate SNARE complexes. Characterization of assembly and biophysical properties. *J Biol Chem* 274(22): 15440-15446.
8. Trimble WS, Cowan DM, Scheller RH (1988) VAMP-1: a synaptic vesicle-associated integral membrane protein. *Proc Natl Acad Sci USA* 85(12): 4538-4542.
9. Inoue A, Obata K, Akagawa K (1992) Cloning and sequence analysis of cDNA for a neuronal cell membrane antigen, HPC-1. *J Biol Chem* 267(15): 10613-10619.
10. Bennett MK, Calakos N, Scheller RH (1992) Syntaxin: a synaptic protein implicated in docking of synaptic vesicles at presynaptic active zones. *Science* 257(5067): 255-259.
11. Oyler GA, Higgins GA, Hart RA, Battenberg E, Billingsley M, et al. (1989) The identification of a novel synaptosomal-associated protein, SNAP-25, differentially expressed by neuronal subpopulations. *J Cell Biol* 109(6 pt 1): 3039-3052.
12. Montecucco C (1980) Protein toxins and membrane transport. *Curr Opin Cell Biol* 10(4): 530-536.
13. Novick P, Field C, Schekman R (1980) Identification of 23 complementation groups required for post-translational events in the yeast secretory pathway. *Cell* 21(1): 205-215.
14. Söllner T, Whiteheart SW, Brunner M, Erdjument-Bromage H, Geromanos S, et al. (1993) SNAP receptors implicated in vesicle targeting and fusion. *Nature* 362(6418): 318-324.
15. Hammarlund M, Palfreyman MT, Watanabe S, Olsen S, Jorgensen EM (2007) Open syntaxin docks synaptic vesicles. *PLoS Biol* 5(8): 1695-1711.
16. Broadie K, Prokop A, Bellen HJ, O’Kane CJ, Schulze KL, et al. (1995) Syntaxin and synaptobrevin function downstream of vesicle docking in Drosophila. *Neuron* 15(3): 663-673.
17. Schoch S, Deák F, Königstorfer A, Mozhayeva M, Sara Y, et al. (2001) SNARE function analyzed in synaptobrevin/VAMP knockout mice. *Science* 294(5544): 1117-1122.
18. Washbourne P, Thompson PM, Carta M, Costa ET, Mathews JR, et al. (2002) Genetic ablation of the t-SNARE SNAP-25 distinguishes mechanisms of neuroexocytosis. *Nat Neurosci* 5(1): 19-26.
19. Deitcher DL, Ueda A, Stewart BA, Burgess RW, Kidokoro Y, et al. (1998) Distinct requirements for evoked and spontaneous release of neurotransmitter are revealed by mutations in the Drosophila gene neuronal-synaptobrevin. *J Neurosci* 18(6): 2028-2039.
20. Vilinsky I, Stewart BA, Drummond J, Robinson I, Deitcher DL (2002) A Drosophila SNAP-25 null mutant reveals context-dependent redundancy with SNAP-24 in neurotransmission. *Genetics* 162(1): 259-271.
21. Jahn R, Scheller RH (2006) SNAREs—engines for membrane fusion. *Nat Rev Mol Cell Biol* 7(9): 631-643.
22. Fasshauer D, Margittai M (2004) A transient N-terminal interaction of SNAP-25 and syntaxin nucleates SNARE assembly. *J Biol Chem* 279(9): 7613-7621.
23. Sørensen JB, Wiederhold K, Müller EM, Milosevic I, Nagy G, et al. (2006) Fasshauer D. Sequential N- to C-terminal SNARE complex assembly drives priming and fusion of secretory vesicles. *EMBO J* 25(5): 955-966.
24. Söllner T, Bennett MK, Whiteheart SW, Scheller RH, Rothman JE (1993) A protein assembly-disassembly pathway in vitro that may correspond to sequential steps of synaptic vesicle docking, activation, and fusion. *Cell* 75(3): 409-418.
25. Newman AP, Shim J, Ferro-Novick S (1990) BET1, BOS1, and SEC22 are members of a group of interacting yeast genes required for transport from the endoplasmic reticulum to the Golgi complex. *Mol Cell Biol* 10(7): 3405-3414.
26. Lewis MJ, Rayner JC, Pelham HR (1997) A novel SNARE complex implicated in vesicle fusion with the endoplasmic reticulum. *EMBO J* 16(11): 3017-3024.
27. Fasshauer D (2003) Structural insights into the SNARE mechanism. *Biochim Biophys Acta* 1641(2-3): 87-97.
28. Fasshauer D, Sutton RB, Brunger AT, Jahn R (1998) Conserved structural features of the synaptic fusion complex: SNARE proteins reclassified as Q- and R-SNAREs. *Proc Natl Acad Sci USA* 95(26): 15781-15786.
29. Pfeffer SR (1999) Transport-vesicle targeting: tethers before SNAREs. *Nat Cell Biol* 1(1): E17-E22.
30. Kim YG, Raunser S, Munger C, Wagner J, Song YL, et al. (2006) The Architecture of the Multisubunit TRAPP I Complex Suggests a Model for Vesicle Tethering. *Cell* 127(4): 817-830.
31. Allan BB, Moyer BD, Balch WE (2000) Rab1 recruitment of p115 into a cis-SNARE complex: programming budding COPII vesicles for fusion. *Science* 289(5478): 444-448.
32. Bentley M, Liang Y, Mullen K, Xu D, Szil C, et al. (2006) SNARE status regulates tether recruitment and function in homotypic COPII vesicle fusion. *J Biol Chem* 281(50): 38825-38833.
33. Beard M, Satoh A, Shorter J, Warren G (2005) A cryptic Rab1-binding site in the p115 tethering protein. *J Biol Chem* 280(27): 25840-25848.
34. Shorter J, Beard MB, Seemann J, Dirac-Svejstrup AB, Warren G (2002) Sequential tethering of Golgins and

- catalysis of SNAREpin assembly by the vesicle-tethering protein p115. *J Cell Biol* 157(1): 45-62.
35. Kümmel D, Heinemann U (2008) Diversity in structure and function of tethering complexes: evidence for different mechanisms in vesicular transport regulation. *Curr Protein Pept Sci* 9(2):197-209.
 36. Lazar T, Götte M, Gallwitz D (1997) Vesicular transport: how many Ypt/Rab-GTPases make a eukaryotic cell? *Trends Biochem Sci* 22(12): 468-472.
 37. Bourne HR, Sanders DA, McCormick F (1990) The GTPase super family: a conserved switch for diverse cell functions. *Nature* 348(6297): 125-132.
 38. Gomes AQ, Ali BR, Ramalho JS, Godfrey RF, Barral DC, (2003) Membrane targeting of Rab GTPases is influenced by the prenylation motif. *Mol Biol Cell* 14(5): 1882-1899.
 39. Barr FA (2013) Rab GTPases and membrane identity: causal or inconsequential? *J Cell Biol* 202(2): 191-199.
 40. Stenmark H (2009) Rab GTPases as coordinators of vesicle traffic. *Nat Rev Mol Cell Biol* 10(8): 513-525.
 41. Bröcker C, Engelbrecht-Vandré S, Ungermann C (2010) Multisubunit tethering complexes and their role in membrane fusion. *Curr Biol* 20(21): 943-952.
 42. Praefcke GJK, McMahon HT (2004) The dynamin super family: universal membrane tubulation and fission molecules? *Nat Rev Mol Cell Biol* 5:133-147.
 43. Ferguson SM, De Camilli P (2012) Dynamin, a membrane-remodelling GTPase. *Nat Rev Mol Cell Biol* 13(2): 75-88.
 44. Hinshaw JE, Schmid SL (1995) Dynamin self-assembles into rings suggesting a mechanism for coated vesicle budding. *Nature* 374(6518): 190-192.
 45. Stowell MH, Marks B, Wigge P, McMahon HT (1999) Nucleotide-dependent conformational changes in dynamin: evidence for a mechanochemical molecular spring. *Nat Cell Biol* 1(1): 27-32.
 46. Sweitzer SM, Hinshaw JE (1998) Dynamin undergoes a GTP-dependent conformational change causing vesiculation. *Cell* 93(6): 1021-1029.
 47. Roux A, Uyhazi K, Frost A, De Camilli P (2006) GTP-dependent twisting of dynamin implicates constriction and tension in membrane fission. *Nature* 441(7092): 528-531.
 48. Ramachandran R, Surka M, Chappie JS, Fowler DM, Foss TR, et al. (2007) The dynamin middle domain is critical for tetramerization and higher-order self-assembly. *EMBO J* 26(2): 559-566.
 49. Ford MG, Jenni S, Nunnari J (2011) The crystal structure of dynamin. *Nature* 477(7366): 561-566.
 50. Henne WM, Boucrot E, Meinecke M, Evergren E, Vallis Y, et al. (2010) FCHO proteins are nucleators of clathrin-mediated endocytosis. *Science* 328(5983): 1281-1284.
 51. McMahon HT, Boucrot E (2011) Molecular mechanism and physiological functions of clathrin-mediated endocytosis. *Nat Rev Mol Cell Biol* 12(8): 517-533.
 52. Ferguson S, Raimondi A, Paradise S, Shen H, Mesaki K, et al. (2009) Coordinated Actions of Actin and BAR Proteins Upstream of Dynamin at Endocytic Clathrin-Coated Pits. *Dev Cell* 17(6): 811-822.
 53. Takei K, Slepnev VI, Haucke V, De Camilli P (1999) Functional partnership between amphiphysin and dynamin in clathrin-mediated endocytosis. *Nat Cell Biol* 1(1):33-39.
 54. Bowers K, Stevens TH (2005) Protein transport from the late Golgi to the vacuole in the yeast *Saccharomyces cerevisiae*. *Biochim Biophys Acta* 1744(3): 438-454.
 55. Ostrowicz CW, Meiringer CTA, Ungermann C (2008) Yeast vacuole fusion: a model system for eukaryotic endomembrane dynamics. *Autophagy* 4(1): 5-19.
 56. Stevens T, Esmon B, Schekman R (1982) Early stages in the yeast secretory pathway are required for transport of carboxypeptidase Y to the vacuole. *Cell* 30(2): 439-448.
 57. Stepp JD, Huang K, Lemmon SK (1997) The yeast adaptor protein complex, AP-3, is essential for the efficient delivery of alkaline phosphatase by the alternate pathway to the vacuole. *J Cell Biol* 139(7): 1761-1774.
 58. Darsow T, Burd CG (1998) Emr SD Acidic di-leucine motif essential for AP-3-dependent sorting and restriction of the functional specificity of the Vam3p vacuolar t-SNARE. *J Cell Biol* 142(4): 913-922.
 59. Wen W, Chen L, Wu H, Sun X, Zhang M, et al. (2006) Identification of the yeast R-SNARE Nyv1p as a novel longin domain-containing protein. *Mol Biol Cell* 17(10): 4282-4299.
 60. Sun B, Chen L, Cao W, Roth AF, Davis NG, et al. (2004) The yeast casein kinase Yck3p is palmitoylated, then sorted to the vacuolar membrane with AP-3-dependent recognition of a YXXPhi adaptin sorting signal. *Mol Biol Cell* 15(3):1397-1406.
 61. Von Mollard GF, Nothwehr SF, Stevens TH (1997) The yeast v-SNARE Vti1p mediates two vesicle transport pathways through interactions with the t-SNAREs Sed5p and Pep12p. *J Cell Biol* 137(7): 1511-1524.
 62. Scott S V, Hefner-Gravink A, Morano KA, Noda T, Ohsumi Y, et al. (1996) Cytoplasm-to-vacuole targeting and autophagy employ the same machinery to deliver proteins to the yeast vacuole. *Proc Natl Acad Sci U S A* 93(22): 12304-12308.
 63. Haas A (1995) A quantitative assay to measure homotypic vacuole fusion in vitro. *Methods Cell Sci* 17(4): 283-294.
 64. Collins KM, Wickner WT (2007) Trans-SNARE complex assembly and yeast vacuole membrane fusion. *Proc Natl Acad Sci U S A* 104(21): 8755-8760.
 65. Li SC, Kane PM (2009) The yeast lysosome-like vacuole: Endpoint and crossroads. *Biochim Biophys Acta* 1793(4): 650-663.
 66. Wickner W, Haas A (2000) Yeast homotypic vacuole fusion: a window on organelle trafficking mechanisms. *Annu Rev Biochem* 69: 247-275.
 67. Smaczynska-de Rooij II, Allwood EG, Aghamohammadzadeh S, Hettema EH, Goldberg MW, et al. (2010) A role for the dynamin-like protein Vps1 during endocytosis in yeast. *J Cell Sci* 123(20): 3496-3506.
 68. Min L, Leung YM, Tomas A, Watson RT, Gaisano HY, et al. (2007) Dynamin is functionally coupled to insulin granule exocytosis. *J Biol Chem* 282(46): 33530-33536.

69. Trouillon R, Ewing AG (2013) Amperometric Measurements at Cells Support a Role for Dynamin in the Dilation of the Fusion Pore during Exocytosis. *Chemphyschem* 14(10): 2295-301.
70. Peters C, Baars TL, Bühler S, Mayer A (2004) Mutual control of membrane fission and fusion proteins. *Cell* 119(5): 667-678.
71. Cherry JM, Adler C, Ball C, Chervitz SA, Dwight SS, et al. (1998) SGD: Saccharomyces Genome Database. *Nucleic Acids Res* 26: 73-79.
72. Ostrowicz CW, Bröcker C, Ahnert F, Nordmann M, Lachmann J, et al. (2010) Defined subunit arrangement and rab interactions are required for functionality of the HOPS tethering complex. *Traffic* 11(10): 1334-1346.
73. Seals DF, Eitzen G, Margolis N, Wickner WT, Price A (2000) A Ypt/Rab effector complex containing the Sec1 homolog Vps33p is required for homotypic vacuole fusion. *Proc Natl Acad Sci U S A* 97(17): 9402-9407.
74. Wurmser AE, Sato TK, Emr SD (2000) New component of the vacuolar class C-Vps complex couples nucleotide exchange on the Ypt7 GTPase to SNARE-dependent docking and fusion. *J Cell Biol* 151(3): 551-562.
75. Stroupe C, Collins KM, Fratti RA, Wickner W (2006) Purification of active HOPS complex reveals its affinities for phosphoinositides and the SNARE Vam7p. *EMBO J* 25(8): 1579-1589.
76. Pieren M, Schmidt A, Mayer A (2010) The SM protein Vps33 and the t-SNARE H(abc) domain promote fusion pore opening. *Nat Struct Mol Biol* 17: 710-717.
77. Sato TK, Rehling P, Peterson MR, Emr SD (2000) Class C Vps protein complex regulates vacuolar SNARE pairing and is required for vesicle docking/fusion. *Mol Cell* 6(3): 661-671.
78. Nickerson DP, Brett CL, Merz AJ (2009) Vps-C complexes: gatekeepers of endolysosomal traffic. *Curr Opin Cell Biol* 21(4): 543-551.
79. Caplan S, Hartnell LM, Aguilar RC, Naslavsky N, Bonifacino JS (2001) Human Vam6p promotes lysosome clustering and fusion in vivo. *J Cell Biol* 154(1): 109-122.
80. Darsow T, Katzmann DJ, Cowles CR, Emr SD (2001) Vps41p function in the alkaline phosphatase pathway requires homo-oligomerization and interaction with AP-3 through two distinct domains. *Mol Biol Cell* 12(1): 37-51.
81. Plemel RL, Lobinger BT, Brett CL, Angers CG, Nickerson DP, et al. (2011) Subunit organization and Rab interactions of Vps-C protein complexes that control endolysosomal membrane traffic. *Mol Biol Cell* 22(8): 1353-1363.
82. Brett CL, Plemel RL, Lobinger BT, Vignali M, Fields S, et al. (2008) Efficient termination of vacuolar Rab GTPase signaling requires coordinated action by a GAP and a protein kinase. *J Cell Biol* 182(2): 1141-1151.
83. Nordmann M, Cabrera M, Perz A, Bröcker C, Ostrowicz C, et al. (2010) The Mon1-Ccz1 complex is the GEF of the late endosomal Rab7 homolog Ypt7. *Curr Biol* 20(18): 1654-1659.
84. Price A, Seals D, Wickner W, Ungermann C (2000) The docking stage of yeast vacuole fusion requires the transfer of proteins from a cis-SNARE complex to a Rab/Ypt protein. *J Cell Biol* 148(6): 1231-1238.
85. Goud B, Salminen A, Walworth NC, Novick PJ (1988) A GTP-binding protein required for secretion rapidly associates with secretory vesicles and the plasma membrane in yeast. *Cell* 53(5): 753-768.
86. Protopopov V, Govindan B, Novick P, Gerst JE (1993) Homologs of the synaptobrevin/VAMP family of synaptic vesicle proteins function on the late secretory pathway in *S. cerevisiae*. *Cell* 74(5): 855-861.
87. Finger FP, Hughes TE (1998) Novick P Sec3p is a spatial landmark for polarized secretion in budding yeast. *Cell* 92(4): 559-571.
88. TerBush DR, Novick P (1995) Sec6, Sec8, and Sec15 are components of a multisubunit complex which localizes to small bud tips in *Saccharomyces cerevisiae*. *J Cell Biol* 130(2): 299-312.
89. Guo W, Roth D, Walch-Solimena C, Novick P (1999) The exocyst is an effector for Sec4p, targeting secretory vesicles to sites of exocytosis. *EMBO J* 18(4): 1071-1080.
90. Garrett MD, Zahner JE, Cheney CM, Novick PJ (1994) GDI1 encodes a GDP dissociation inhibitor that plays an essential role in the yeast secretory pathway. *EMBO J* 13(7): 1718-1728.
91. Calakos N, Scheller RH (1996) Synaptic vesicle biogenesis, docking, and fusion: a molecular description. *Physiol Rev* 76(1): 1-29.
92. Palfrey HC, Artalejo CR (1998) Vesicle recycling revisited: Rapid endocytosis may be the first step. *Neuroscience* 83(4): 969-989.
93. Wilson DW, Wilcox CA, Flynn GC, Chen E, Kuang WJ (1989) A fusion protein required for vesicle-mediated transport in both mammalian cells and yeast. *Nature* 339(6223): 355-359.
94. Weidman PJ, Melancon P, Block MR, Rothman JE (1989) Binding of an N-ethylmaleimide-sensitive fusion protein to Golgi membranes requires both a soluble protein(s) and an integral membrane receptor. *J Cell Biol* 108(5): 1589-1596.
95. Clary DO, Griff IC, Rothman JE (1990) SNAPS, a family of NSF attachment proteins involved in intracellular membrane fusion in animals and yeast. *Cell* 61(4): 709-721.
96. Hay JC, Fisette PL, Jenkins GH, Fukami K, Takenawa T, et al. (1995) ATP-dependent inositol phosphorylation required for Ca(2+)-activated secretion. *Nature* 374(6518): 173-177.
97. Cremona O, De Camilli P (2001) Phosphoinositides in membrane traffic at the synapse. *J Cell Sci* 114(16): 1041-1052.
98. Banerjee A, Barry VA, DasGupta BR, Martin T (1996) N-Ethylmaleimide-sensitive factor acts at a prefusion ATP-dependent step in Ca2+-activated exocytosis. *J Biol Chem* 271: 20223-20226.
99. Hay JC, Fisette PL, Jenkins GH, Fukami K, Takenawa T, (1995) ATP-dependent inositol phosphorylation required for Ca(2+)-activated secretion. *Nature* 374(6518): 173-177.
100. Eberhard DA, Cooper CL, Lowt MG, Holz RW (1990) Evidence that the inositol phospholipids are necessary for exocytosis. *J Biochem* 268(1): 15-25.

101. Chamberlain LH, Roth D, Morgan A, Burgoyne RD (1995) Distinct effects of alpha-SNAP, 14-3-3 proteins, and calmodulin on priming and triggering of regulated exocytosis. *J Cell Biol* 130(5): 1063-1070.
102. Barnard RJ, Morgan A, Burgoyne RD (1997) Stimulation of NSF ATPase activity by alpha-SNAP is required for SNARE complex disassembly and exocytosis. *J Cell Biol* 139(4): 875-883.
103. Zheng X, Bobich JA (1998) MgATP-dependent and MgATP-independent [³H]noradrenaline release from perforated synaptosomes both use N-ethylmaleimide-sensitive fusion protein. *Biochemistry* 37(36): 12569-12575.
104. Tolar LA, Pallanck L (1998) NSF function in neurotransmitter release involves rearrangement of the SNARE complex downstream of synaptic vesicle docking. *J Neurosci* 18(24): 10250-10256.
105. Hunt JM, Bommert K, Charlton MP, Kistner A, Habermann E, et al. (1994) A post-docking role for synaptobrevin in synaptic vesicle fusion. *Neuron* 12(6): 1269-1279.
106. Haas A, Schegemann D, Lazar T, Gallwitz D, Wickner W (1995) The GTPase Ypt7p of *Saccharomyces cerevisiae* is required on both partner vacuoles for the homotypic fusion step of vacuole inheritance. *EMBO J* 14(21): 5258-5270.
107. Mayer A, Wickner W (1997) Docking of yeast vacuoles is catalyzed by the Ras-like GTPase Ypt7p after symmetric priming by Sec18p (NSF). *J Cell Biol* 136(2): 307-317.
108. Barbieri MA, Hoffenberg S, Roberts R, Mukhopadhyay A, Pomrehn A, et al. (1998) Evidence for a symmetrical requirement for Rab5-GTP in *in vitro* endosome-endosome fusion. *J Biol Chem* 273(40): 25850-25855.
109. Fischer von Mollard G, Mignery GA, Baumert M, Perin MS, Hanson TJ, et al. (1990) rab3 is a small GTP-binding protein exclusively localized to synaptic vesicles. *Proc Natl Acad Sci U S A* 87(5): 1988-1992.
110. Fischer von Mollard G, Südhof TC, Jahn R (1991) A small GTP-binding protein dissociates from synaptic vesicles during exocytosis. *Nature* 349(6304): 79-81.
111. Cao X, Ballew N, Barlowe C (1998) Initial docking of ER-derived vesicles requires Uso1p and Ypt1p but is independent of SNARE proteins. *EMBO J* 17(18): 2156-2165.
112. Parlati F, McNew JA, Fukuda R, Miller R, Söllner TH, Rothman JE (2000) Topological restriction of SNARE-dependent membrane fusion. *Nature* 407(6801): 194-198.
113. Weber T, Zemelman B V, McNew JA, Westermann B, Gmachl M, et al. (1998) SNAREpins: Minimal machinery for membrane fusion. *Cell* 92(6): 759-772.
114. Zwilling D, Cypionka A, Pohl WH, Fasshauer D, Walla PJ, (2007) Early endosomal SNAREs form a structurally conserved SNARE complex and fuse liposomes with multiple topologies. *EMBO J* 26(1): 9-18.
115. Alpadi K, Kulkarni A, Comte V, Reinhardt M, Schmidt A, et al. (2012) Sequential Analysis of Trans-SNARE Formation in Intracellular Membrane Fusion. *PLoS Biol* 10(1): e1001243.
116. Nichols BJ, Ungermann C, Pelham HR, Wickner WT, Haas A (1997) Homotypic vacuolar fusion mediated by t- and v-SNAREs. *Nature* 387(6629): 199-202.
117. Etzen G, Will E, Gallwitz D, Haas A, Wickner W (2000) Sequential action of two GTPases to promote vacuole docking and fusion. *EMBO J* 19(24): 6713-6720.
118. Sato TK, Darsow T, Emr SD (1998) Vam7p, a SNAP-25-like molecule, and Vam3p, a syntaxin homolog, function together in yeast vacuolar protein trafficking. *Mol Cell Biol* 18(9): 5308-5319.
119. Bethani I, Lang T, Geumann U, Sieber JJ, Jahn R, Rizzoli SO (2007) The specificity of SNARE pairing in biological membranes is mediated by both proof-reading and spatial segregation. *EMBO J* 26(17): 3981-3992.
120. Weninger K, Bowen ME, Chu S, Brunger AT (2003) Single-molecule studies of SNARE complex assembly reveal parallel and antiparallel configurations. *Proc Natl Acad Sci U S A* 100(25): 14800-14805.
121. Cao X, Barlowe C (2000) Asymmetric requirements for a Rab GTPase and SNARE proteins in fusion of COPII vesicles with acceptor membranes. *J Cell Biol* 149(1): 55-66.
122. Hickey CM, Wickner W (2010) HOPS initiates vacuole docking by tethering membranes before trans-SNARE complex assembly. *Mol Biol Cell* 21(13): 2297-2305.
123. Lo S-Y, Brett CL, Plemel RL, Vignali M, Fields S, Gonen T, Merz AJ (2011) Intrinsic tethering activity of endosomal Rab proteins. *Nat Struct Mol Biol* 19(1): 40-47.
124. Xu H, Jun Y, Thompson J, Yates J, Wickner W (2010) HOPS prevents the disassembly of trans-SNARE complexes by Sec17p/Sec18p during membrane fusion. *EMBO J* 29(12): 1948-1960.
125. Sohda M, Misumi Y, Yamamoto A, Nakamura N, Ogata S, et al. (2010) Interaction of Golgin-84 with the COG complex mediates the intra-Golgi retrograde transport. *Traffic* 11(12): 1552-1566.
126. Callaghan J, Simonsen A, Gaullier JM, Toh BH, Stenmark H (1999) The endosome fusion regulator early-endosomal autoantigen 1 (EEA1) is a dimer. *Biochem J* 338 (Pt 2): 539-543.
127. Yip CK, Berschenski J, Walz T (2010) Molecular architecture of the TRAPP II complex and implications for vesicle tethering. *Nat Struct Mol Biol* 17(11): 1298-1304.
128. Sacher M, Barrowman J, Wang W, Horecka J, Zhang Y, et al. (2001) TRAPP I implicated in the specificity of tethering in ER-to-Golgi transport. *Mol Cell* 7(2): 433-442.
129. Brocker C, Kuhlee A, Gatsogiannis C, kleine Balderhaar HJ, et al. (2012) Molecular architecture of the multisubunit homotypic fusion and vacuole protein sorting (HOPS) tethering complex. *Proc Natl Acad Sci* 109(6): 1991-1996.
130. Reese C, Heise F, Mayer A (2005) Trans-SNARE pairing can precede a hemifusion intermediate in intracellular membrane fusion. *Nature* 436(7049): 410-414.
131. Arneson LN, Segovis CM, Gomez TS, Schoon RA, Dick CJ, et al. (2008) Dynamin 2 regulates granule exocytosis during NK cell-mediated cytotoxicity. *J Immunol* 181(10): 6995-7001.

132. Bürmann F, Ebert N, van Baarle S, Bramkamp M (2011) A bacterial dynamin-like protein mediating nucleotide-independent membrane fusion. *Mol Microbiol* 79(5): 1294-1304.
133. Vater CA, Raymond CK, Ekena K, Howald-Stevenson I, Stevens TH (1992) The VPS1 protein, a homolog of dynamin required for vacuolar protein sorting in *Saccharomyces cerevisiae*, is a GTPase with two functionally separable domains. *J Cell Biol* 119(4): 773-786.
134. Alpadi K, Kulkarni A, Namjoshi S, Srinivasan S, Sippel KH, et al. (2013) Dynamin-SNARE interactions control trans-SNARE formation in intracellular membrane fusion. *Nat Commun* 4: 1704.
135. Van den Bogaart G, Jahn R (2011) Counting the SNAREs needed for membrane fusion. *J Mol Cell Biol* 3(4): 204-205.
136. Sinha R, Ahmed S, Jahn R, Klingauf J (2011) Two synaptobrevin molecules are sufficient for vesicle fusion in central nervous system synapses. *Proc Natl Acad Sci U S A* 108(34): 14318-14323.
137. Domanska MK, Kiessling V, Stein A, Fasshauer D, Tamm LK (2009) Single vesicle millisecond fusion kinetics reveals number of SNARE complexes optimal for fast SNARE-mediated membrane fusion. *J Biol Chem* 284(46): 32158-32166.
138. Shi L, Shen Q-T, Kiel A, Wang J, Wang H-W, et al. (2012) SNARE Proteins: One to Fuse and Three to Keep the Nascent Fusion Pore Open. *Science* 335(6074): 1355-1359.
139. Mohrmann R, de Wit H, Verhage M, Neher E, Sørensen JB (2010) Fast vesicle fusion in living cells requires at least three SNARE complexes. *Science* 330(6003): 502-505.
140. Hua Y, Scheller RH (2001) Three SNARE complexes cooperate to mediate membrane fusion. *Proc Natl Acad Sci U S A* 98(14): 8065-8070.
141. Shnyrova AV, Bashkirov PV, Akimov SA, Pucadyil TJ, Zimmerberg J, et al. (2013) Geometric catalysis of membrane fission driven by flexible dynamin rings. *Science* 339(6126): 1433-1436.
142. Karunakaran S, Fratti RA (2013) The lipid composition and physical properties of the yeast vacuole affect the hemifusion-fusion transition. *Traffic* 14(6): 650-662.
143. Han X, Wang C-T, Bai J, Chapman ER, Jackson MB (2004) Transmembrane segments of syntaxin line the fusion pore of Ca²⁺-triggered exocytosis. *Science* 304(5668): 289-292.
144. Bai J, Wang CT, Richards DA, Jackson MB, Chapman ER (2004) Fusion pore dynamics are regulated by synaptotagmin-t-SNARE interactions. *Neuron* 41(6): 929-942.
145. Galas MC, Chasserot-Golaz S, Dirrig-Grosch S, Bader MF (2000) Presence of dynamin-syntaxin complexes associated with secretory granules in adrenal chromaffin cells. *J Neurochem* 75(4): 1511-1519.
146. Kulkarni A, Alpadi K, Namjoshi S, Peters C (2012) A tethering complex dimer catalyzes trans-SNARE complex formation in intracellular membrane fusion. *Bioarchitecture* 2(2): 59-69.
147. Koseoglu S, Dilks JR, Peters CG, Fitch-Tewfik JL, Fadel NA, et al. (2013) Dynamin-related protein-1 controls fusion pore dynamics during platelet granule exocytosis. *Arterioscler Thromb Vasc Biol* 33(3): 481-498.
148. Harata NC, Aravanis AM, Tsien RW (2006) Kiss-and-run and full-collapse fusion as modes of exo-endocytosis in neurosecretion. *J Neurochem* 97(6): 1546-1570.
149. Sherwood MW, Prior IA, Voronina SG, Barrow SL, Woodsmith JD, et al. (2007) Activation of trypsinogen in large endocytic vacuoles of pancreatic acinar cells. *Proc Natl Acad Sci U S A* 104(13): 5674-5679.
150. Schonthaler HB, Fleisch VC, Biehlmaier O, Makhanov Y, Rinner O, et al. (2008) The zebrafish mutant lkb/vam6 resembles human multisystemic disorders caused by aberrant trafficking of endosomal vesicles. *Development* 135(2): 387-399.
151. Kim BY, Ueda M, Kominami E, Akagawa K, Kohsaka S, et al. (2003) Identification of mouse Vps16 and biochemical characterization of mammalian Class C Vps complex. *Biochem Biophys Res Commun* 311(3): 577-582.
152. Rojo E, Gillmor CS, Kovaleva V, Somerville CR, Raikhel NV (2001) VACUOLELESS1 Is an Essential Gene Required for Vacuole Formation and Morphogenesis in Arabidopsis. *Dev Cell* 1(2): 303-310.
153. Kinchen JM, Doukoumetzidis K, Almendinger J, Stergiou L, Tosello-Trampont A, et al. (2008) A pathway for phagosome maturation during engulfment of apoptotic cells. *Nat Cell Biol* 10(5): 556-566.
154. Koumandou VL, Dacks JB, Coulson RMR, Field MC (2007) Control systems for membrane fusion in the ancestral eukaryote evolution of tethering complexes and SM proteins. *BMC Evol Biol* 7: 29.
155. Spinosa MR, Progida C, De Luca A, Colucci AMR, Alifano P, et al. (2008) Functional characterization of Rab7 mutant proteins associated with Charcot-Marie-Tooth type 2B disease. *J Neurosci* 28(7): 1640-1648.
156. Wu X, Steet RA, Bohorov O, Bakker J, Newell J, et al. (2004) Mutation of the COG complex subunit gene COG7 causes a lethal congenital disorder. *Nat Med* 10(5): 518-523.
157. Misura KM, Scheller RH, Weis WI (2001) Self-association of the H3 region of syntaxin 1A. Implications for intermediates in SNARE complex assembly. *J Biol Chem* 276(16): 13273-13282.
158. Misura KM, Gonzalez LC, May AP, Scheller RH, Weis WI (2001) Crystal structure and biophysical properties of a complex between the N-terminal SNARE region of SNAP25 and syntaxin 1a. *J Biol Chem* 276: 41301-41309.
159. Margittai M, Fasshauer D, Pabst S, Jahn R, Langen R (2001) Homo- and heterooligomeric SNARE complexes studied by site-directed spin labeling. *J Biol Chem* 276(16): 13169-13177.
160. Zhang F, Chen Y, Kweon D-H, Kim CS, Shin Y-K (2002) The four-helix bundle of the neuronal target membrane SNARE complex is neither disordered in the middle nor uncoiled at the C-terminal region. *J Biol Chem* 277(27): 24294-24298.

161. Parlati F, Varlamov O, Paz K, McNew JA, Hurtado D, et al. (2002) Distinct SNARE complexes mediating membrane fusion in Golgi transport based on combinatorial specificity. *Proc Natl Acad Sci U S A* 99(8): 5424-5429.
162. Grote E, Novick PJ (1999) Promiscuity in Rab-SNARE interactions. *Mol Biol Cell* 10(12): 4149-4161.
163. Mallozzi C, D'Amore C, Camerini S, Macchia G, Crescenzi M, et al. (2013) Phosphorylation and nitration of tyrosine residues affect functional properties of Synaptophysin and Dynamin I, two proteins involved in exo-endocytosis of synaptic vesicles. *Biochim Biophys Acta - Mol Cell Res* 1833(1): 110-121.
164. Kelly BL, Vassar R, Ferreira A (2005) Beta-amyloid-induced dynamin 1 depletion in hippocampal neurons. A potential mechanism for early cognitive decline in Alzheimer disease. *J Biol Chem* 280(36): 31746-31753.
165. Bitoun M, Maugrenre S, Jeannet P-Y, Lacène E, Ferrer X, et al. (2005) Mutations in dynamin 2 cause dominant centronuclear myopathy. *Nat Genet* 37(11): 1207-1209.
166. Züchner S, Noureddine M, Kennerson M, Verhoeven K, Claeys K, et al. (2005) Mutations in the pleckstrin homology domain of dynamin 2 cause dominant intermediate Charcot-Marie-Tooth disease. *Nat Genet* 37(3): 289-294.
167. Alexander C, Votruba M, Pesch UE, Thiselton DL, Mayer S, et al. (2000) OPA1, encoding a dynamin-related GTPase, is mutated in autosomal dominant optic atrophy linked to chromosome 3q28. *Nat Genet* 26(2): 211-215.
168. Sever S, Altintas MM, Nankoe SR, Möller CC, Ko D, et al. (2007) Proteolytic processing of dynamin by cytoplasmic cathepsin L is a mechanism for proteinuric kidney disease. *J Clin Invest* 117(15): 2095-2104.
169. Anantharam A, Bittner MA, Aikman RL, Stuenkel EL, Schmid SL, (2011) A new role for the dynamin GTPase in the regulation of fusion pore expansion. *Mol Biol Cell* 22(11): 1907-1918.
170. González-Jamett AM, Báez-Matus X, Hevia MA, Guerra MJ, Olivares MJ, et al. (2010) The association of dynamin with synaptophysin regulates quantal size and duration of exocytotic events in chromaffin cells. *J Neurosci* 30(32): 10683-10691.
171. Samasilp P, Chan S-A, Smith C (2012) Activity-Dependent Fusion Pore Expansion Regulated by a Calcineurin-Dependent Dynamin-Syndapin Pathway in Mouse Adrenal Chromaffin Cells. *J Neurosci* 32(30): 10438-10447.
172. Reid AT, Lord T, Stanger SJ, Roman SD, McCluskey A, et al. (2012) Dynamin Regulates Specific Membrane Fusion Events Necessary for Acrosomal Exocytosis in Mouse Spermatozoa. *J Biol Chem* 287(45): 37659-37672.
173. Leikina E, Melikov K, Sanyal S, Verma SK, Eun B, Get al. (2013) Extracellular annexins and dynamin are important for sequential steps in myoblast fusion. *J Cell Biol* 200(1): 109-123.
174. De la Vega M, Marin M, Kondo N, Miyauchi K, Kim Y, Epanad RF, Epanad RM, Melikyan GB (2011) Inhibition of HIV-1 endocytosis allows lipid mixing at the plasma membrane, but not complete fusion. *Retrovirology* 8: 99.
175. Zhao L, Shi X, Li L, Miller DJ (2007) Dynamin 2 associates with complexins and is found in the acrosomal region of mammalian sperm. *Mol Reprod Dev* 74(6): 750-757.
176. Alabi A, Tsien RW (2013) Perspectives on kiss-and-run: role in exocytosis, endocytosis, and neurotransmission. *Annu Rev Physiol* 75: 393-422.
177. De Matteis MA, Luini A (2011) Mendelian disorders of membrane trafficking. *N Engl J Med* 365(10): 927-938.
178. Duclos S, Diez R, Garin J, Papadopoulou B, Descoteaux A, et al. (2000) Rab5 regulates the kiss and run fusion between phagosomes and endosomes and the acquisition of phagosome leishmanicidal properties in RAW 264.7 macrophages. *J Cell Sci* 113 Pt 19: 3531-3541.